



**SRI LANKAN GEOTECHNICAL SOCIETY**

A Member Society of the International Society for Soil Mechanics and Geotechnical Engineering (ISSMGE)

**ANNUAL CONFERENCE 2024**

**GEOTECHNICAL ENGINEERING  
CHALLENGES IN EXPRESSWAY  
CONSTRUCTION**



**08<sup>th</sup> October 2024**

**At Galle Face Hotel, Colombo, Sri Lanka**



# **ANNUAL CONFERENCE 2024**

## **GEOTECHNICAL ENGINEERING CHALLENGES IN EXPRESSWAY CONSTRUCTION**

**08<sup>th</sup> October 2024**

**At Galle Face Hotel, Colombo, Sri Lanka**

**To Download the Proceedings:**







## Associate Partner:



International top-tier engineering contractor, investment operator, urban developer and ecological manager, and enjoys complete industrial chain advantages and boasts strong resource integration capabilities in such fields as ports, buildings, roads and bridges, rails, comprehensive urban developments, environmental protection, pipe networks and green power.

Guided by the "Belt and Road" Initiative, CHEC is upholding its notion of "Pricing is the core of Marketing" and is striving to balance among "the Clients' willingness to accept", "Company's reasonable profit" and the Social Responsibilities. Aiming at "high standard, sustainability and benefiting the people", CHEC will contribute to building a community with a shared future for mankind.





**SRI LANKAN GEOTECHNICAL SOCIETY**

**EXECUTIVE COMMITTEE - 2023/2024**

President	:	Eng. K L S Sahabandu
Past Presidents	:	Prof. S A S Kulathilaka Eng. K S Senanayake
Vice President	:	Prof. H S Thilakasiri
Hony. Secretary	:	Prof. U P Nawagamuwa
Treasurer	:	Eng. R M Rathnasiri
Editor –Journal	:	Prof. N H Priyankara
Editor – Newsletter	:	Dr. S K Navaratnarajah
Asst. Secretary	:	Dr. K H S M Sampath
Asst. Treasurer	:	Eng. M D J P Wickramasooriya
Committee Members	:	Dr. W A Karunawardena Dr. J S M Fowze Prof. L I N De Silva Eng. R M Abeysinghe Eng. (Mrs.) L Padmasiri





Gold Sponsor:



# ICC PRECAST SOLUTIONS

Transforming construction efficiency, delivering faster, stronger, and sustainable solutions for modern building needs.



ICC WEBSITE



- ▶ WIDE RANGE OF PRODUCTS
- ▶ SUPERIOR QUALITY
- ▶ COST EFFICIENCY
- ▶ FASTER CONSTRUCTION
- ▶ DURABILITY AND STRENGTH
- ▶ DESIGN FLEXIBILITY

A leading Precast & Prestressed product manufacturer, offering a wide range of products & solutions to the Sri Lankan construction industry, manufactured at a fully fledged, state of the art production facilities.

## ICC Precast & Prestressed Factory Colombo

# 508/2 New Gadabuwana Road,  
Piliyandala, Sri Lanka.

Email: [precast@icc-construct.com](mailto:precast@icc-construct.com)



**INTERNATIONAL CONSTRUCTION CONSORTIUM PVT LTD**

Address #57, S. De. S. Jayasinghe Mawatha, Kohuwala, Nugegoda, Sri Lanka  
Website : [www.icc-construct.com](http://www.icc-construct.com)



**077 383 6386**



## PRESIDENT'S MESSAGE

It is with great pleasure and honour that I send this message to the 2024 Annual Conference of the Sri Lankan Geotechnical Society (SLGS), held under the theme **“Geotechnical Engineering Challenges in Expressway Construction,”** which customarily precedes the Annual General Meeting.



In the past few decades, numerous expressway projects have been successfully completed in Sri Lanka, with several more scheduled to commence or be completed in the near future. Throughout these projects, significant geotechnical engineering challenges were encountered, and innovative solutions were developed. The experiences gained from these projects will be invaluable for future expressway and infrastructure developments.

SLGS, as you may know, was founded nearly three and a half decades ago under the visionary leadership of Prof. A. Thurairajah, who returned to his homeland after an illustrious and influential career at the University of Cambridge. He is widely regarded as the father of Soil Mechanics in Sri Lanka.

Since its inception, SLGS has played a pivotal role in advancing the field of Geotechnical Engineering in Sri Lanka, serving as the professional body for practicing engineers and academics in this field. Our influence has further grown since becoming a member of the *International Society for Soil Mechanics and Geotechnical Engineering (ISSMGE)*.

SLGS has engaged in a wide range of activities, including conferences, seminars, and workshops featuring renowned national and international experts. We also host the Geotechnical Forum or Webinar, a monthly evening lecture (mostly conducted in Hybrid Mode) that provides a platform for local and regional engineers to learn from the experiences of both academics and practitioners around the world. Additionally, we organize technical visits to project sites of geotechnical significance.

SLGS has successfully conducted three major international conferences in 2007, 2015, and 2021, attracting leading academics and practitioners in the fields of Geotechnical Engineering and Foundations.

During this tenure, we have held two forums, a webinar and a workshop on contemporary topics in Geotechnical Engineering. As the final event of this term, we are hosting our Annual Conference, which, in line with our statutes, precedes the Annual General Meeting. This year, we have organized the conference in a hybrid format to maximize the benefits of both in-person and virtual participation.

We are fortunate to have a distinguished line-up of resource persons, selected from both industry and academia, who will share their valuable insights on the theme “Geotechnical Engineering Challenges in Expressway Construction.” We are deeply grateful to them for taking time from their busy schedules to join us in this knowledge-sharing endeavour. I am confident that this conference will spark thought-provoking discussions and will be of great interest to all of us in the geotechnical engineering community.

Ladies and gentlemen, it is my privilege, on behalf of the Society, to extend a warm welcome and express my appreciation to Mr. Shi Fulu, Technical Manager from China Harbour Engineering Company (CHEC), Emeritus Prof. Athula Kulathilaka of the Department of Civil Engineering at the University of Moratuwa, Prof. Neelima Satyam from IIT Indore and a National Executive Committee Member of the Indian Geotechnical Society, Dr. Asiri Karunawardena, Director General of the National Building Research Organisation (NBRO), Prof. Saman Thilakasiri, from the Sri Lanka Institute of Information Technology (SLIIT), and Prof. Nadeej Priyankara from the Department of Civil and Environmental Engineering at the University of Ruhuna, for accepting our invitation to serve as resource personnel and share their knowledge with our members and professionals in Sri Lanka and the region.

I would also like to express my deep gratitude to Dr. Anil Joseph, President of the Indian Geotechnical Society, for his invaluable assistance in organizing this conference.

With immense appreciation, I welcome all distinguished invitees, including past presidents and current and former executive committee members of SLGS, for gracing us with their presence at this event.

I extend my sincere thanks to our Associate Partner, China Harbour Engineering Company, as well as our sponsors: M/s International Construction Consortium (Pvt.) Ltd, M/s Maga Engineering (Pvt.) Ltd, M/s Pile Test Consultants (Pvt.) Ltd, M/s Getech Engineering (Pvt.) Ltd, M/s Sanken Construction (Pvt.) Ltd, M/s Sierra Construction (Pvt.) Ltd and M/s ELS Construction (Pvt.) Ltd, for their support and generous sponsorship of this event.


I also warmly welcome Prof. Udeni Nawagamuwa for accepting my invitation to chair the sessions of the conference with me.

My heartfelt gratitude goes to all the members of the organizing and executive committees, particularly Prof. Udeni Nawagamuwa, Eng. Mahinda Rathnasiri, Dr. Sampath Hewage, Eng. (Ms) Lasanda Padmasiri, and Eng. Janaka Priyantha, for their unwavering support in making this event a success.

Finally, I extend a warm welcome to all participants, whose presence will undoubtedly make this event a memorable one.

Without a doubt, this conference will be another exciting and informative event hosted by SLGS, and I wish everyone a highly productive and fruitful experience.

Thank you.



**Eng. K.L.S. Sahabandu**

*B.Sc.Eng.(Hons.), Pg. Dip.(Hyd.Eng.), M.Sc.(Struct. Eng.), C.Eng.,  
M.I.C.E.(London), M.Cons.E.(S.L.), F.I.E.(S.L.), Hon. F.S.S.E.(S.L.)*

**President-SLGS**



**SLGS ANNUAL CONFERENCE, 2024**

**“GEOTECHNICAL ENGINEERING CHALLENGES IN EXPRESSWAY CONSTRUCTION”**

**PROGRAMME**

8:30 – 9:00	Registration of Participants / Morning Tea	
9:00 – 9:15	Ceremonial Opening	
9:15 – 9:30	Welcome Address	<b>Eng. K.L.S. Sahabandu</b> President - SLGS
<b>Morning Session: Session Chair: Eng. K.L.S. Sahabandu</b>		
9:30 – 10:10	Risk Investigation and Damage Treatment of High Slopes on Expressways	<b>Mr. Shi Fulu</b> Technical Manager, China Harbour Engineering Company (CHEC)
10:10 – 10:50	Slope Stabilization Techniques and Earth Retaining Systems in Expressways	<b>Emeritus Prof. Athula Kulathilaka</b> Department of Civil Engineering, University of Moratuwa
10.50 – 11.30	Geotechnical and Structural Aspects of Tunnel Design in Highway Projects	<b>Prof. Neelima Satyam</b> Professor, IIT Indore, National Executive Committee Member, Indian Geotechnical Society
11.30 – 12.00	Discussion Session	
12:00 – 13:00	<b>Lunch Break</b>	
<b>Evening Session: Session Chair: Prof. Udeni Nawagamuwa</b>		
13:00 – 13:40	Advancements in Ground Improvement Techniques for Sri Lankan Expressway Construction	<b>Dr. Asiri Karunawardena</b> Director General, National Building Research Organisation (NBRO)
13:40 – 14:20	Post-Construction Settlements of Expressways	<b>Prof. Saman Thilakasiri</b> Senior Professor, Sri Lanka Institute of Information Technology (SLIIT)
14.20 – 15.00	Failure of Gravel Compaction Pile (GCP) Improved Embankment – A Case Study	<b>Prof. Nadeej Priyankara</b> Professor, Department of Civil and Environmental Engineering, University of Ruhuna
15.00 – 15.30	Discussion Session	
15:30 – 15:40	Vote of Thanks & Closing Remarks	<b>Prof. Udeni Nawagamuwa</b> Hony. Secretary - SLGS
15:40 – 16:00	Evening Tea	
16.00 – 16.45	27 <sup>th</sup> Annual General Meeting of SLGS	



**SLGS ANNUAL CONFERENCE, 2024****“GEOTECHNICAL ENGINEERING CHALLENGES IN EXPRESSWAY CONSTRUCTION”****CONTENT**

<b>No.</b>	<b>Topic</b>	<b>Page</b>
<b>01</b>	<b>Risk Investigation and Damage Treatment of High Slopes on Expressways</b> <i>Mr. Shi Fulu, Technical Manager, China Harbour Engineering Company (CHEC)</i>	<b>03</b>
<b>02</b>	<b>Slope Stabilization Techniques and Earth Retaining Systems in Expressways</b> <i>Emeritus Prof. Athula Kulathilaka, Department of Civil Engineering, University of Moratuwa</i>	<b>18</b>
<b>03</b>	<b>Geotechnical and Structural Aspects of Tunnel Design in Highway Projects</b> <i>Prof. Neelima Satyam, Professor, IIT Indore, National Executive Committee Member, Indian Geotechnical Society</i>	<b>51</b>
<b>04</b>	<b>Advancements in Ground Improvement Techniques for Sri Lankan Expressway Construction</b> <i>Dr. Asiri Karunawardena, Director General, National Building Research Organisation (NBRO)</i>	<b>59</b>
<b>05</b>	<b>Post-Construction Settlements of Expressways</b> <i>Prof. Saman Thilakasiri, Senior Professor, Sri Lanka Institute of Information Technology (SLIIT)</i>	<b>70</b>
<b>06</b>	<b>Failure of Gravel Compaction Pile (GCP) Improved Embankment – A Case Study</b> <i>Prof. Nadeej Priyankara, Professor, Department of Civil and Environmental Engineering, University of Ruhuna</i>	<b>76</b>

**Eng. K. L. S. Sahabandu**

**Session Chair**

**SLGS Annual Conference, 2024**



Eng. K.L.S. Sahabandu has over 40 years of experience in the engineering consultancy industry, having served several major organizations in Sri Lanka, most notably the Central Engineering Consultancy Bureau (CECB), the largest multidisciplinary engineering consultancy firm in the country. Throughout his career, he held various positions, with a primary focus on structural and geotechnical design for numerous nationally significant projects, spanning sectors such as hydro-power, high-rise buildings, highways and railways, harbours, and airports. He retired as the General Manager of CECB in 2019 and now serving as the Head, Engineering Consultancy Division of Urban Development Authority (UDA).

He was actively involved in Expressway and Railway construction in Sri Lanka in many capacities such as a Team Leader-Designs, Procurement / Technical Committee Member, Investigator etc. from the First ever Expressway Construction Project, i.e. Southern Expressway Project in Sri Lanka.

In terms of professional service, Eng. Sahabandu currently serves as the President of both the Sri Lankan Geotechnical Society (SLGS) and the Association of Consulting Engineers – Sri Lanka (ACESL). He is a former President of the Society of Structural Engineers, Sri Lanka (SSESL), and the Immediate Past Vice President of the Sri Lanka National Committee on Large Dams (SLNCOLD).

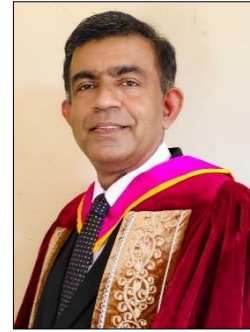
Eng. Sahabandu has been honoured with several prestigious awards, including the once-in-a-lifetime "Award of Eminence - 2016" from the Construction Industry Development Authority (CIDA) of Sri Lanka, the "Chartered Engineer Excellence Award - 2018," and the "Eng. (Dr.) A. C. Visvalingam Award for the Most Outstanding Engineer – 2023" from the Institution of Engineers, Sri Lanka (IESL), in recognition of his significant contributions to the advancement of the construction industry and the engineering profession in Sri Lanka.



**Prof. Udeni Nawagamuwa**

**Session Chair**

**SLGS Annual Conference, 2024**



Prof. Udeni Nawagamuwa is a professor in the Department of Civil Engineering at the University of Moratuwa, Sri Lanka, specializing in geotechnical engineering. He obtained his BSc (Eng) Hons in Civil Engineering from the University of Moratuwa in 1999, followed by an MEng in Geotechnical Engineering from the Asian Institute of Technology (AIT) in 2002. He further advanced his studies by earning a Doctor of Engineering degree from Yokohama National University in 2005.

With extensive experience in both academia and practical applications, Prof. Nawagamuwa has made significant contributions to various areas within geotechnical engineering, including earth-retaining structures, ground improvement techniques, and geo-environmental engineering. His research emphasizes sustainable engineering solutions, particularly the utilization of domestic and industrial waste materials in soil stabilization, slope stabilization, and infrastructure development.

Throughout his career, he has actively supervised numerous undergraduate and postgraduate students, with a research focus on nature-based landslide mitigation and sustainable ground improvement practices. Prof. Nawagamuwa is a member of several professional organizations, including the Institution of Engineers Sri Lanka (IESL), the International Society of Soil Mechanics and Geotechnical Engineering (ISSMGE), the Sri Lankan Geotechnical Society (SLGS), and the Sri Lanka Association for the Advancement of Science (SLAAS).

In addition to his academic contributions, he has served as a consultant on various infrastructure projects, applying his expertise to address real-world geotechnical challenges. His outstanding research performance has been recognized through multiple awards, including the Appreciation of Outstanding Research Performance in 2015 and 2016 and the Best Paper Award at ACEPS 2016.



Silver Sponsor:

*Changing landscapes...  
Changing lives*



The largest and most trusted construction company in Sri Lanka, Mäga Engineering specializes in multi-disciplinary projects in buildings, highways, bridges, water supply schemes and marine structures.



200, Nawala Road, Narahenpita, Colombo 05, Sri Lanka  
Tel: +94 11 2808835 - 2808844 | E-mail: [maga@maga.lk](mailto:maga@maga.lk) | Web: [www.maga.lk](http://www.maga.lk)





**RISK INVESTIGATION AND DAMAGE TREATMENT OF  
HIGH SLOPES ON EXPRESSWAYS**

**By**

**Mr. Shi Fulu,**

**Technical Officer, China Harbour Engineering Company (CHEC)**



Shi Fulu is a highly skilled expert in highway and bridge design, with a specialization in project management, highway design, structural design, and structural reinforcement. He has extensive experience in project implementation across more than ten countries, including Singapore, Malaysia, Sri Lanka, and Costa Rica.

His notable projects include the Sri Lanka Extension of the Southern Expressway Project (Section 4) and the Kong-Zhuhai-Macao Bridge Hong Kong Link Viaduct Project. Through these projects, he has developed strong technical expertise, particularly in high slope treatment and the design of special-shaped structures, enabling him to deliver optimal technical solutions for his clients.

In addition to his practical experience, Shi is passionate about technology research. He has completed four forward-looking technology studies in the highway sector, published three key papers, and secured four patent licenses. Some of his research findings have been recognized as internationally advanced.

Shi Fulu is committed to becoming an expert in international engineering technology and project management, and he is dedicated to working diligently to achieve this goal.





# Risk Management and Disaster Emergency Treatment of High Slopes in Expressways

October 2024


1



Report content

- 1 Highway High Slope Disaster
- 2 Risk Management
- 3 Risk Treatment of Meida Expressway
- 4 Emergency Disaster Treatment of Wenma Expressway
- 5 Conclusion and Recommendations


2




## 1. Highway High Slope Disaster

**Highway high slope** **Definition:** Soil slopes with a height greater than 20m or rock slopes with a height greater than 30m.

- Highway slope is a part of geological body transformed into artificial facilities. Its stability depends on the natural slope stability, geological conditions and the artificial transformation.
- The artificial transformation changes the stress state of natural slope and the seepage conditions of groundwater. The stress adjustment takes some time.
- Highway slopes are under the influence of various natural forces, such as sunlight, rainfall, weathering and earthquakes. But the change caused by artificial transformation effects more intensely.



3

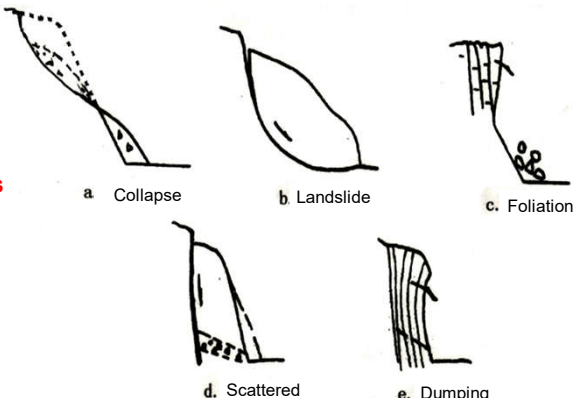


## 1. Highway High Slope Disaster

**Highway high slope** There are five failure types of high slope.

**Failure types**

- a. Collapse
- b. Landslide
- c. Foliation
- d. Scattered
- e. Dumping

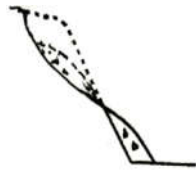


4

1. Highway High Slope Disaster

HEC 中国港湾 CHINA HARBOUR

Highway high slope Failure types



a. Collapse



Collapse occur ommonly in mountainous areas.


**Collapse** - If the slope is too steep, or if groundwater seeps to the slope toe after excavation, softening the rock and soil and reducing its strength, causing layer-by-layer collapse and deformation.

5


1. Highway High Slope Disaster

HEC 中国港湾 CHINA HARBOUR

Highway high slope Failure types



b. Landslide



The accident occurred below the airport runway in Panzhihua airport.  
The designer made a mistake in project site selection because there has been a landslide below occurred 30 years ago.


**Landslide** -The deformation of the slope is mainly horizontal sliding downward along the fixed sliding curve in the slope under the action of natural or human behaviors. The main differences between landslides and other slope deformations are the fixed sliding curve, overall sliding, and the rich groundwater.

6


1. Highway High Slope Disaster

HEC 中国港湾 CHINA HARBOUR

Highway high slope Failure types



c. Foliation



Rock foliation occurred at outlet of tunnel in Kaiji, Guizhou Province. The foliation rock blocked the outlet of tunnel.


**Rock Foliation** -The weathered and broken rock mass on the steep slope collapsed or slipped due to natural and human behaviors. The foliation rock completely destroying the original structure.

7


1. Highway High Slope Disaster

HEC 中国港湾 CHINA HARBOUR

Highway high slope Failure types



d. Scattered



Scattered occurred on the G346 highway in Shanxi Province. Reducing the weight of the upper part of the slope is the main measure to prevent scattered.

**Scattered** -For the relatively steep (35°~45°) slopes, the joint interface separates the outer weathered rock mass from the inner intact rock mass. After the river scouring or artificial excavation, the underlying soft layer cannot withstand the upper pressure and deforms, causing the upper rock mass to deform.

8

1. Highway High Slope Disaster

HEC 中国港湾 CHINA HARBOUR

Highway high slope

Failure types



e. Dump



Dumping - Steeply inclined thin rock layer bend and tilt in an unsupported direction due to river flushing or artificial excavation.

Dumping occurred on the jingzhu expressway in Guangdong Province. One motorcycle was buried.

9

1. Highway High Slope Disaster

HEC 中国港湾 CHINA HARBOUR

Consequences of Highway High Slope Diseases

Slope failure can lead to severe consequences. This was a serious slope failure accident that occurred in China 5 months ago.

During the holiday, most city residents drive to their hometowns by expressway. Unfortunately, a landslide occurred on the Meida Expressway, 18 meters long embankment collapsed. The cars driving on the highway cannot find the deep pit ahead because the pit is below the line of sight, they rushed into the pit one by one at a fast speed.



23 smashed vehicles were found in the pit  
48 deaths and 30 injuries was caused.  
A very serious and painful accident !

10

1. Highway High Slope Disaster

HEC 中国港湾 CHINA HARBOUR

Consequences of Highway High Slope Diseases

What exactly caused the accident?

Design defects, Construction quality, or Poor maintenance?  
Or it is a natural disaster caused by continuous heavy rain?

The government has started evidence collection and investigation work and will give an investigation conclusion.

But we can be sure that  
The highway operator failed to do a good job in Risk inspection and failed to take measures in advance to prevent the accident .

So it is necessary to manage the high slope Risk in advance.

11

2. Risk Management

HEC 中国港湾 CHINA HARBOUR


Risk management

Risk of highway high slope shall be managed as following procedure.

<b>Inspection</b>	➤	<b>Assessment</b>	➤	<b>Treatment</b>
Monitoring Weekly inspection Manual special inspection		Current status and future trends assessment Classification		Data collection Soil investigation Cause analysis Stability analysis & treatment selection Treatment construction

12




**2. Risk Management** 

**Risk inspection**

Risk inspection on high slopes is mainly carried out through monitoring, weekly inspection and special inspection.

Type	Content
Inspection content	1. Development of pavement cracks 2. Slope drainage, protection damage, and slope deformation 3. Surface water and groundwater condition
Inspection methods	1. Monitoring system 2. Drone inspections 3. Manual inspections
Inspection frequency	1. Weekly inspection: Once a week. During the raining season from April to July, the frequency should be increased. 2. Special inspections of key sections during special periods, such as before the rainy season, after an earthquake or in emergency situations.
Key sections	Sections with arc-shaped cracks, sections with filled areas on the opposite side or low-lying areas between mountains with M terrain on the opposite side, sections with steep slopes filled with muddy sandstone, and sections with soft rock.

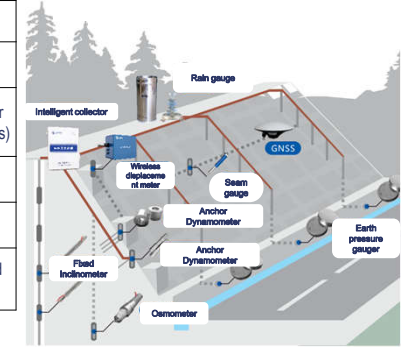
13

**2. Risk Management** 


**Risk inspection** **Monitoring system**

For high slopes and slopes with potential stability risks, a monitoring system needs to be installed.

No.	Type	Monitoring content	Monitoring methods
1	Slope monitoring	Surface displacement	GNSS
2		Deep displacement	Deep inclinometer (for complex slopes)
3	Protection structure monitoring	Anchor cable stress	Dynamometer
4		Anti-sliding piles, retaining walls	GNSS, Inclinometer
5	Slope and structure monitoring	Strain	OTDR(Distributed Fiber)




14


**2. Risk Management** 

**Risk inspection** **Manual inspection**

**Top of slope :** Water accumulation, Natural ditches and drainage ditches



**Road pavement :** Water accumulation ; focus on longitudinal cracks, whether the cracks are arc-shaped at both ends ; whether the cracks reopen after sealing; whether the cracks continue to extend ; Verify if the cracks are offset.



15

**2. Risk Management** 


**Risk inspection** **Manual inspection**





**Traffic safety facilities :**

- Deformations or sinking of the guardrail and concrete parapet,
- Column/Support detachment;
- Gap or deformation between embankment guardrail and bridge parapet.

16


2. Risk Management 

**Risk inspection** **Manual inspection**



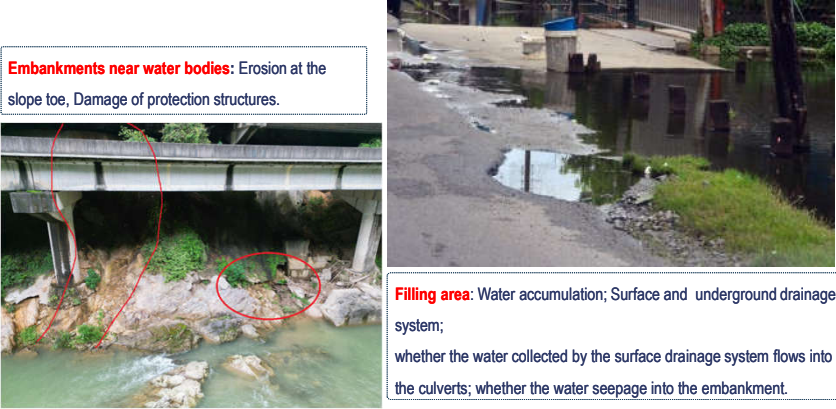
**Slope surface:** Water seepage from slope face ; Protection structures deformation; Slope toe deformation; Ditch wall deformation; Local failures on the slope; Drainage system, Berm cracks; Retaining wall deformation and cracks, Drainage holes.

17

2. Risk Management 

**Risk inspection** **Manual inspection**

**Embankments near water bodies:** Erosion at the slope toe, Damage of protection structures.





**Filling area:** Water accumulation; Surface and underground drainage system; whether the water collected by the surface drainage system flows into the culverts; whether the water seepage into the embankment.

18

2. Risk Management 


**Risk assessment**

Risk shall be classified based on site inspection data and monitoring data.




-  **Class A**  
Slopes with **serious seepage**, **Clear sign of deformation** of slope and a tendency to **continue to develop**, and the **retaining walls with severe deformation**.
-  **Class B**  
Slopes with **Clear signs of deformation but not yet develop**.
-  **Class C**  
Slopes **with Risks but currently less dangerous**.

**Other types of slopes:** The slope is in a stable state.

19


2. Risk Management 

**Risk treatment**

-  **Class A**  
Emergency treatment should be started immediately. **Horizontal drains** shall be installed on site and **emergency monitoring** shall be implemented . Toe loading or unloading at the top shall be carried out. **The soil investigation and design work shall be carried out immediately.**
-  **Class B**  
**Horizontal drains** shall be installed. Toe loading or unloading at the top and other slope stability enhancement treatment shall be carried out at the **appropriate time**.
-  **Class C**  
**Repair and clean the drainage** system.

**Other types of slopes:** No treatment required.

20

**2. Risk Management** 

**Risk treatment**

For the high slopes classified as Class A or Class B, treatment shall be taken to eliminate the Risks.

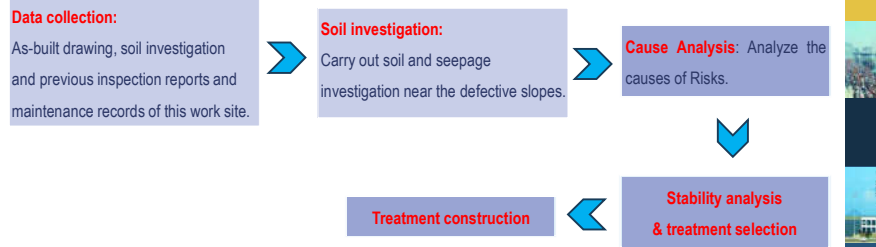
**Data collection:**  
As-built drawing, soil investigation and previous inspection reports and maintenance records of this work site.

**Soil investigation:**  
Carry out soil and seepage investigation near the defective slopes.


**Cause Analysis:** Analyze the causes of Risks.

**Stability analysis & treatment selection**

**Treatment construction**



21

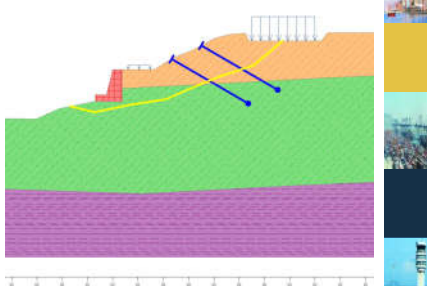
**2. Risk Management** 

**Risk treatment**


**Stability analysis & treatment selection**

Reasonably determine the factor of safety of the embankment slope, potential deformation range, and sliding curve, and determine the parameters of the rock and soil through calculation and verification.

**Calculation condition** where the embankment is under continuous heavy rain or continuous rainfall.



22

**2. Risk Management** 

**Risk treatment** **Stability analysis & treatment selection**

For excavation slopes completely in soil or strongly weathered or fully weathered rock layers, the potential failure mode is arc sliding failure, the **simplified Bishop method** should be used for stability calculation:

$$F_s = \frac{\sum [c_i b_i + (W_i + Q_i) \tan \varphi_i] / m_{\alpha i}}{\sum (W_i + Q_i) \sin \alpha_i}$$

Where :


- F<sub>s</sub> is the embankment stability factor;
- b<sub>i</sub> is the width of the i<sup>th</sup> soil strip ( m )
- α<sub>i</sub> is the inclination angle of the bottom Sliding curve of the i<sup>th</sup> soil strip ( ° )
- c<sub>i</sub>, φ<sub>i</sub> are the cohesion and internal friction angle of the soil or rock layer where the sliding arc of the i - th soil strip is located. According to the location of the sliding arc, the cohesion ( kPa ) and internal friction angle ( ° ) of the corresponding soil or rock layer are taken.
- m<sub>α</sub> is the coefficient, calculated according to the following formula:

$$m_{\alpha} = \cos \alpha_i + \frac{\sin \alpha_i \tan \varphi_i}{F_s}$$

W<sub>i</sub> is the gravity of the i<sup>th</sup> soil strip ( kN )

Q<sub>i</sub> is the vertical external force of the i<sup>th</sup> soil strip ( kN )

23

**2. Risk Management** 

**Risk treatment** **Stability analysis & treatment selection**

For rock slopes with sliding curve along the layer, the **plane sliding curve method** should be used for calculation

$$F_s = \frac{\tan \varphi \sum N + \sum P_i \cos \psi + cL}{\sum T - \sum P_i \sin \psi}$$

Where :

- F<sub>s</sub> — stability factor;
- φ — Internal friction angle of the rock mass on the Sliding curve ( ° );
- c — cohesion of rock mass on Sliding curve ( kPa );
- N — Component force of the sliding body on the normal line of the Sliding curve ( KN/m );
- P<sub>w</sub> — Working anchoring force ( KN/m );
- T — component force of sliding body on the tangent line of Sliding curve ( KN/m );
- ψ — Angle between the anchor axis and the normal of the Sliding curve;
- L — Length of Sliding curve ( m ).

The rock mass mechanical parameters are determined comprehensively based on geological survey data, regional experience and actual site conditions.

24



## 2. Risk Management

Risk treatment

Stability analysis & treatment selection

If the potential sliding curve of slope is a broken line, the unbalanced thrust method should be used for stability calculation :

$$E_i = W_{qi} \sin \alpha_i - \frac{1}{F_s} (c_i l_i + W_{qi} \cos \alpha_i \tan \phi_i) + E_{i-1} \psi_{i-1}$$

$$\psi_{i-1} = \cos(\alpha_{i-1} - \alpha_i) - \frac{\tan \phi_i}{F_s} \sin(\alpha_{i-1} - \alpha_i)$$

Where :

- W<sub>qi</sub> — the sum of the gravity and external vertical load of the i-th soil strip ( kN )
- α<sub>i</sub> — inclination angle of the bottom Sliding curve of the ith soil strip ( ° )
- c<sub>i</sub>, φ<sub>i</sub> — cohesion ( kPa ) and internal friction angle ( ° ) at the bottom of the ith soil strip
- l<sub>i</sub> — length of the bottom Sliding curve of the ith soil strip (m)
- α<sub>i-1</sub> — the inclination angle of the bottom Sliding curve of the i-1th soil strip ( ° )
- E<sub>i-1</sub> — The sliding force transmitted from the i-1th soil strip to the i- th soil strip ( kN )

25

## 2. Risk Management

Risk treatment

The measure should be selected according to the features and level of the Risks.

The measure mainly includes repairing the defects found during the inspection and strengthening the slope stability.

Usual repair measures mainly include:

**Top of slope :** Repair and clean ditches, set up circular intercepting ditch in the filled areas.

**Pavement surface :** Seal cracks to prevent rainwater infiltration into the embankment

**Embankments near water:** Set up toe wall to prevent toe erosion.

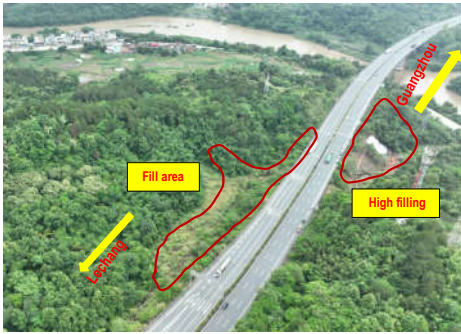
**Slope body:** Take measures to improve slope stability based on site damage and verification results. Including but not limited to: **toe loading** or unloading at the top, set up retaining walls, anti-sliding piles, and prestressed anchor cables, or reduce the slope angle

26

## 3. Risk Treatment of Meida Expressway

Project Introduction

A experience case how to manage the Risk of high slope.



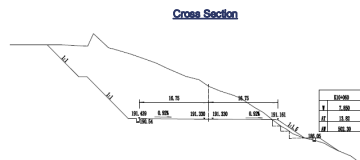
Meida Expressway is located in the mountainous area of northern Guangdong. The mountain ranges are mostly distributed in an east-west direction. There are many bridges, high-filling, and deep excavation slopes along the route.

The slope to be managed this time is located at chainage 10+040. There are mountains and filling areas on the left, and a high filling slope on the right.

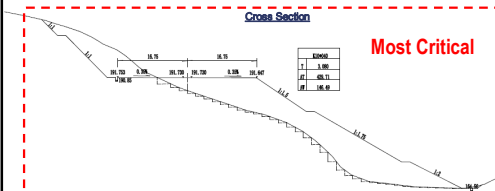
27

## 3. Risk Treatment of Meida Expressway

Project Introduction



Cross Section



Most Critical

The total height of the right filling slope is 13 to 26 meters.

The first-level slope: 8 meters high, slope ratio of 1:1.5, grass turfing was adopted;

The second-level slope: 12 meters high, slope ratio of 1:1.75, concrete frame was adopted.

The third-level slope: 6 meters high, slope ratio of 1:2. Rip-rap stone slope protection was adopted.

28

### 3. Risk Treatment of Meida Expressway

**Risk inspection**

**On-site inspection**

A landslide occurred on the first-level berm, with a length of about 15m and a thickness of 2 to 4m. Due to rainwater, the landslide formed a gully on the second-level slope, with a width of about 4m and a depth of 2m.

Water outflow

Collapse area

Slope seepage

Slope collapse

29

### 3. Risk Treatment of Meida Expressway

**Risk inspection**

There is no circular intercepting ditch in the opposite side filling area, and there are natural pits outside that have not been filled, and holes can be seen on the surface. The surface water in the area cannot be discharged properly, leading to serious seepage. Longitudinal cracks appeared in the third lane of this section.

Waterlogged areas

Fill area

Pavement crack

30

### 3. Risk Treatment of Meida Expressway

**Risk assessment**

According to the on-site inspection data, this slope has serious seepage, deformation of slope and a tendency to continue to develop. It is **classified as Class A**.

**Emergency treatment should be started immediately.**

31

### 3. Risk Treatment of Meida Expressway

**Risk treatment**

Emergency monitoring and toe loading was carried out immediately.  
The data collection, soil investigation, survey and design work shall be carried out immediately.

**Data collection:**  
As-built drawing, previous inspection and soil investigation reports and maintenance records.


**Soil investigation:**  
Combined with the geological data in the original design phase, 3 new geological boreholes were arranged.

32

### 3. Risk Treatment of Meida Expressway

**Risk treatment**

**Cause analysis**



The left side of the road is a filling area where surface water seeps into the embankment.

The drainage system is insufficient to handle rainwater runoff from the pavement surface during rainstorms, leading to severe erosion of the earth shoulders and slopes, and accelerating the infiltration of rainwater into the embankment.

The high-fill embankment is composed of muddy siltstone and soil. Prolonged heavy rainfall and rainwater infiltration have reduced the embankment's bearing capacity.



After years operation, the differential settlement of the embankment has increased, partial landslides have occurred.

33

### 3. Risk Treatment of Meida Expressway

**Risk treatment**

**Stability analysis & treatment selection**

**Stability analysis method**

The simplified Bishop method is used to analyze the stability of the embankment body and the overall stability of the section.

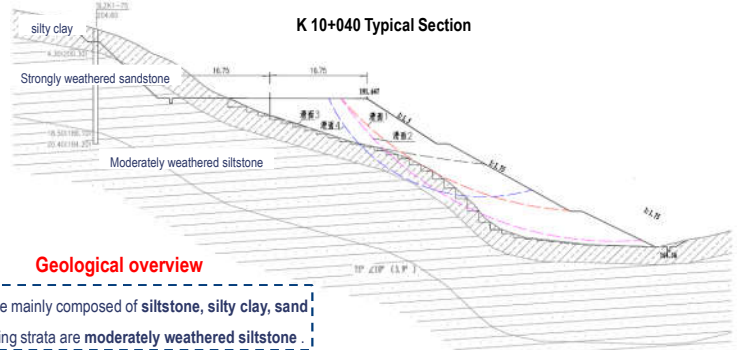
34

### 3. Risk Treatment of Meida Expressway

**Risk treatment**

**Stability analysis & treatment selection**

According to the site inspection, taking the last longitudinal crack on the pavement surface as the rear edge of the potential sliding curve, the sliding curve of the section are shown in the figure below.



**Geological overview**

The strata are mainly composed of siltstone, silty clay, sand

The underlying strata are moderately weathered siltstone.

35

### 3. Risk Treatment of Meida Expressway

**Risk treatment**

**Stability analysis & treatment selection**

According to the site inspection, the slope is in a basically stable state, FoS of the slope is 1.05. The soil parameters were back-calculated based on the sliding curve and the safety factor.

The shear strength are influenced by factors such as the roughness of the interface, water content and the composition of the sliding interface material. The long-term water seepage changes the strength of the soil and reduces the effective normal stress and friction resistance. The soil parameters are different from the test data from laboratory test and shall be back-calculated.

Geotechnical category	Calculation parameters	Inverse Parameters		Stability factor $F_s$			
	Saturated density (kN/m <sup>3</sup> )	Cohesion $c$ (kPa)	Internal friction angle $\phi$ (°)	Sliding curve 1	Sliding curve 2	Sliding curve 3	Sliding curve 4
Embankment: Filling soil	20	5	27	1.25	1.05	1.54	1.05
Foundation soil: Silty clay	18.5	14	13				
Foundation soil: Strongly weathered siltstone	20	18	30				

36



### 3. Risk Treatment of Meida Expressway

**Risk treatment**      **Stability analysis & treatment selection**

Refer to local experience, anchor cable frame for the first-level slope and backfilling with stone (block) for the third-level slope are proposed. The verification results can meet the requirements of the specification.

The most critical section	Sliding curve	Analyze content	Calculation method	Stability coefficient before treatment	Residual sliding force (horizontal /kN) Ks=1.25	Main treatment measures	Stability coefficient after treatment
K 10 + 0 40	Sliding curve 1	Embankment stability	Simplified Bishop method	1.25	/	Prestressed anchor cable frame is set up on the first-level slope, and the third-level slope are backfilled with stone (block).	/
	Sliding curve 2	Overall stability of embankment + foundation	Simplified Bishop method	1.05	238.7		1.38
	Sliding curve 3	Stability along the slope	Unbalanced thrust method	1.54	/		/
	Sliding curve 4	Overall stability of embankment + foundation	Simplified Bishop method	1.05	249.7		1.26

37

### 3. Risk Treatment of Meida Expressway

**Risk treatment**      **Final treatment**

- (1) Install circular intercepting ditches around the filling area and level the site to prevent seepage.; set up horizontal drainage pipes in the slope seepage area and restore the drainage system;
- (2) Anchors with grid frames are set up on the first-level slope, the third-level slope are backfilled with stone blocks to counter earth pressure;
- (3) For the collaps in second-level slope, the collapsed body is cleared and backfilled with stone and sealed with concrete;

38

### 4. Emergency Disaster Treatment of Wenma Expressway

**Disaster treatment**

In some cases, highway operators fail to detect the high slope Risks in advance, causing Risk to develop into disaster. Then the highway operators need to take immediate action.

**Close traffic** and stop construction, Publish accident notices in public media and provide vehicle detour suggestions.

➔

**Take emergency measures** such as counter-pressure at the toe or unloading at the top, to control the further development of slope deformation.

➔

**Take permanently meatures** to enhance the slope, such as retaining walls, anti-sliding piles, and prestressed anchor cables, or reducing the slope angle.

39

### 4. Emergency Disaster Treatment of Wenma Expressway

**Project introduction**

This case provides insight into managing disasters on high slopes. Mistakes were made during the treatment process, offering both valuable experiences and important lessons.

The Wenma Expressway, located in the southeastern mountainous region of Yunnan Province, spans 87 kilometers. The excavation slope is situated at chainage 39+400 on a natural slope, with a height difference of 70 meters between the natural slope and the pavement surface.

40

### 4. Emergency Disaster Treatment of Wenma Expressway

**Project introduction**

The maximum excavation height is about 32m, the slope is divided into four levels along the height direction. Concrete grid beam slope protection was adopted in the original design.

During the excavation construction, the landslides occurred several times.

Strongly weathered shale  
Moderately weathered shale  
Angular silty clay

41

### 4. Emergency Disaster Treatment of Wenma Expressway

**Disaster development**

Cracks appeared in April 2018

- The excavation of the third-level slope has been completed, and excavation of the second-level and first-level slopes is being carried out.
- After continuous heavy rainfall, cracks appeared on the slope for the first time.

The construction team stopped construction immediately and contacted the client and the design institute to start solving the problem.

42

### 4. Emergency Disaster Treatment of Wenma Expressway

**Disaster development**

The designers visit the construction site to investigate, conduct soil investigation, and compare treatment proposal. After verification, Designer proposed treatment: **Anchor cable + 36 anti-sliding pile**

The treatment construction was completed in December 2020

43

### 4. Emergency Disaster Treatment of Wenma Expressway

**Disaster development**

In December 2020, the anti-sliding piles were displaced.

After the anti-sliding pile construction, during the excavation of the first-level slope, the monitoring data showed that the displacement of the No. 14 pile reaching 28mm/d.

In August 2021. Affected by continuous heavy rainfall, the displacement of anti-sliding piles top was up to 40mm in one month.

In October 2021, The construction team backfill soil on the first-level slope and carry out the pile body integrity of the existing anti-sliding piles, 7 piles was classified as Class III and invalid.

The displacement of slope anti-sliding piles

44

### 4. Emergency Disaster Treatment of Wenma Expressway

**Disaster treatment**

Because the incorrect measures were taken at the beginning, a small issue developed to a big problem. New measures have to be implemented and must be fully-justified to ensure they permanently resolve the problem.

The flowchart shows a cyclical process: Inspection leads to Soil investigation, which leads to Cause analysis. Cause analysis leads to Treatment selection, which leads to Stability analysis, which leads to Construction. Construction then feeds back into Inspection.

45

### 4. Emergency Disaster Treatment of Wenma Expressway

**Inspection**

**Surface water**

A big erosion channel was found on the slope surface. The source of the gully is located within the slope, and there are two water outlets (springs) in the gully. The gully was formed by spring erosion.

Water outflow from slope surface

**Ground water**

The groundwater is rich, groundwater level is 8m. The main source of groundwater is the accumulated water in the karst depression at the rear of the area. Some of the water enters the slope area along the rock structural fissures.

Water outflow from retaining wall

Water seepage from baffle

46

### 4. Emergency Disaster Treatment of Wenma Expressway

**Soil investigation**

**Geological conditions**

- Rock layer is bent and fractured
- The upper rock layer is flat
- The lower rock layer is almost vertical

> The upper layer is composed of gravel silty clay and gravel residual soil, with a thickness of 7~ 14m. The lower layer is shale and its weathering layer. But the most important thing to note is **the weak layer (infill) between strongly weathered shale and moderately weathered shale.**

> According to the geological profile derived from multiple boreholes, the rock layer exhibits a steep inclination angle. The upper rock mass has experienced bending and fracture deformation along the weak infill due to self-weight.

> The rock inclination varies greatly, with the upper part being relatively flat and the lower being relatively steep (almost vertical).

47

### 4. Emergency Disaster Treatment of Wenma Expressway

**Cause analysis**

**Reflection on the first treatment**

Insufficient geological surveys were conducted to get clear the rock and groundwater conditions.

Failed to control the water immediately:

- (1) Failure to isolate surface water and groundwater;
- (2) Surface rainwater seeps into the slope, the groundwater level rises, and the water softens the weathered rock and soft interlayer;
- (3) The sliding interfaces in different sections are connected, the local landslide develops into a deep overall sliding.

The anti-sliding piles only constrain the slope toe, but cannot constrain the huge rock mass with large changes.

48



### 4. Emergency Disaster Treatment of Wenma Expressway

**Stability analysis & treatment selection**

The unbalanced thrust method is used to analyze the stability of the embankment sliding along the slope foundation or weak layer.

The ground level and sliding curve are simplified into broken lines. According to the geological profile and the slope deformation, a sliding calculation model is established.

49

### 4. Emergency Disaster Treatment of Wenma Expressway

**Stability analysis & treatment selection**

In the back-calculation, it is considered that the fourth-level slope is in the limit stability during the excavation process under the heavy raining condition.  $F_s=1.05$ .

Under the heavy raining condition, the slope is in the limit stability. Therefore, this state can be used to back-calculate the  $C$  and  $\phi$  values.

Parameter Value	Saturated density (kN/m <sup>3</sup> )	Saturated density	Calculation parameters under heavy rain conditions	
			Cohesion $c$ (kPa)	Internal friction angle $\phi$ (°)
Test value	19.7	20.7	21.0	15.0
Inverse calculated value	Angular silty clay		18.7	19.1
Selected value	19.7	20.7	18.7	19.1

50

### 4. Emergency Disaster Treatment of Wenma Expressway

**Stability analysis & treatment selection**

**Verification conditions:** The safety factor is 1.15, considering the dynamic water pressure and buoyancy, the soil porosity is 0.1, the buoyancy of the confined water is not considered.

**Anti-slide piles are proposed to enhance slope stability.**

Loading case	Residual sliding force(kN/m)	
	Existing anti-sliding pile	New anti-sliding pile
Loading case 1	7091	7797
Loading case 2	1896	2728

51

### 4. Emergency Disaster Treatment of Wenma Expressway

**Stability analysis & treatment selection**      **Final treatment**

- 38 new anti-sliding piles. Pile top connects the existing piles;
- Deep drainage of water collection wells;

52

### 4. Emergency Disaster Treatment of Wenma Expressway

**HEC 中国港湾 CHINA HARBOUR**

**Stability analysis & treatment selection      Final treatment**

- Deep drainage pipes are set up on the retaining wall, anti-sliding pile baffles and upper slope surface;
- Seepage ditches are set up in the gully;
- Intercepting drainage tunnel are set up in the slope body.

Drainage tunnel profile      Drainage tunnel cross section

53

### 4. Emergency Disaster Treatment of Wenma Expressway

**HEC 中国港湾 CHINA HARBOUR**

**Stability analysis & treatment selection      Operation effect**

**Current progress**

- The seepage ditch and the water collection well has been completed;
- The construction of new anti-sliding piles has been completed;
- The drainage tunnel has been completed for 170m.

**Current monitoring result**

- The displacement of the retaining wall and the anti-sliding pile has slowed down and the convergence trend is obvious;
- The surface displacement slowed down significantly.

**The second treatment solved the slope stability problem and achieved the expected results**

54

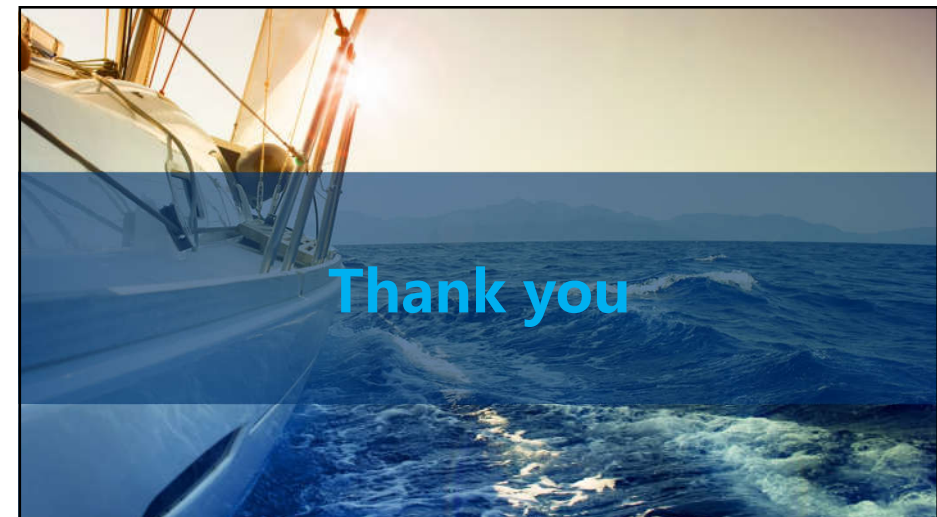
### 5. Conclusion and Recommendations

**HEC 中国港湾 CHINA HARBOUR**

**Conclusion and Recommendations**

- It is significant to manage the high slope Risk in advance for the highways in operation especially before the rainy season.
- Road routes** should avoid areas with poor geological conditions, and route need to be shifted if the high slope is located in poor geological area.;
- Water interception** and isolation measure shall be taken as early as possible;
- When **groundwater** is rich, measures should be taken to drain the groundwater and lower the groundwater level;
- Carry out **monitoring work**, and when the data is abnormal, find out the cause and eliminate the Risk in time.

55



56



Silver Sponsor:



**Pile Testing Service**

**Non-Destructive  
Testing Service**

**Geotechnical/  
Environmental  
Monitoring**

**Soil Investigation  
Services**

**Civil Engineering  
Structures &  
Material Testing  
Services**

**PILETEST CONSULTANTS  
(PVT) LTD**

Tele. 0 112080088  
0112157844, Hot Line/  
WhatsApp 0703600600

Email: [piletestcon@gmail.com](mailto:piletestcon@gmail.com)

Web: [www.piletest.lk](http://www.piletest.lk)



**SLOPE STABILIZATION TECHNIQUES AND EARTH  
RETAINING SYSTEMS IN EXPRESSWAYS**

**By**

**Emeritus Prof. Athula Kulathilaka, Department of Civil  
Engineering, University of Moratuwa**



Prof. Athula Kulathilaka obtained BSc Eng (Hons) in Civil Engineering from the University of Moratuwa in 1981 and PhD from Monash University in 1990. He retired from the University of Moratuwa in September 2023.

He has conducted lectures, and research and provided expert advice in the areas of Earth Retaining Structures, Ground Improvement Techniques, unsaturated soil mechanics, Rain induced Slope Failure, and Stabilization of Slopes. He has supervised many undergraduate projects in these areas and more than 30 master's projects. He has published around 100 referred papers in conferences and Journals.


He has provided guidance to RDA in the field of geotechnical engineering in the construction of expressways in the country in the areas of Soft Ground Improvement and Stabilization of Cut Slopes. As a consultant to NBRO he has provided expert guidance to NBRO in many Landslide Rectification projects throughout the country and guided many young Engineers.

He has contributed immensely to advancing the field of Geotechnical Engineering in Sri Lanka through numerous activities conducted by the Sri Lankan Geotechnical Society. He was the Honorary Secretary from 1994-2004, Vice President from 2005-2011, and President from 2011 to 2021.

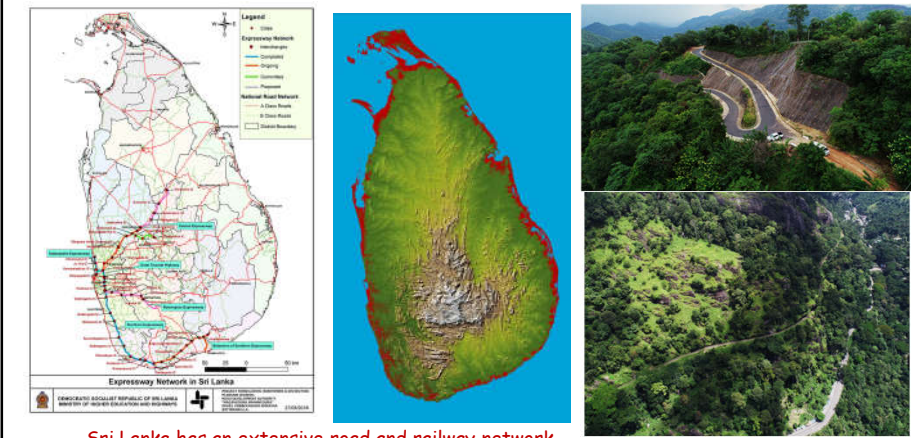


# Slope Stabilization Techniques and Earth Retaining Systems in Sri Lankan Expressways


Prof Athula Kulathilaka



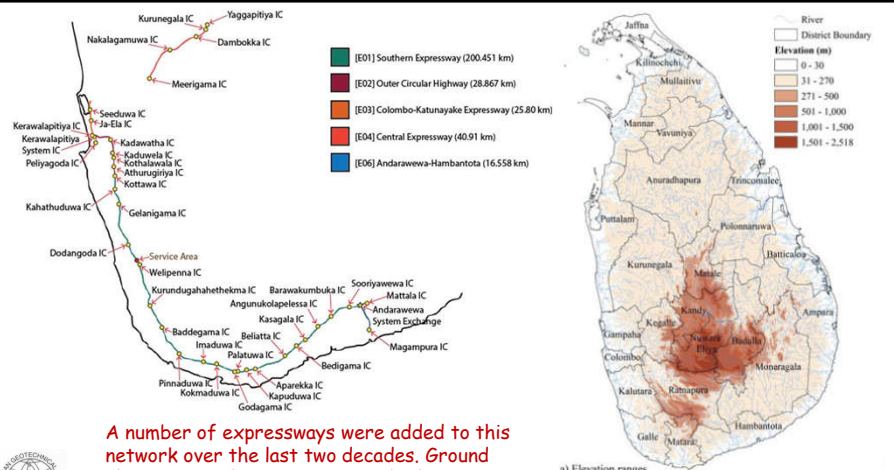
1



Sri Lanka has an extensive road and railway network covering the whole country through a very picturesque landscape.



2




a) Elevation ranges

3

A number of expressways were added to this network over the last two decades. Ground elevations in the 0-270m range had been encountered in these projects.

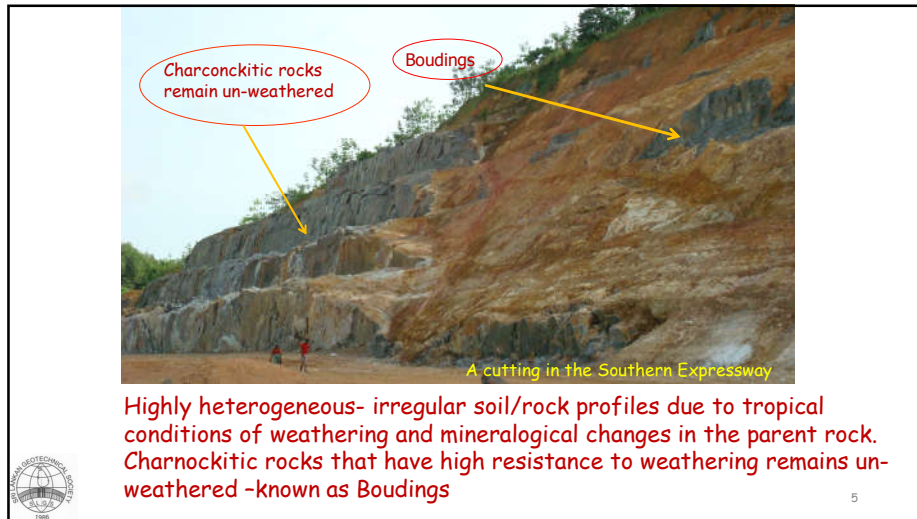
## Geological Background

- Sloping grounds and flood plains of low-ground elevations were encountered in constructing these expressways.
- Sloping grounds encountered are formed of; rocks of different levels of weathering, residual soils and colluvial soils. Rocks present are mainly Metamorphic. Principal rock types are Gneisses, Charnockites, Marble and Quartzite.
- Thick layers of soft clays and soft peaty clays were encountered in flood plains.
- It was necessary to make deep excavations in sloping grounds and construct high embankments over flood plains.



4

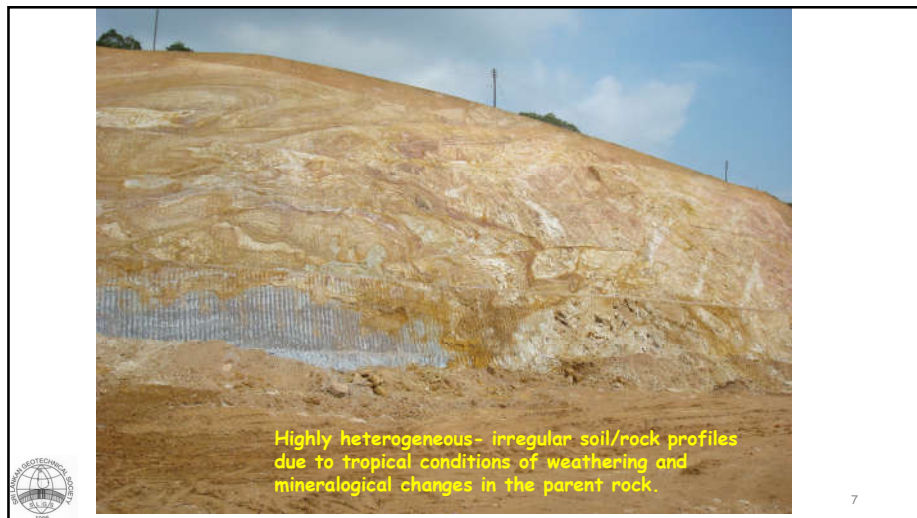




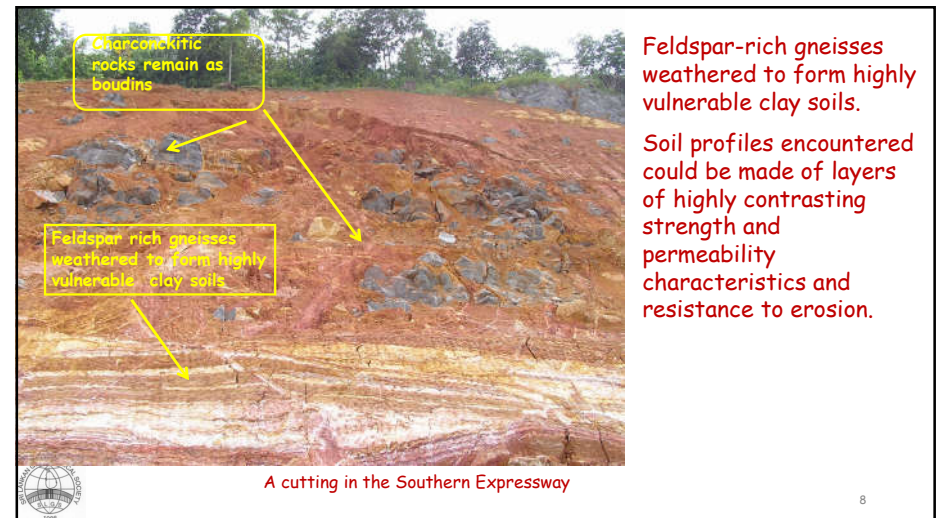
5



6



7



8

### Slope Instability Triggered by Rainfall

- Many of these slopes are with a low water table during periods of dry weather. Prevailing high matric suctions make them stable.
- Infiltration of rainwater, loss of matric suctions and perhaps the development of a perched water table condition will cause a reduction in shear strength  $\tau_f$  making the slopes unstable.
- In the background of layers of contrasting strength and permeability characteristics, failures could in the colluvial layer or in boundary of; the colluvial and residual layer or residual layer and rock (weathered).
- Relict joints in the sloping grounds facilitate infiltration. Adversely oriented relict joints make the slopes further unstable.



9

- Rocks could have banded structures with one or more joint planes. Joint planes will remain as relict joints in the residual soils. Relict joints remain as weak zones in the sloping ground. Sliding and toppling failure modes will occur when relict joints are adversely oriented.



10

Extremely soft ground conditions encountered were overcome with different ground improvement techniques



11



12



- When the embankments of expressways were constructed over flood plains and low-lying ground to achieve grade separation, appropriate ground improvement techniques were used.
- When there were space limitations different forms of Earth Retaining Structures were used.

**Different types presented here are;**


**Externally Stabilized Category**

- Mass Concrete walls
- Gabion Walls

**Internally Stabilized Category**

- Reinforced Earth
- Anchored Earth
- Soil nailing

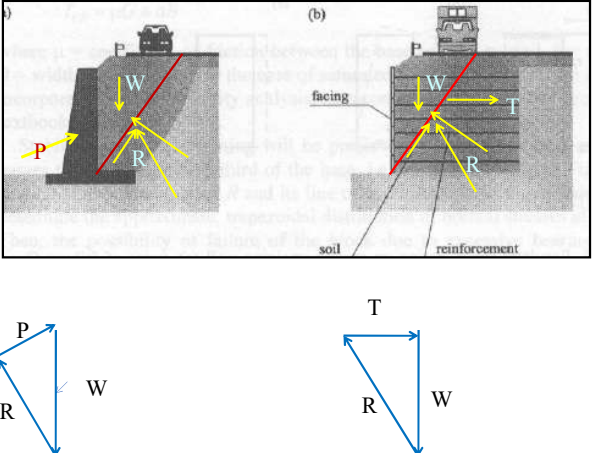

- Surface and sub surface drainage measures coupled with different types of earth retaining systems were used to enhance the stability of cut slopes or rectify the failed cut slopes.



13

13

**Comparison of the two systems**

14

14

**The embankment constructed to provide the grade separation at the Fly over Bridge was supported by a gabion wall - Southern Expressway**




- Can be constructed rapidly
- Usable immediately
- Free draining structure
- Geotextile filter
- Packed at the site using locally found rock
- A larger cross section is required due to the lower density of the wall.



15

15

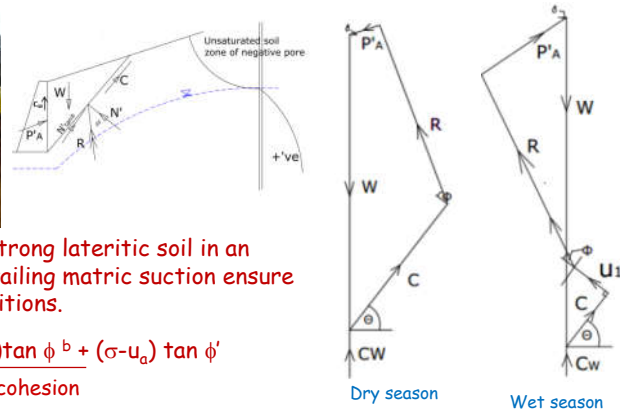




16

16

**Construction of A Mass Concrete wall to support a cutting in the CKE - Approach to the underpass at A3**



The soil in the cut is a strong lateritic soil in an unsaturated state. Prevailing matric suction ensure stability under dry conditions.

$$\tau_f = \frac{c' + (u_a - u_w) \tan \phi^b + (\sigma - u_a) \tan \phi^i}{\text{Apparent cohesion}}$$

A wall is required to ensure stability in the wet season



17



Shuttering is fabricated after cutting to the necessary profile

Construction of the wall is done in segments during a spell of dry weather



18

**Underpass at A3 - Bridge (two spans) supported on piles. Done in two halves.**



Ground was excavated vertically to find space for CKE. Vertical excavation was supported by soil nailing



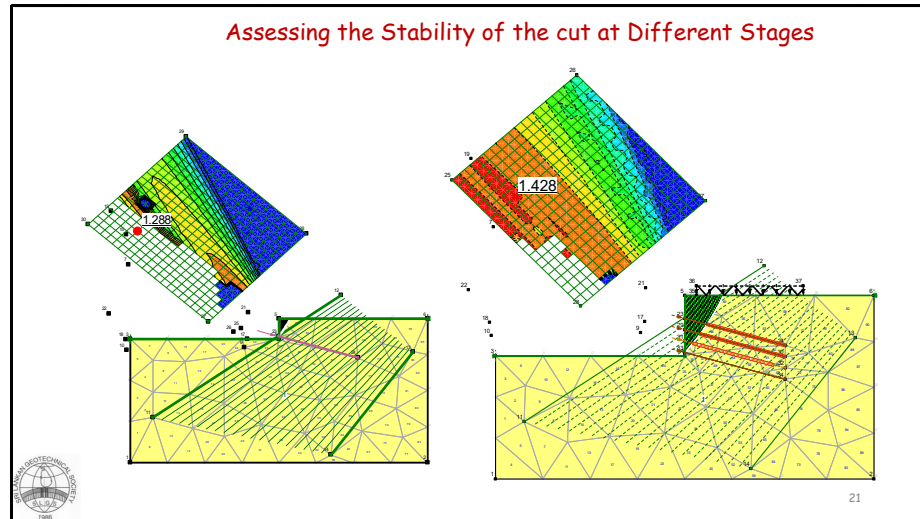
19

19

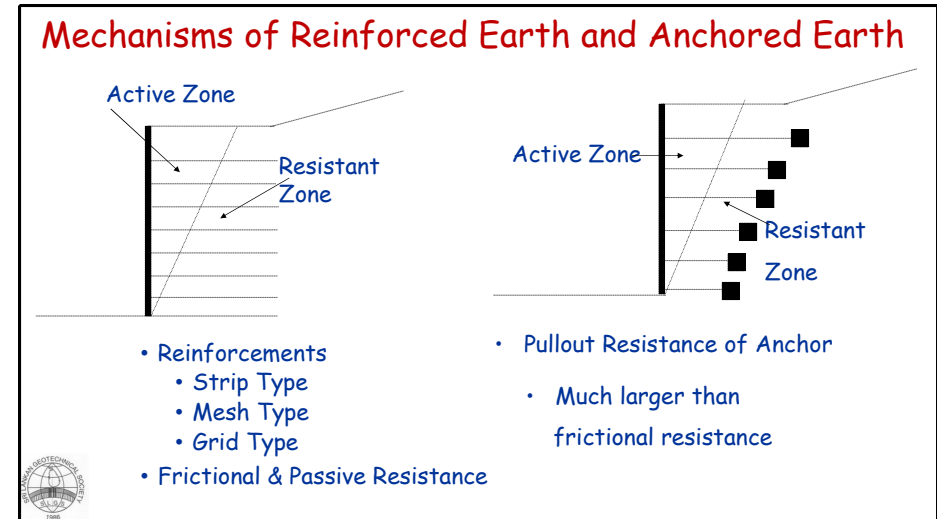


20

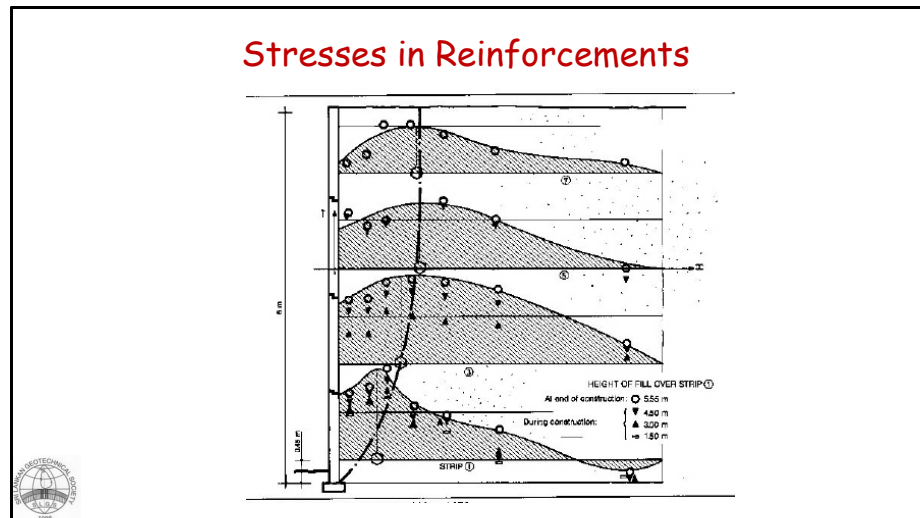
20



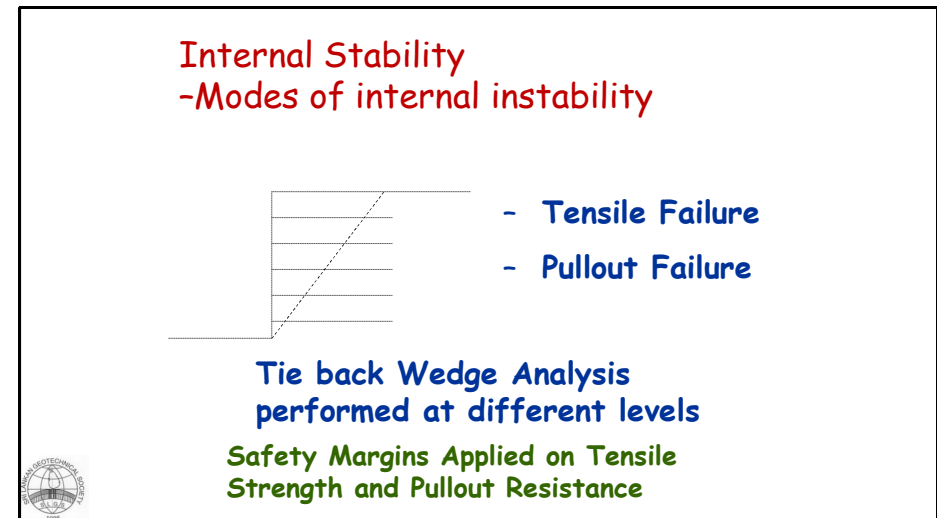
21



22



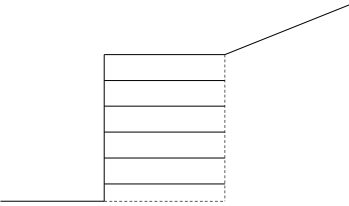
23



24




### External Stability - As a gravity Structure



Stability on

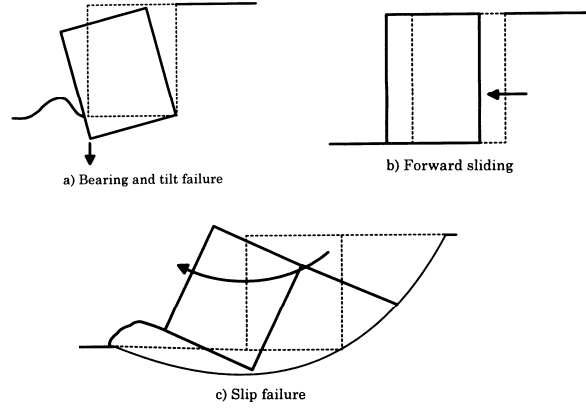
- Overturning
- Sliding
- Bearing Capacity

Provide sufficient Safety Margins against all these modes



25


### External Instability Mechanisms



a) Bearing and tilt failure

b) Forward sliding

c) Slip failure



26

### Internal Stability Consideration - Reinforced Earth and Anchored Earth - Tieback Analysis Performed at different levels

Try different trial wedges to obtain the most critical one

Consider modes of internal instability

- Tensile Failure
- Pullout Failure

Safety Margins Applied on Tensile strength and pullout resistance

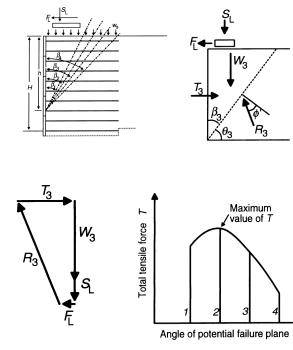
Find  $\Sigma T_{\text{Pullout}}$  and  $\Sigma T_{\text{Tensile}}$

Lower of Above


FOS on Internal Stability =  $\frac{\text{Lower of Above}}{T_{\text{Eqm}}}$

$T_{\text{Tensile}}$  - Based on the tensile capacity of the reinforcing element

$T_{\text{Pullout}}$  - Based on the interaction between the reinforcing element and the surrounding soil.




Find the  $T_{\text{Eqm}}$  for the Critical Wedge



27


### Strip - Friction on planer surface



Tensile capacity =  $\sigma_{\text{all}} \times b \times t$   
 $t$  - design thickness  $t = e_o - 2vN$

Pullout capacity =  $2 \sigma_v \mu \times b \times L_e$

### Grid- Mesh - When there are transverse members



There are formulae to account for transverse members. Generally simplified by a coefficient  $f_b$

Pullout capacity =  $2 \sigma_v \times f_b \tan \phi \times L_e$

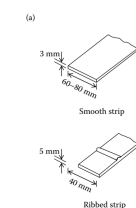
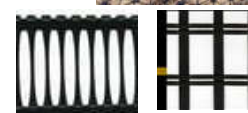




Figure 11.2 Mechanisms of soil-reinforcement bond. (a) Friction on planar surfaces. (b) Bearing on transverse members.



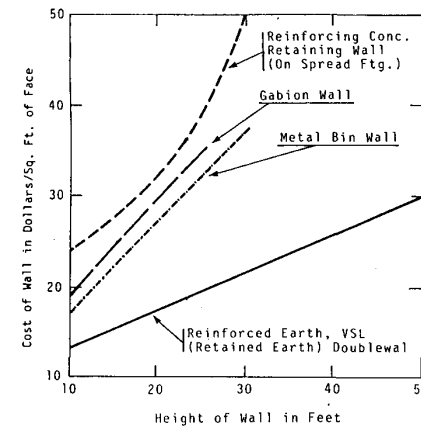
28

## Advantages

- Lower Cost
  - Flexible, can tolerate large deformations
  - Rapid Construction
  - No need of special equipment
  - Immediately usable
- But it required sufficient width
- Use of local material may offer further advantages



29



Cost Comparisons for Six Wall Types -California Department of Transport (1981)



30

Reinforced Earth Retaining wall to provide approach to Viaduct at Hunupitiya -CKE



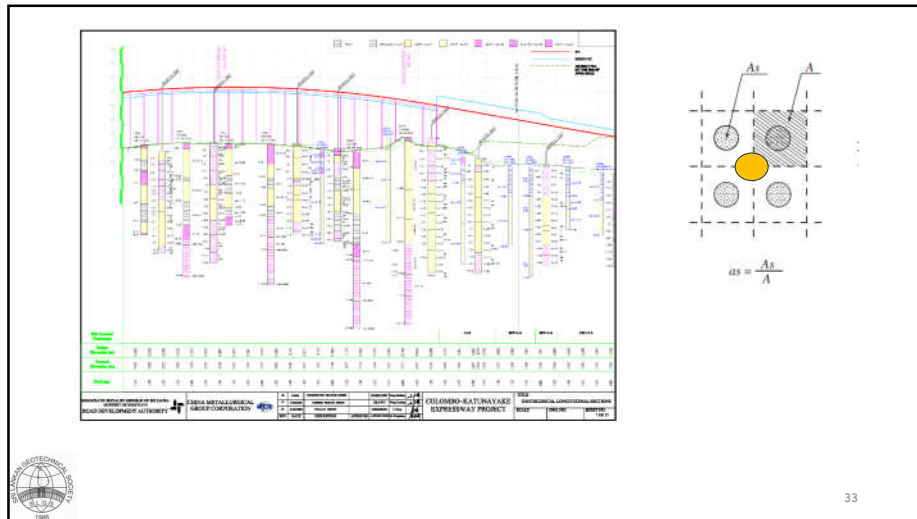
31



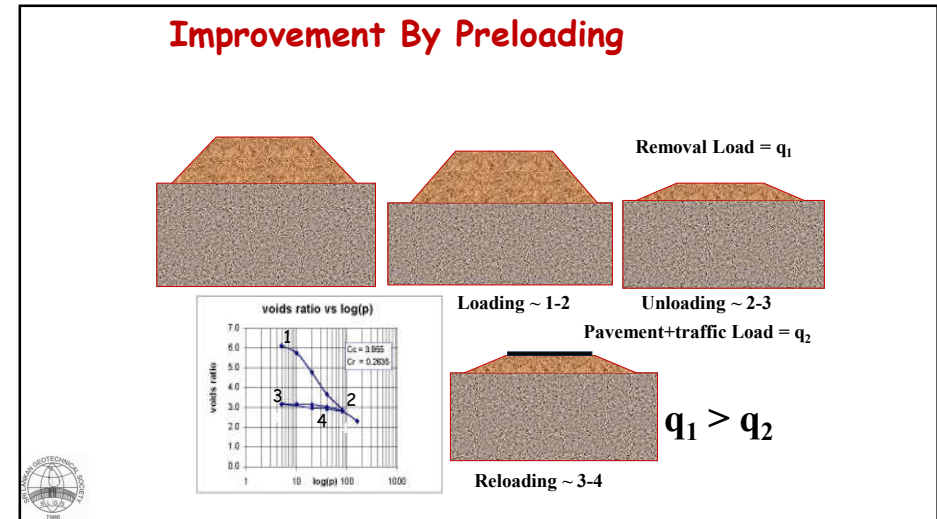
Facing blocks and Geogrid Reinforcements Placed



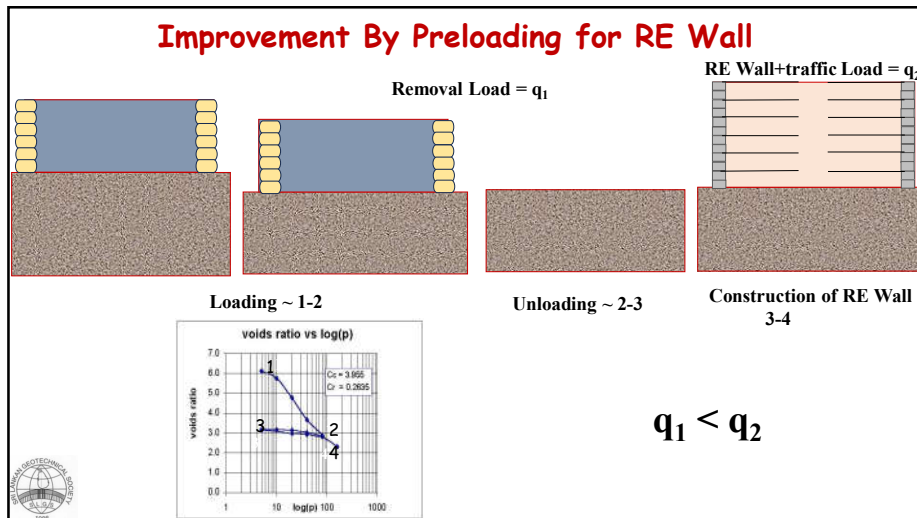
32



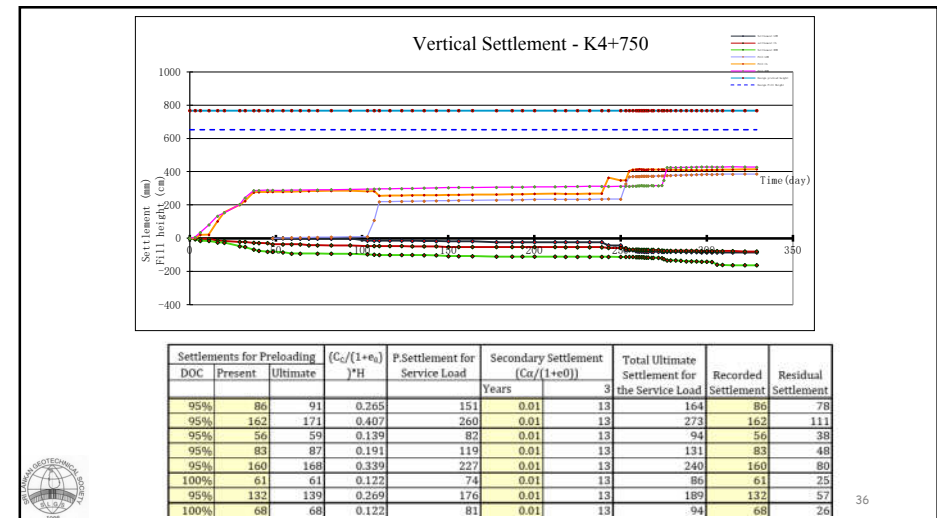
33



34



35

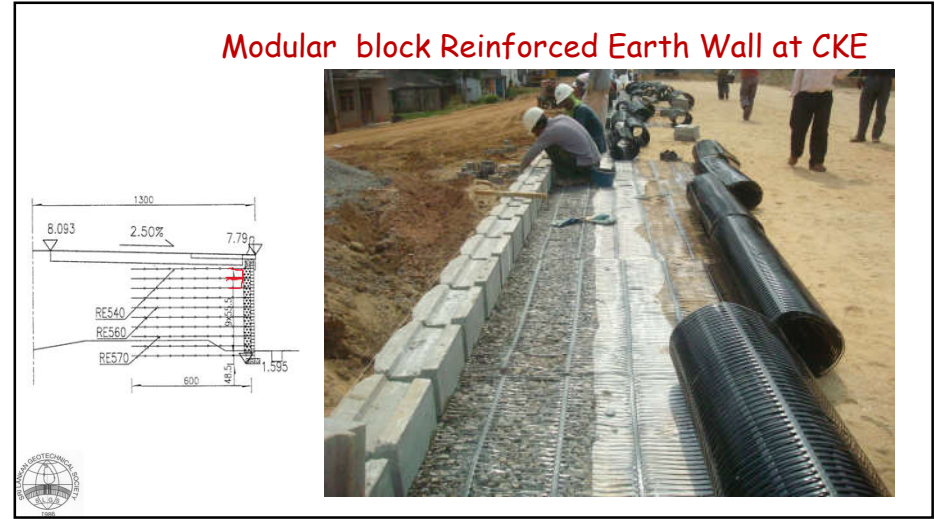


36





37



38



39



40





Two RERW Perpendicular to each other -approach to fly over bridge at Thelangapatha Road - 2+485 CKE

41



Geogrid Reinforcement layers for two RERW are placed at different levels

42



A view of the Facing

43

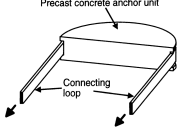
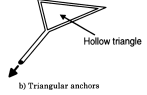
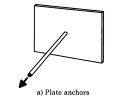
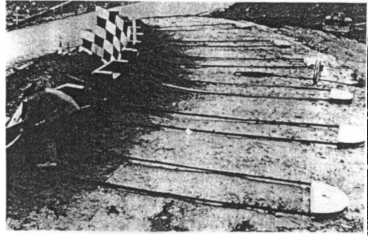



Failed Reinforced Earth Wall in Australia - Poor Drainage Details

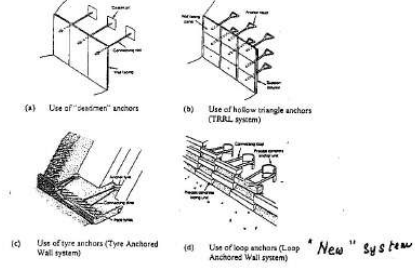
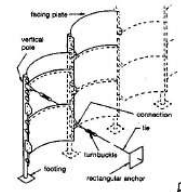
44

## Different forms of Anchored Earth Retaining systems

- Loop Anchored System - Austria
- Bent Triangular System - TRRL-UK
- Multi Anchored System - Japan

45

Fu Kuoka  
Multi Anchor System

46

### Triangular Anchors (TRRL)

- Two possible failure modes are considered

#### Flow around failure

$$P = \sigma_b \times A_b$$

$$A_b = 2 \omega t$$

$$\sigma_b b = 4 K_p \sigma_v'$$

$$P = (4 K_p \sigma_v') (2 \omega t) = 8 \omega t K_p$$

#### Retained wedge Failure

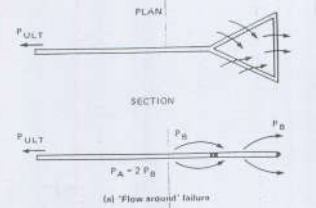
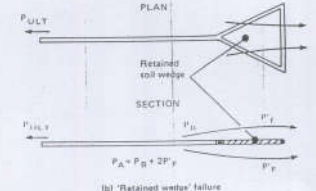
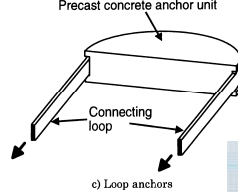
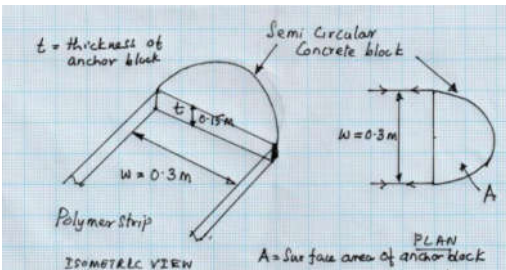
$$P = \sigma_b \omega t + \sigma_v \tan \phi \times 2 A_{TR}$$



Fig. 2 Pull out mechanisms for a triangular anchor

47

### Loop Anchored Wall - Austria

$$P = 3 K_p \sigma_v' \omega t + 2 \times 0.8 \times \sigma_v \tan \phi \times A$$

Frictional resistance along the synthetic strip is usually ignored

48



**Basic Repetitive Unit** **Anchored Tyre Structures**

**Pullout resistance of an anchor tyre**

$T_p = \text{Passive Resistance in front} + \text{Frictional resistance on top and bottom}$

$$= 3 K_p \sigma_v' T D + 2 \times A (\sigma_v' \tan \phi')$$

Number of horizontal layers  
Length of the anchor

Co-impregnation

$$= \sigma_v' \tan \phi' + c'$$

in a cohesive soil

$$T_p = 3 K_p \sigma_v' \times T \times D + 2 A (\sigma_v' \tan \phi' + c)$$

Frictional resistance along the connecting nylon wire is usually ignored

49

**Anchored Earth Structures for Bridge Abutments in Southern Expressway**

50

**Hexagonal Facing Unit**

**Connecting Detail**

**Anchor Blocks for two mutually perpendicular walls**

51

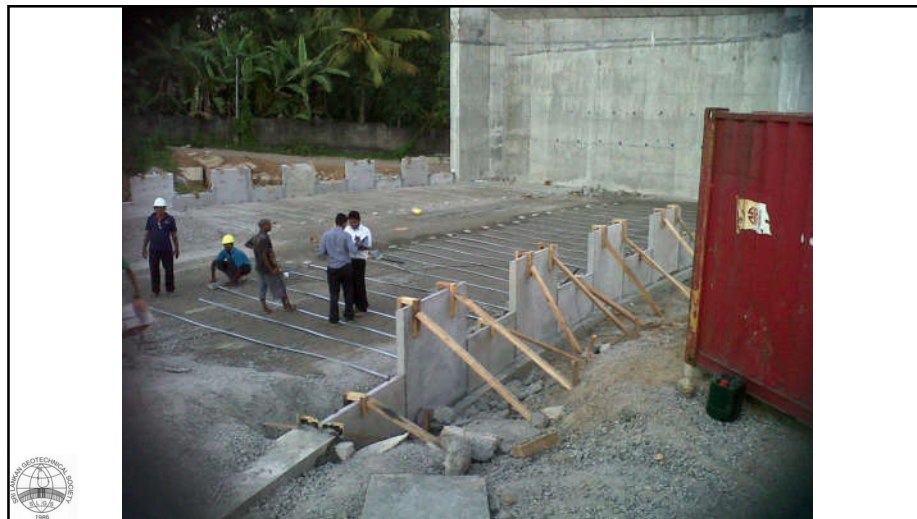
52



53



54



55



56





57



58



59

**Ensuring the Stability of cut slopes and Stabilization of Slopes in Expressways**

- With the infiltration of water due to rainfall, matric suction will be reduced or completely lost.
- Positive pore water pressures (perched water table condition) may also develop
- The presence of layers of different degrees of weathering (permeability) will affect the changes in the pore water pressure regime.
- The shear strength  $\tau_f$  will decrease

$$\tau_f = c' + (u_a - u_w) \tan \phi^b + (\sigma - u_a) \tan \phi'$$

and the Factor of safety  $\tau_f / \tau_m$  will reduce. When it approaches unity slope failures will occur

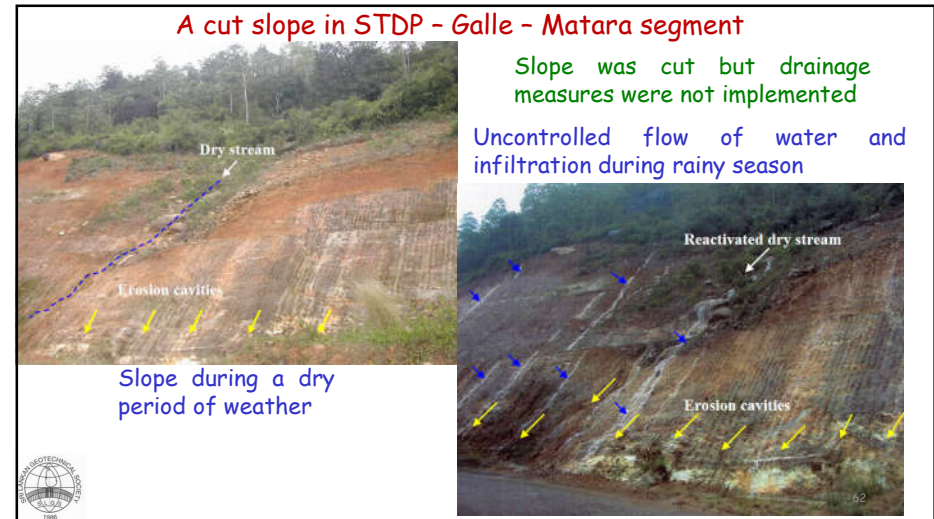
$$FOS = \tau_f / \tau_m$$

60





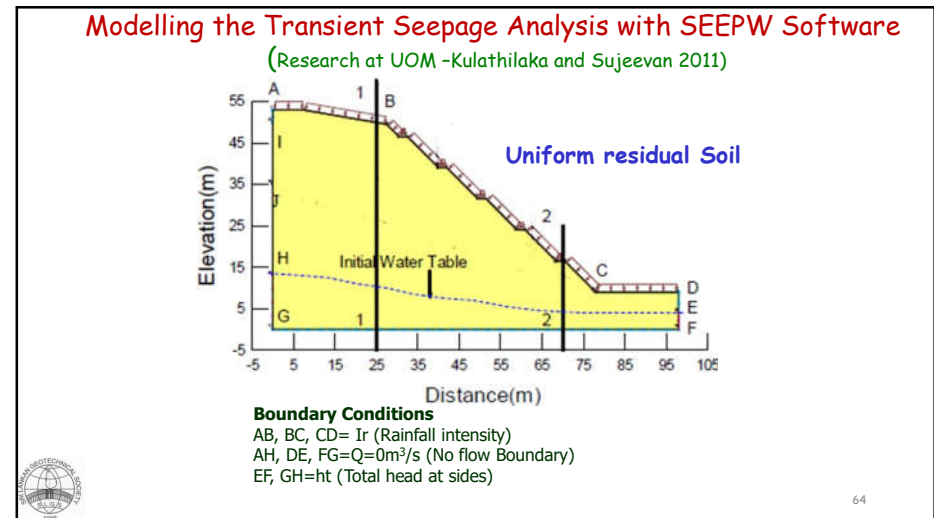
61



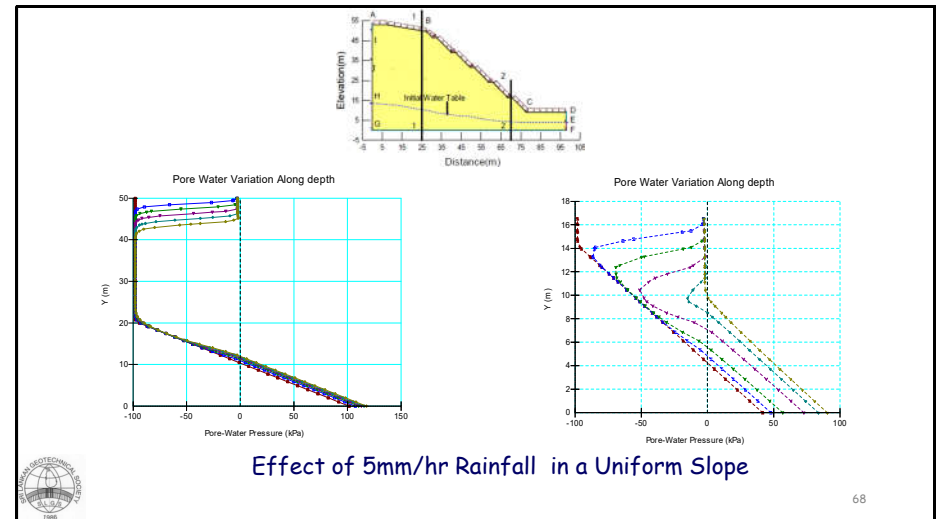
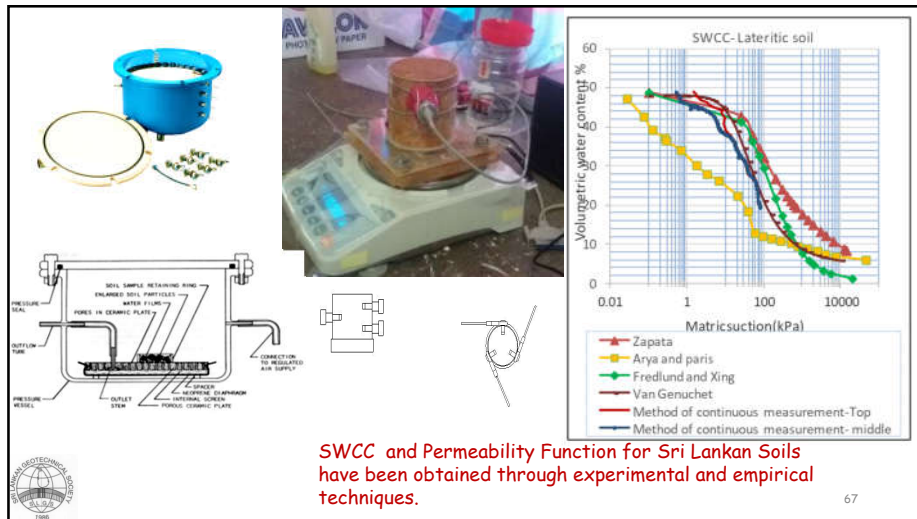
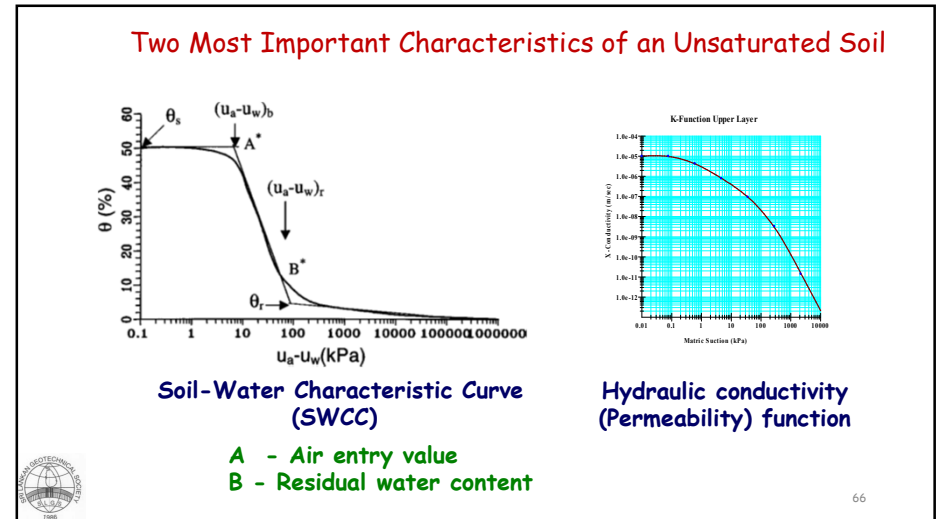
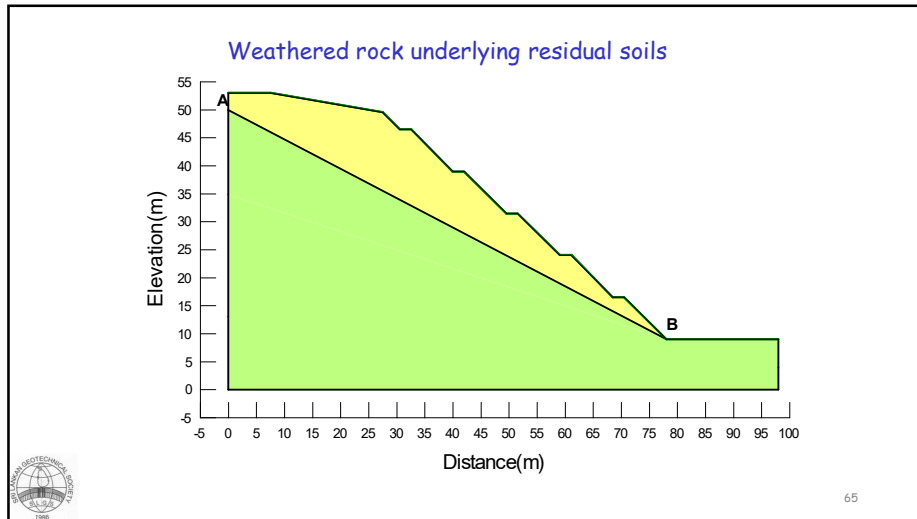
62

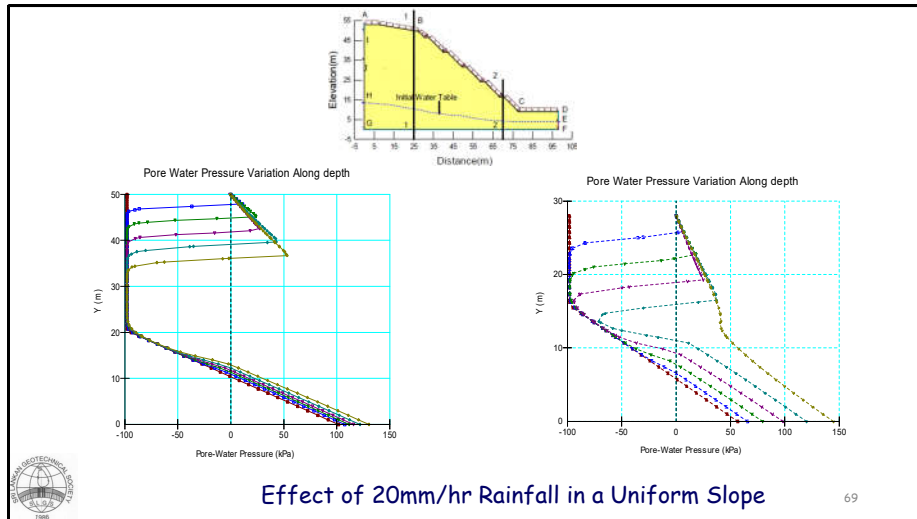


63

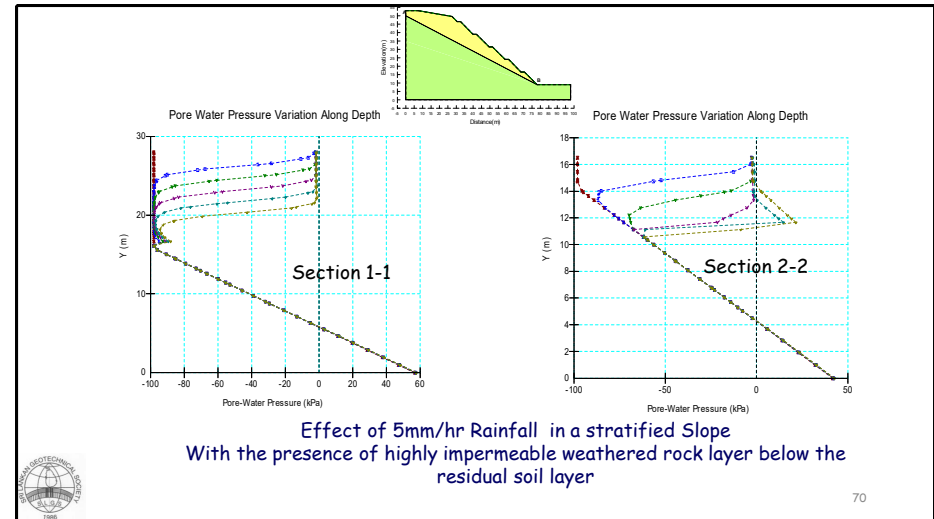


64

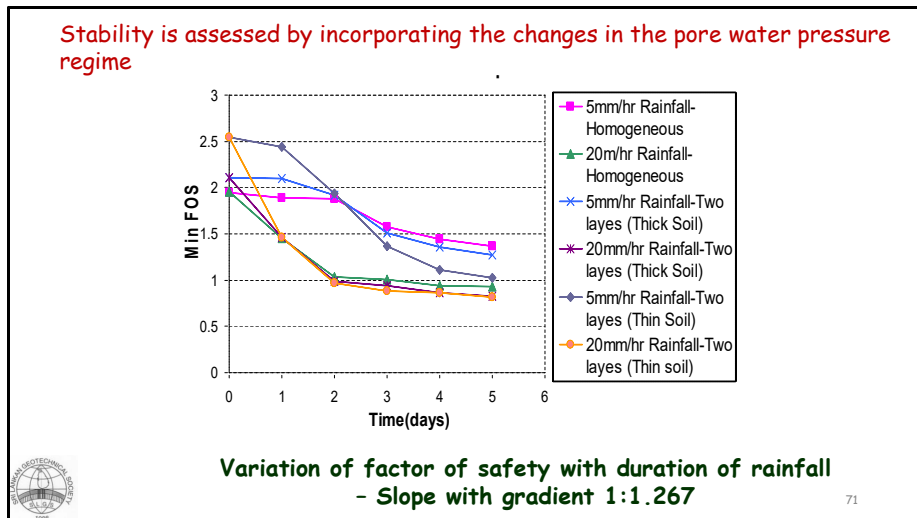




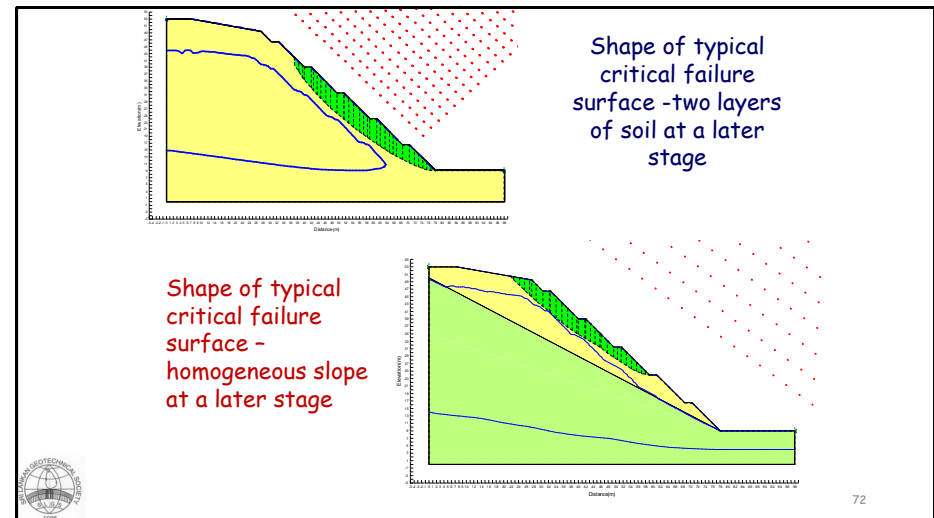
69



70



71



72



### Stabilization by Drainage

Instability of these cut slopes could be prevented by minimizing infiltration through the construction of Cut off drains and berm drains.

Appropriate Vegetation or artificial Slope Cover such as shotcrete could minimize infiltration and prevent erosion as well.

Infiltration into relict joints should be prevented by sealing.

Sub surface drains of different forms may be required in some situations.



73

73



Surface Drainage Measures in Southern Expressway

Cutoff Drains

Berm Drains



74



75

75



76



77



78

Present Situation

78

**Cut off drain at the crest of the slope**

- Has to be done with minimum cutting to prevent disturbance to the boulders at the crest

79

79

Different forms of surface protective measures are used

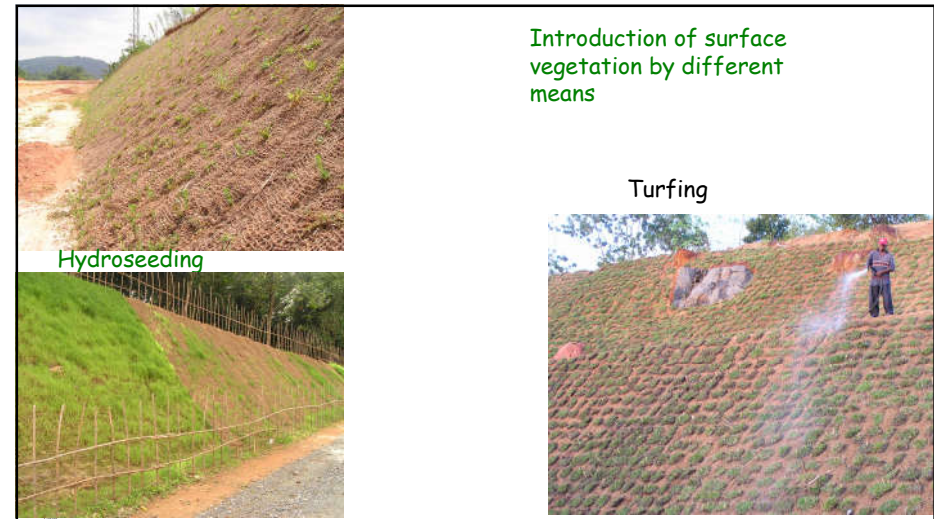
80

80





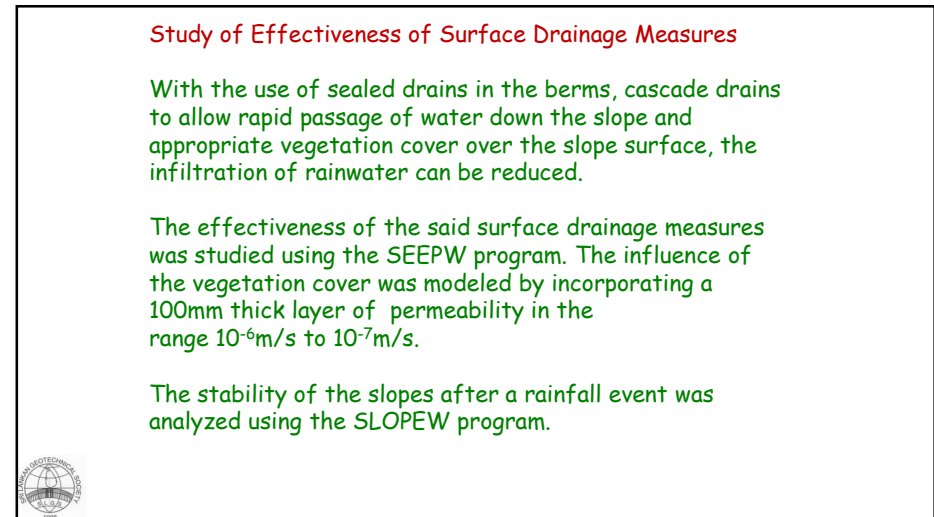
81



82



83



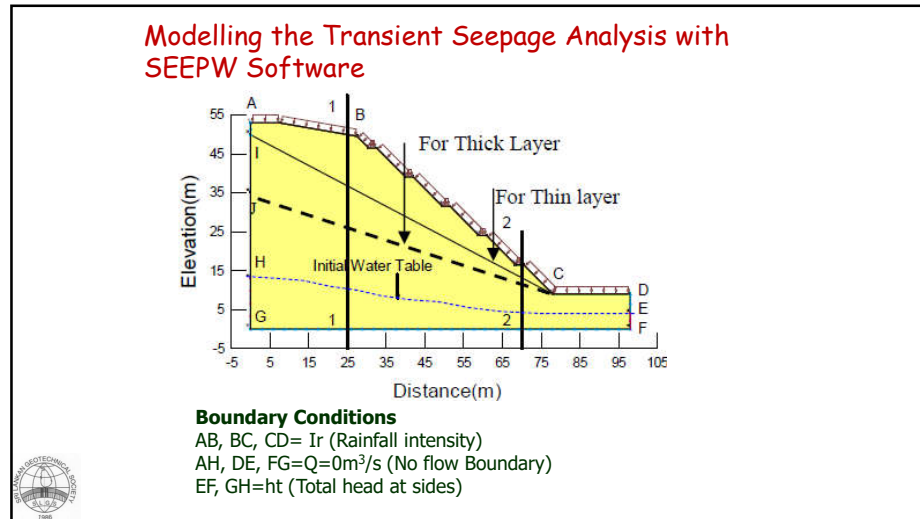
84

**Study of Effectiveness of Surface Drainage Measures**

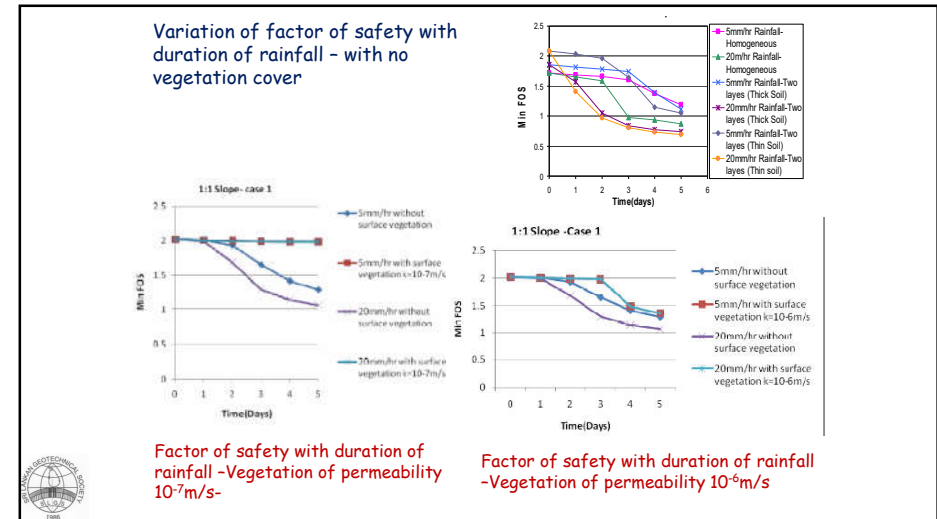
With the use of sealed drains in the berms, cascade drains to allow rapid passage of water down the slope and appropriate vegetation cover over the slope surface, the infiltration of rainwater can be reduced.

The effectiveness of the said surface drainage measures was studied using the SEEPW program. The influence of the vegetation cover was modeled by incorporating a 100mm thick layer of permeability in the range  $10^{-6}$ m/s to  $10^{-7}$ m/s.

The stability of the slopes after a rainfall event was analyzed using the SLOPEW program.



85



86

The results showed that the use of a 100 mm thick vegetation cover of permeability  $10^{-7}\text{m/s}$ , which is practically achievable, could cause a significant reduction in infiltration and the prevent formation of a perched water table and minimize the destruction of the matric suction.

The study also revealed that a vegetation cover with a permeability of the order of  $10^{-6}\text{m/s}$  would be less effective in maintaining a sufficient safety factor during prolonged rainfall. As such, Studies should be conducted to identify appropriate type of vegetation.

87

### Sub Surface Drains

To maintain a sufficient safety margin, some Slopes surface drainage alone may not be sufficient in some slopes.

Then sub surface drainage measures to facilitate rapid movement of water that has already infiltrated would be required .

Orientation of these drains and length of drains should be decided to ensure rapid dissipation of excess pore water pressures in the slope.


88

**Use of Structural Measures**

In some situations further external support through

- **Earth Retaining Structure of different types**
  - Gravity Retaining Walls
  - Passive piles, piers and caissons
  - Cast in situ reinforced concrete walls
  - Reinforced earth retaining structures
  - Buttress counter forts of coarse grained material
- **Internal Stabilizing Systems such as Soil nailing**
  - Soil Nailing
  - Anchoring or

• may also be required

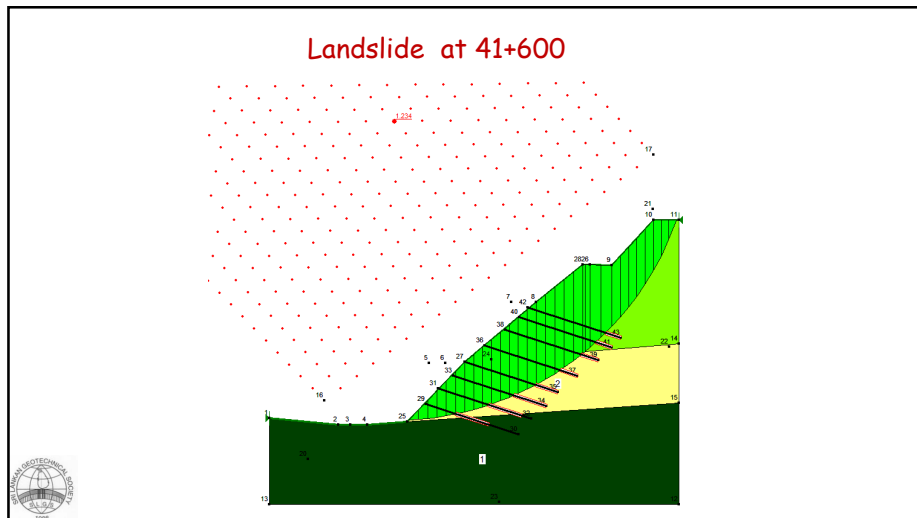


89

**Failure of cut slope near a valley during construction**  
At 41+ STDP Galle - Matara segment




90



91

**Soil Nailing with shotcrete facing**

Improvement of surface drainage. A basin drain at the valley to collect all the water and direct that to a cascade drain




92



**Rectification of Landslide at Welipenna in the Southern Transport Development Project**

Failure after adopting all drainage measures due to faulty surface drains- lack of maintenance

Initial tension cracks appear at 9AM




93



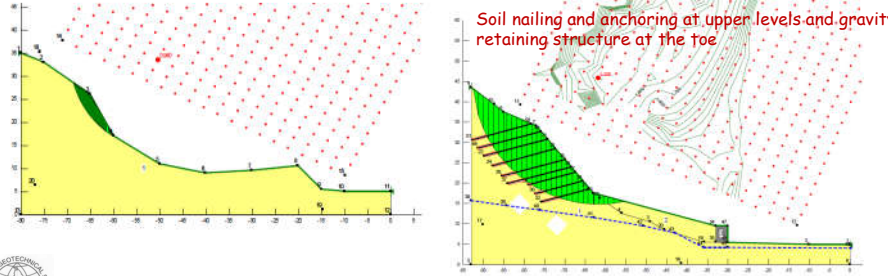





94

Scar left behind by the failure is unstable. Need to stabilize by multiple techniques

- Soil nailing and anchoring at upper level
- Gravity retaining structure at the toe
- Surface drainage -berm drains and cascade drains
- Sub surface drains at lower levels

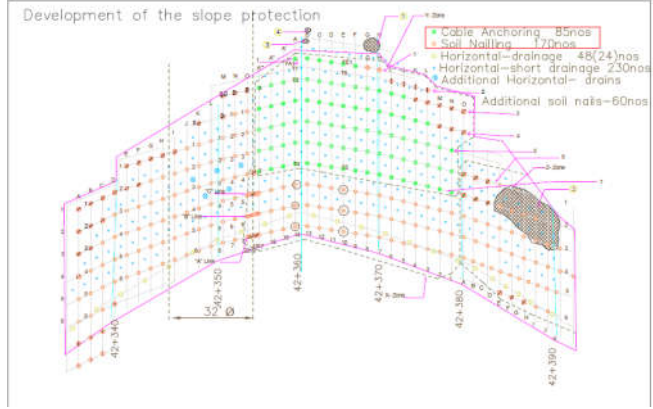


Soil nailing and anchoring at upper levels and gravity retaining structure at the toe




95

Development of the slope protection

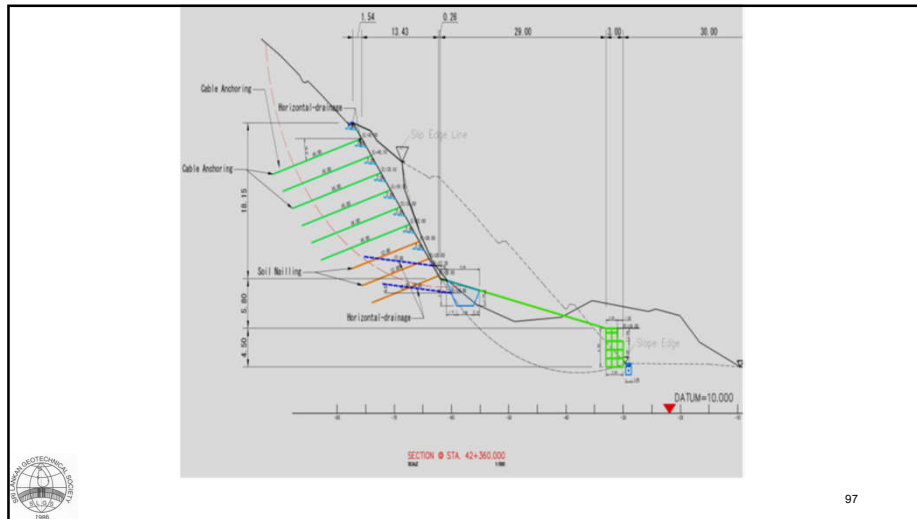


- Cable Anchoring - 85nos
- Soil Nailing - 170nos
- Horizontal - drainage 48(24)nos
- Horizontal - short drainage 230nos
- Additional Horizontal - drains
- Additional soil nails - 60nos



96

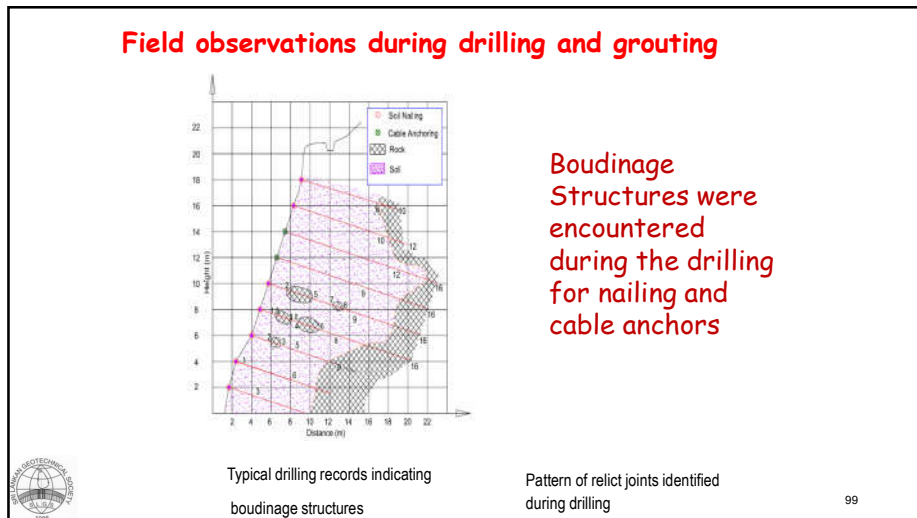




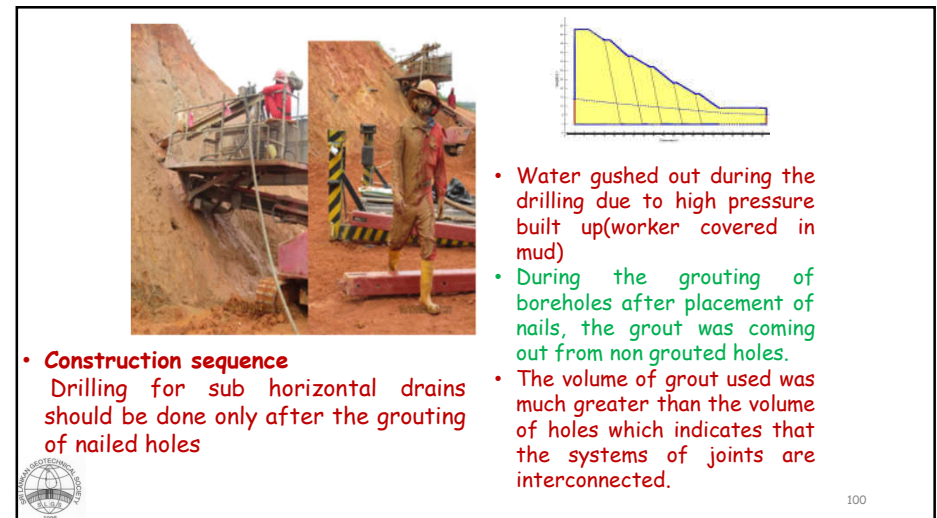
97



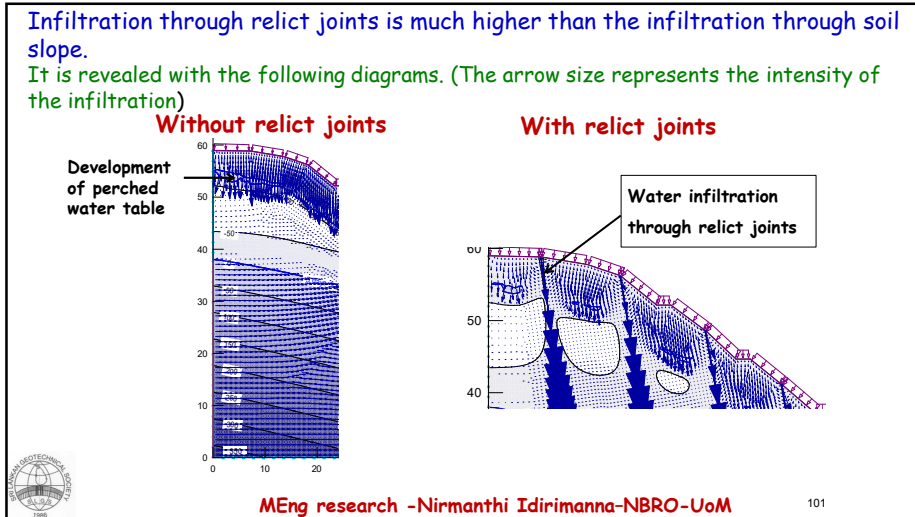
98



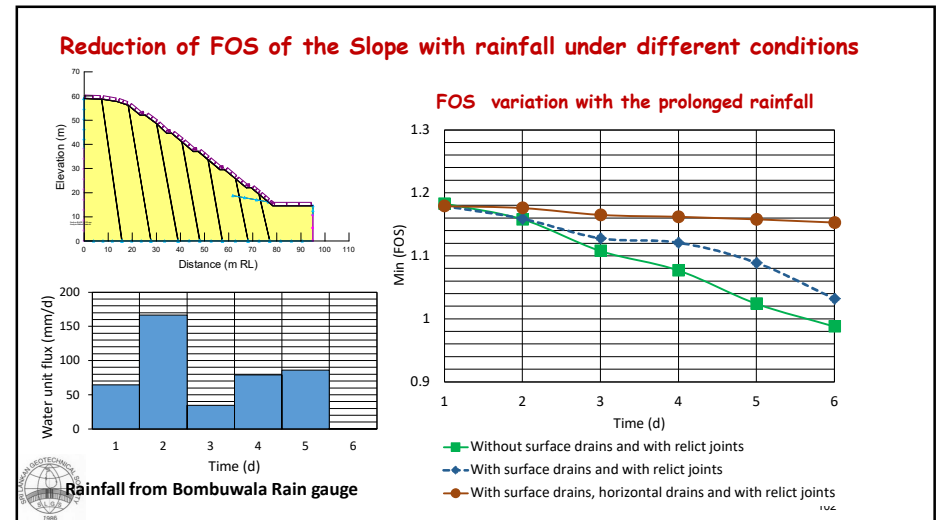
99



100



101



102



103

**Rectification of Failure at Kokmaduwa**

- Berms (3) were provided with berm drains and are connected to cascade drains.
- Part of the middle berm has been reinforced with soil nailing.
- The major tension cracks developed at the crest area were observed with lateral displacement of 50 to 200mm and vertical displacement of 1 m to 2m.
- Berms have been severely damaged by the movements of the cut slope.

**Tension Crack at the crest of the road cut**

**Initial failure with damages in soil nailing segment also**

**104**

104



105



106

**Immediate mitigation measures**

- Forty five numbers (45 Nos.) of horizontal drains into angle of 15° were installed at the first berm level get the infiltrated water trapped inside.



Installed Horizontal drains

Water discharge from horizontal gravity drains



107

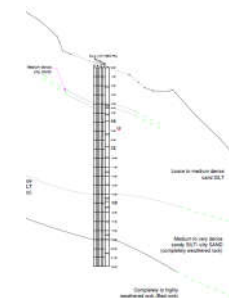
**Geotechnical Investigations and findings**

- Through borehole investigations four soil layers were deduced. Engineering properties of the soils were identified through lab testing.
- Piezometers installed in boreholes. An extensometer was installed to identify slope movements.
- Ground Penetrating Radar (GPR) survey and Resistivity survey to confirm the subsurface information

- Layer 1**- Loose to very dense sandy silt/ silty sand
- Layer 2**- Medium dense to very dense sandy silt/silty sand/gravelly silt (Completely weathered rock)
- Layer 3**- Completely to highly weathered rock
- Layer 4**- Moderately to slightly weathered Charnockitic gneiss

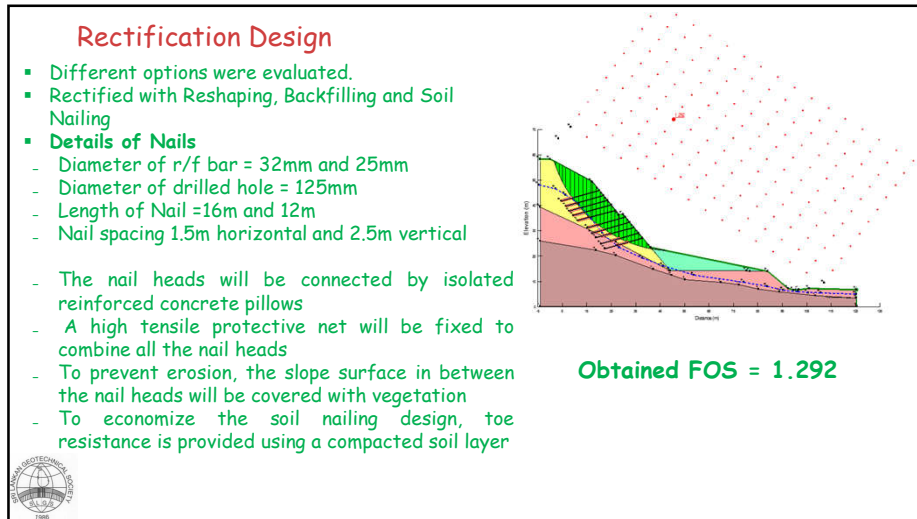
The existing condition was Back Analysis using the deduced sub surface profile

Rectification options were evaluated

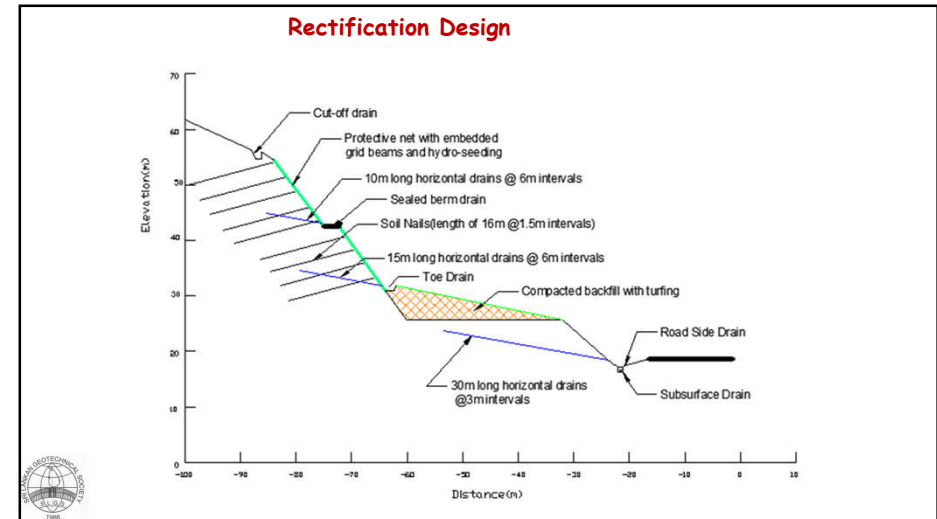


108

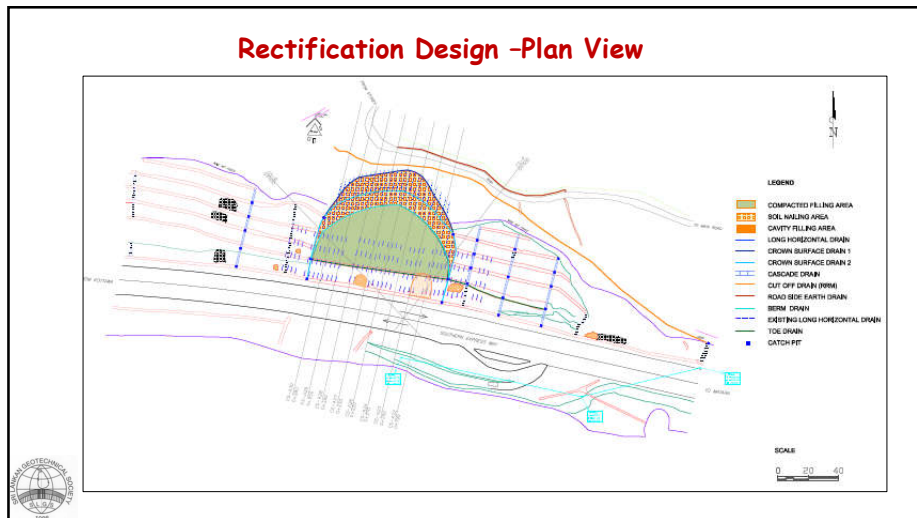




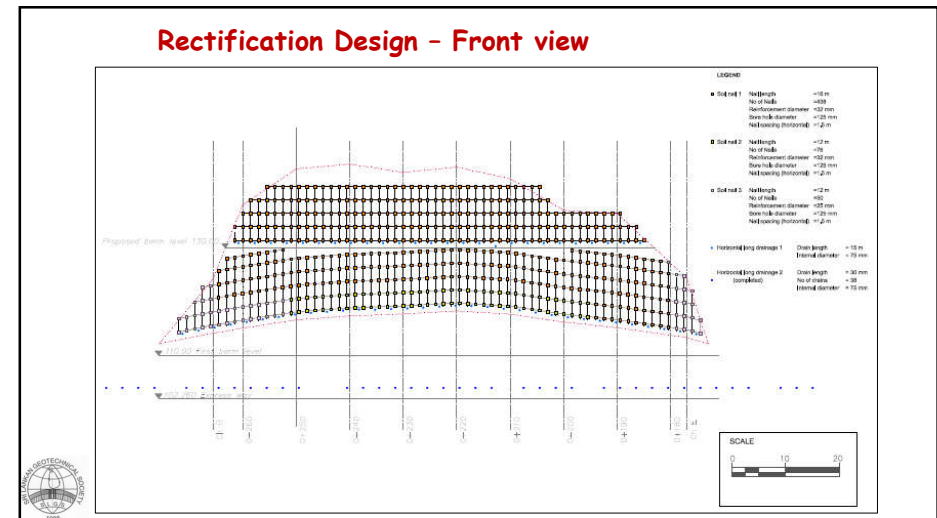
109



110



111



112

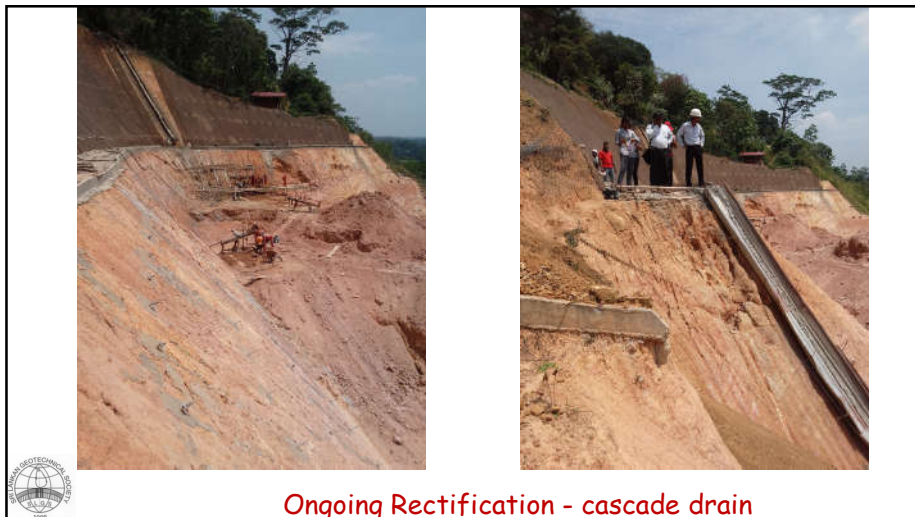




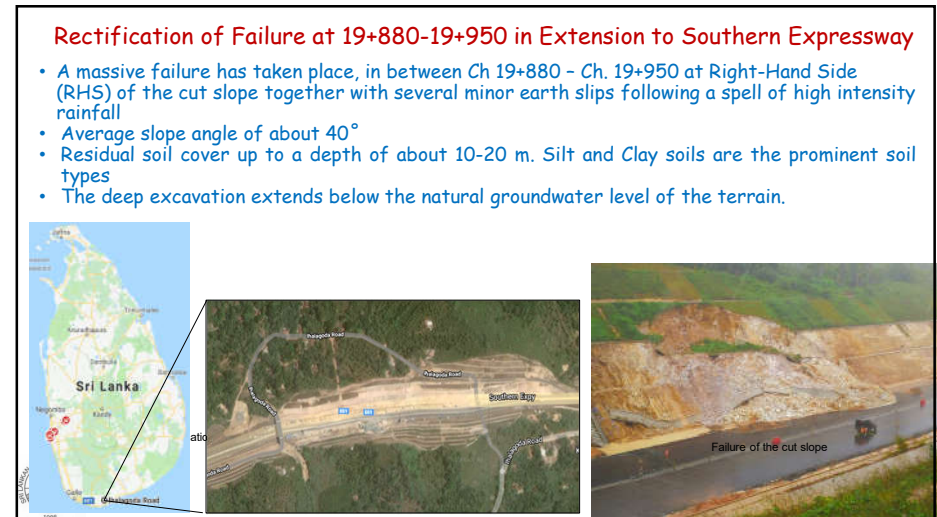
113



114





115

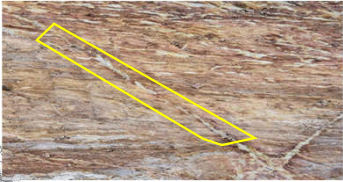


116


### Geological Observations


Plane failure condition



Feldspar rich pegmatite body



Soft infillings



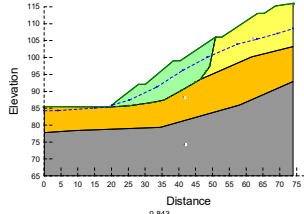
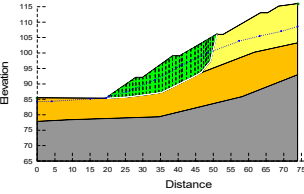
Observations at collapsed location

117

117

### Geological Investigations, testing and back analysis

- A back analysis of the failure was carried out using the section at Ch 19+910 using SLOPE/W 2016
- 20 boreholes were done and undisturbed box samples were collected for laboratory testing
- Sub surface geology and the strength parameters for sub-soil and groundwater table at the time of failure were validated based on the results of the back analysis
- The failure was observed at the boundary of feldspar rich pegmatitic body and residual soil

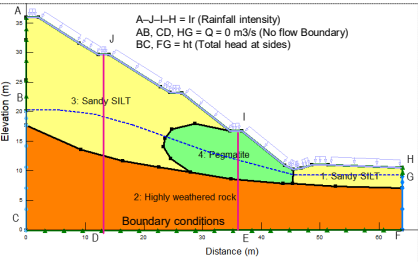



Soil type	$\gamma$ (kN/m <sup>3</sup> )	$\phi'$ (°)	$c'$ (kPa)
Kaolinite rich (Pegmatitic body)	18	30	06
Completely Weathered Rock	19	34	09
Residual soil	18	25	06

118

118

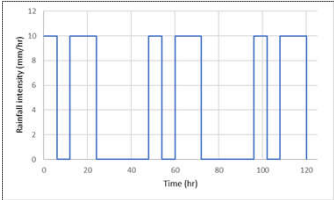
### Infiltration Study



A-J-L-H = Ir (Rainfall intensity)  
 AB, CD, HG = Q = 0 m<sup>3</sup>/s (No flow Boundary)  
 BC, FG = ht (Total head at sides)

3: Sandy SILT  
 4: Pegmatite  
 2: Highly weathered rock  
 1: Sandy SILT

Boundary conditions



Rainfall pattern

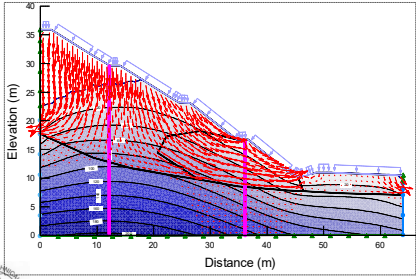
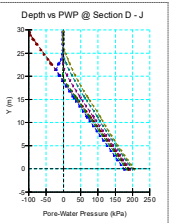
- For the analysis, actual rainfall recorded was idealized and applied under appropriate slope boundary conditions
- Soil Water Characteristic Curve and Permeability function obtained for the Sandy SILT soil at the site of similar soil by Vasanthan (2016) was used in this study.
- For other soils sample functions (Van Genuchten) given in the software were used.

119

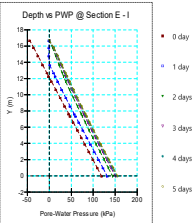
119

### Variation of stability with prolonged rainfall

- The results of the analysis show that as rainfall continues, the matric suction values in the upper section 1 is lost within one day and the groundwater table is rising.
- The groundwater table has risen 5 m at Section 1 within 5 days. Over the lower section 2 the groundwater table has risen to the ground level within 5 days

PWP distribution of section 1



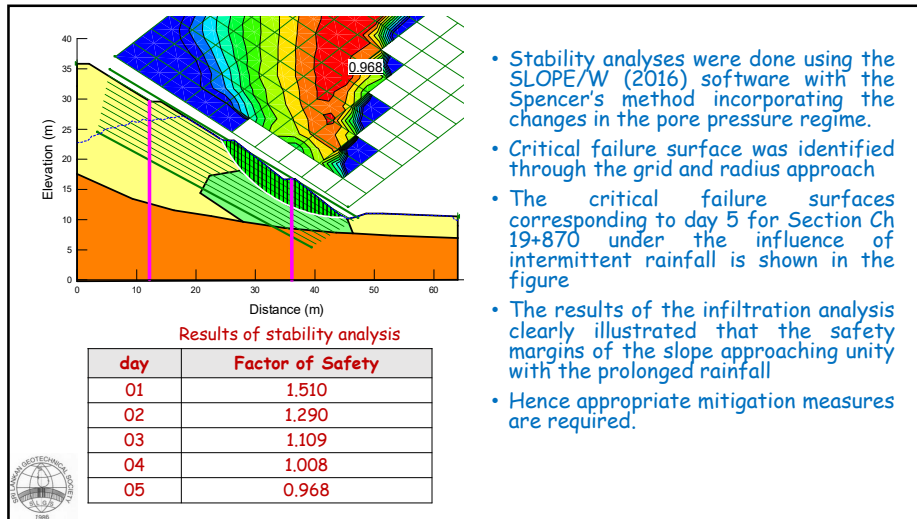
PWP distribution of section 2

Results of infiltration analysis

120

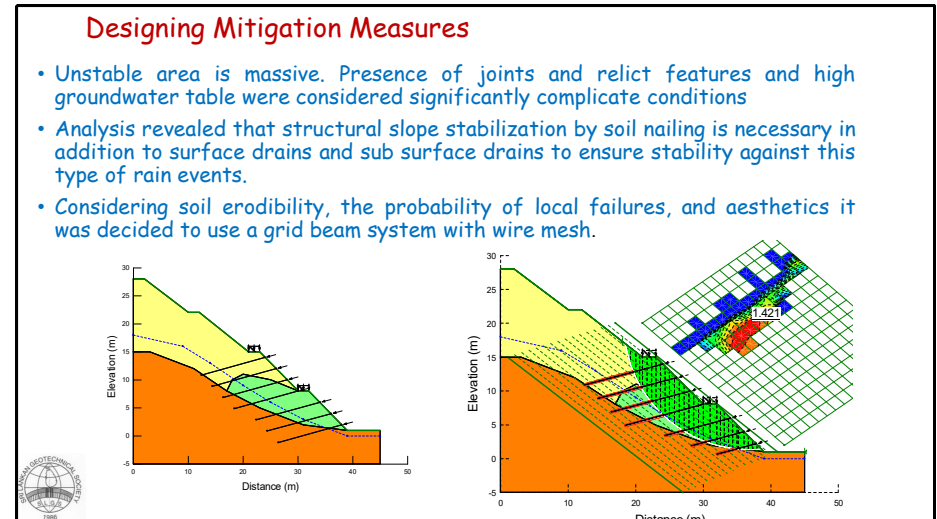
120





- Stability analyses were done using the SLOPE/W (2016) software with the Spencer's method incorporating the changes in the pore pressure regime.
- Critical failure surface was identified through the grid and radius approach
- The critical failure surfaces corresponding to day 5 for Section Ch 19+870 under the influence of intermittent rainfall is shown in the figure
- The results of the infiltration analysis clearly illustrated that the safety margins of the slope approaching unity with the prolonged rainfall
- Hence appropriate mitigation measures are required.

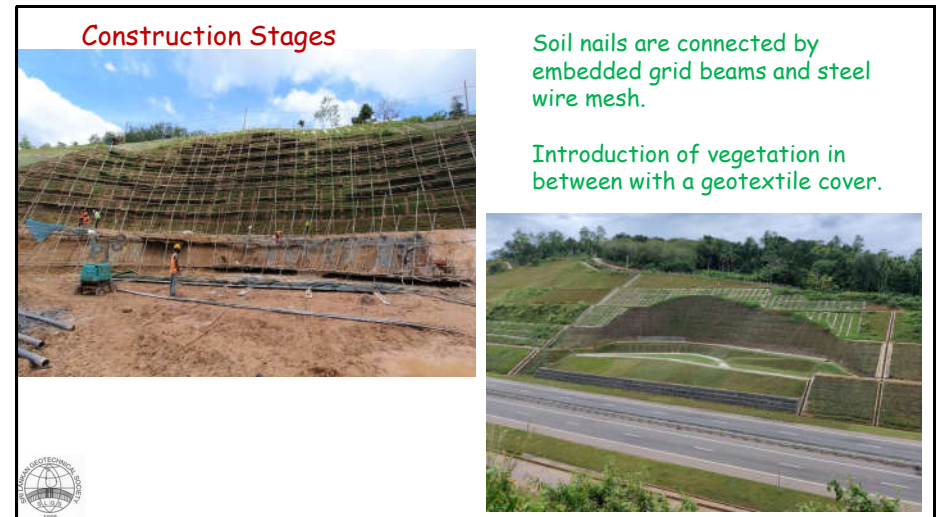
121



122



123



124

### Concluding Comments

**It is essential to monitor all these slope protective measures and earth retaining systems periodically and attend to whatever necessary maintenance and repair work promptly. - "Build and Watch "**

**With "Build and Forget" approach there could be some defects (minor), preventing them from performing the designed functions.**

**If neglected over time this would develop into major issues and may lead to catastrophic failures.**



125

**Thank You**



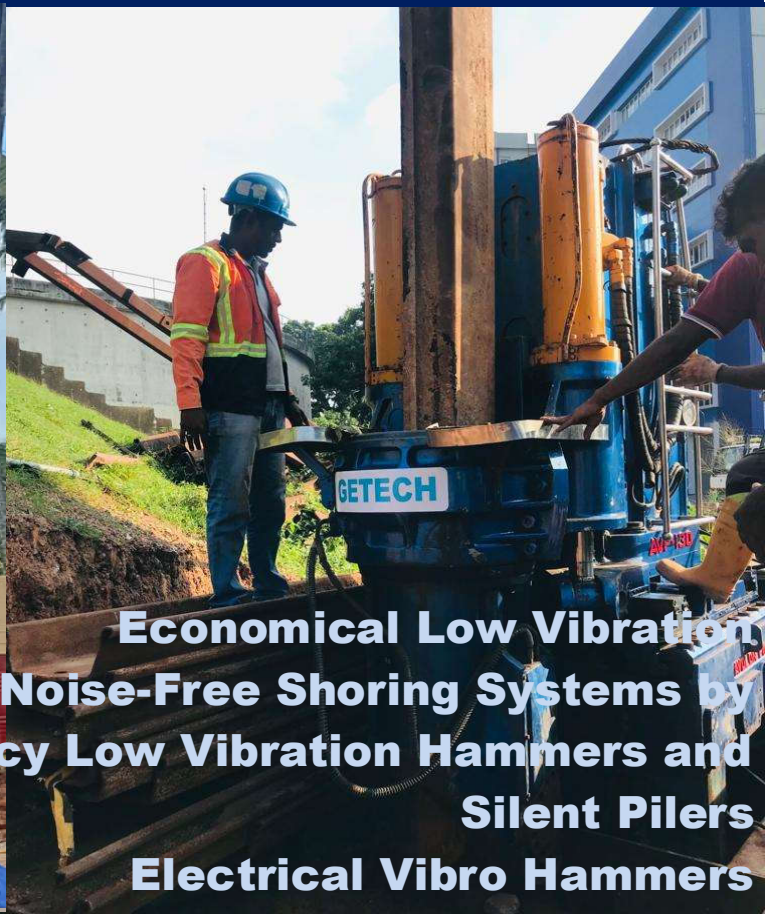
126

126



Silver Sponsor:

# GETECH ENGINEERING



**Economical Low Vibration  
Noise-Free Shoring Systems by  
High-Frequency Low Vibration Hammers and  
Silent Pilers  
Electrical Vibro Hammers**



**GETECH**

No 80A, Udumulla Road,  
Himbutana, Mulleriyawa New  
Town, Sri Lanka.

Tele/Fax 011 208 0 088,  
Email: [getech2050@gmail.com](mailto:getech2050@gmail.com),  
WhatsApp 071 022 6 366,

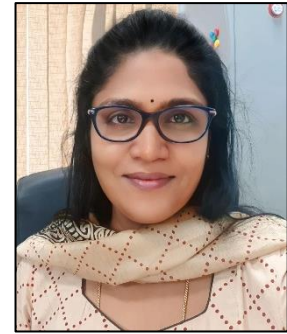




**GEOTECHNICAL AND STRUCTURAL ASPECTS OF  
TUNNEL DESIGN IN HIGHWAY PROJECTS**

**By**

**Prof. Neelima Satyam, Professor, IIT Indore, National  
Executive Committee Member, Indian Geotechnical Society**



Prof. Neelima Satyam is a Professor in the Department of Civil Engineering at IIT Indore, holding a Ph.D. and M.Tech from IIT Delhi, and a B.Tech from SV University, Tirupati. Previously, she served as an Assistant Professor at the Earthquake Engineering Research Centre, IIIT Hyderabad. Prof. Satyam has been a visiting researcher at prestigious institutions, including Kyushu University (2023), the University of Stuttgart (2018), and the University of Tokyo (2013).

Her expertise encompasses Geotechnical Earthquake Engineering, Micro-zonation, Site Response studies, Landslide hazard monitoring, and Rock engineering. Actively involved in teaching, research, and consultancy, she is a National Executive Committee Member of the Indian Geotechnical Society (IGS) and Chairman of the IGS Indore Local Chapter.

Prof. Satyam has received numerous research grants and published 119 papers in esteemed international journals, along with five patents and 21 book chapters. Her work has garnered several best paper awards from organizations like IGS and AGU. She has received numerous accolades, including the IEI Young Engineers Award and the CIDC Vishwakarma Award. A fellow of several professional societies, she also serves on editorial boards of reputable journals and is involved in various standards committees under the Bureau of Indian Standards (BIS).







# Analysis of earthquake impact on circular tunnels in varying rock mass

Neelima Satyam

*Department of Civil Engineering, Indian Institute of Technology Indore, Simrol, Indore, India*

**ABSTRACT:** Tunnels play a crucial role in public infrastructure, water transport, and hydroelectric power production. Tunnel stability is often challenged by varying geological conditions, particularly in seismically active regions. A pseudo-static approach using Phase 2 software was applied to study earthquake impacts on circular tunnels. The rock mass surrounding the tunnel was modeled using both continuum and continuum with interface approaches, where joints were incorporated as interfaces. The study examined a tunnel with a 6 m diameter and 100 m depth across a rock mass quality (Q) range of 1–30. Results indicated that seismic axial force increases as rock mass quality decreases, even when seismic load remains constant. Additionally, increasing the tunnel diameter from 6 m to 24 m reduced the seismic axial force for  $Q = 1$  ("very low" rock quality) and stronger rock types, indicating that larger tunnel diameters experience less impact under seismic loading conditions.

## 1 INTRODUCTION

Infrastructure development in mountainous regions has been steadily increasing, with a major focus on road networks that connect remote areas to major cities. This often involves tunnel construction by cutting through hills and rock masses. These tunnels are particularly vulnerable due to the complex geological conditions and high seismic activity in these areas. Consequently, studying the vulnerability of tunnels under seismic loading has garnered significant attention from researchers (Jain and Rao, 2022; Jaramillo, 2017). Key failure mechanisms in tunnels during earthquakes include ground failures such as portal landslides, soil liquefaction, and tunnel collapse due to fault slip (Rawat and Satyam, 2024a, 2024b; Sharma et al., 2022b, 2022a). In cases where tunnels intercept active faults, the damage to the support system—such as lining cracking, cement lining failure, spalling, and steel bending—can be severe. These studies have provided critical insights into the stability of mountain tunnels under seismic conditions.

To construct earthquake-resistant underground structures, it is important to understand how seismic waves interact with tunnels and the surrounding rock mass. In most underground structures, the rock mass's inertia is much greater than that of the tunnel structure, meaning the tunnel's seismic response is primarily governed by the rock's response to seismic waves. This differs from surface structures, where the seismic response is determined by the structure's own inertia (Forcellini, 2019, 2017).

Mountainous tunnels are typically built within rock masses, whose stability is directly related to the quality of the rock (Pandey et al., 2024, 2023). The

rock mass can be characterized as discontinuous, anisotropic, inhomogeneous, and non-elastic (DIANE). In modeling these rock masses, they can be categorized into four basic physical models: (a) continuum, (b) continuum with predominant joints, (c) rock with well-defined joint sets, and (d) frequently and randomly fractured rock mass. In a continuum model, rock is treated as continuous, and the effects of discontinuities are accounted for by reducing the rock's properties and strength. In the second approach, the rock is modeled as a combination of intact rock with predominant joint sets included.

The seismic load on underground structures was first analyzed by Barton et al., 1974, who developed the Q-system to categorize rock mass quality, with the assumption that the seismic Q value ( $Q_{\text{seismic}}$ ) is half of the static Q value ( $Q_{\text{static}}$ ). Hashash et al., 2001 conducted a detailed study of seismic analysis in underground structures, outlining key steps such as determining seismic characteristics, studying the ground's response to seismic waves, and designing the underground structure to withstand earthquakes. Seismic response can be analyzed using three methodologies: static, pseudo-static, and dynamic (Sedarat et al., 2009). Of these, pseudo-static analysis is based on empirical approaches and is simpler to perform compared to the others, making it widely used.

The pseudo-static analysis incorporates seismic loads by adding a body force in the direction of the earthquake within a static finite element analysis. This can be performed using finite element-based software like Phase 2.

This study aims to analyze the impact of seismic loading on tunnel linings using a numerical modeling approach. Specifically, the study

examines how the axial force on the tunnel lining increases as a function of rock mass quality (Q) and tunnel dimensions. Three sedimentary rock masses, ranging from "very poor" to "very good," were modeled with different geomechanical parameters derived through empirical relations. The surrounding rock mass was modeled using two different approaches: continuum and continuum with interfaces (discontinuities). The results were compared for both static and seismic case studies to understand how incorporating discontinuities affects tunnel stability (Sun and Dias, 2019).

A tunnel model with diameters of 6 m, 12 m, 18 m, and 24 m, at a depth of 100 m, was analyzed under seismic conditions, with surrounding rock masses of Q values ranging from 1 to 30. The study compared results from the continuum and continuum with interface models to evaluate their differences in seismic response. This research provides valuable insights for researchers and engineers by highlighting the importance of considering joint orientation and discontinuities when assessing tunnel stability under seismic loading. The findings contribute to better seismic design practices for tunnels in seismically active regions.

## 2 METHODOLOGY

The impact of seismic loading on tunnel deformation was studied using a parametric experimental model in Phase 2, a 2D finite element stress analysis software for rock and soil excavation. The study focuses on the axial force in the tunnel lining under static and seismic conditions. The difference in axial force during seismic and static loading, termed "seismic axial force," describes the earthquake's effect on the lining. The model's parameters include variations in tunnel diameter, rock mass quality, and joint orientation. This analysis helps predict potential failure scenarios by assessing the axial force in the lining during seismic events.

### 2.1 Model geometry and mesh details

In this study, the influence of seismic loading on tunnels was analyzed through a parametric investigation considering various case scenarios. These scenarios involved variations in tunnel diameter, rock mass quality, and joint orientation. Table 1 presents the rock mass classifications and corresponding Q values used for this analysis.

Table 1 Classification of rock mass quality

Rock class	I	II	III	IV	V
Description	Very good	Good	Fair	Poor	Very poor
Q value	> 40	10–40	4–10	1–4	< 1

The study examined how seismicity affects tunnels by evaluating the axial force developed in the liner under varying tunnel diameters and rock mass qualities. For the continuum with the interface model, the joint orientation was altered to explore potential tunnel lining failures at the intersection of the liner and rock joints. The diameters considered ranged from 6 m to 24 m, with increments of 6 m, and the depth was fixed at 100 m, representing the typical depth of tunnels in practice.

Pseudo-static finite element analyses were performed to assess the impact of rock joint deformation on the seismic response of circular tunnels. Figure 1 illustrates the computational domain and boundary conditions. The lower boundary was constrained in both vertical and horizontal directions, while the lateral boundaries were fixed in the vertical direction. The ground level was treated as a stress-free surface, while the bottom boundary was fixed, and both sides were considered rollers.

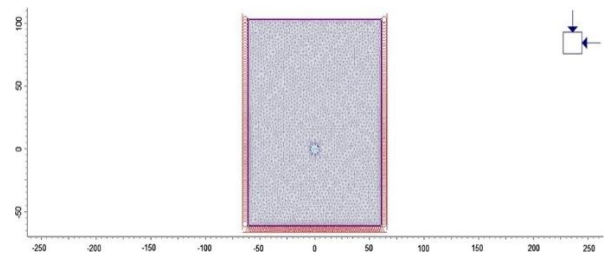


Fig. 1 Phase 2 model of the 6 m diameter circular tunnel

To ensure computational efficiency and accuracy, a three-noded graded mesh was used, with stress and strain calculated at the vertices of the triangular finite elements. The tunnel was modeled as a circular opening with diameters of 6 m and 12 m, and a 0.1-m-thick liner was applied around the circumference for plane strain conditions.

The in-situ stress was assumed to be both lithostatic and hydrostatic, with horizontal and vertical seismic coefficients of 0.3 and 0.2,

respectively. The analysis examined the axial forces developed in the tunnel lining under both static and seismic loading for three rock mass qualities ( $Q = 1$  to  $Q = 30$ ), considering both continuum and continuum-with-interface cases. Geotechnical parameters for different rock classes were derived using Roclab software (RocScience, 2007), as detailed in Tables 2 and 3.

Table 2 Geotechnical parameters of rock mass considered

Q value	$E_{\text{rockmass}}$ (GPa)	Cohesion (MPa)	Friction angle ( $^{\circ}$ )
30	10.78	1.7	51
10	8.3	1.1	50.5
1	3.5	0.6	44.8

Table 3 Geotechnical parameters of joints considered

Parameter	Value
Cohesion	0
Friction	$20^{\circ}$ and $10^{\circ}$
Normal stiffness	10,0000 mPa/m
Shear stiffness	10,0000 mPa/m

### 2.2 Case 1: Continuum rock mass

The continuum rock mass represents a rock mass without joints, modeled as a continuous medium with reduced strength to account for joint effects. This approach is widely used for underground excavation analyses due to its simplicity, applicability in practical scenarios, and capability to yield reasonably accurate results. Figure 1 illustrates the numerical model employed in this study.

### 2.3 Case 2: Continuum with the interface

In this approach, the tunnel is modeled as an equivalent continuum, incorporating a critical joint set within the rock mass. Unlike continuum methods, this approach allows for the explicit inclusion of interfaces, enabling the modeling of anisotropic variations. Such scenarios are analyzed using the discrete element method, which examines joint interactions with the tunnel. Vardakos et al., 2007 utilized in situ blasting measurements to investigate how joint layouts affect stress wave propagation. Similarly, Li and Ma, 2010 explored the interaction between blast waves and arbitrarily positioned rock joints. For this study, joints were simulated at three orientations:  $0^{\circ}$ ,  $45^{\circ}$ , and  $90^{\circ}$ , as shown in Fig. 2.

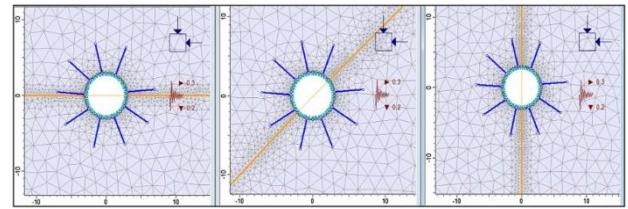


Fig. 2 Joint model for a 6-meter diameter circular tunnel with horizontal, diagonal, and vertical joints under quasi-static seismic loading conditions.

### 2.4 The sequence of excavation and support installation

In this analysis, the excavation and support installation processes were simulated in detail across several stages. Stage 1 represents the unexcavated tunnel under hydrostatic conditions, while Stage 2 captures stress relaxation occurring during the slight delay between excavation and support deployment. Prior to support installation, some stress is released, so calculating the load borne by the support system requires determining the amount of stress released during this relaxation, assumed to be 70%, using the convergence confinement method (CCM).

Stage 3 examines the interaction between the rock mass and support system, featuring a 10-cm-thick standard beam liner simulating shotcrete, along with 4-m-long rock bolts spaced 2.0 m apart. Table 4 details the modeled properties of shotcrete.

Table 4 Strength properties of shotcrete

Parameters	Value or description
E modulus (MPa)	25000
Poisson's ratio	0.2
Thickness (m)	0.1
Material type	Elastic
Liner type	Beam and formulated as Timoshenko beam

Finally, Stage 4 analyzes the impact of seismic loading, where the difference between axial forces during seismic (Stage 4) and static loading (Stage 3) determines the Seismic Axial Force, quantifying the earthquake's effect on tunnel stability.

## 3 RESULTS AND DISCUSSION

The methodology outlined in Section 3 was employed to assess seismic loading conditions for both scenarios, focusing on the post-failure behavior of the rock mass surrounding the tunnel. Although definitive guidelines for understanding post-failure characteristics are lacking, Hoek and Brown, 1997 pioneered the classification of these

behaviors into three scenarios: (1) elastic-brittle plastic for hard rock masses ( $GSI > 75$ ), (2) strain-softening for moderate rock masses ( $GSI 25-75$ ), and (3) elastic-perfectly plastic for weak rock masses ( $GSI < 25$ ). This study specifically addresses weaker rock masses, accounting for the effects of seismic activity, and assumes an elastic-perfectly plastic post-failure characteristic. The analysis considers two cases—continuum rock mass and continuum with interfaces—examining major principal stresses ( $\sigma_1$ ) and the increases in axial force within the lining following seismic loading (Fig. 3).

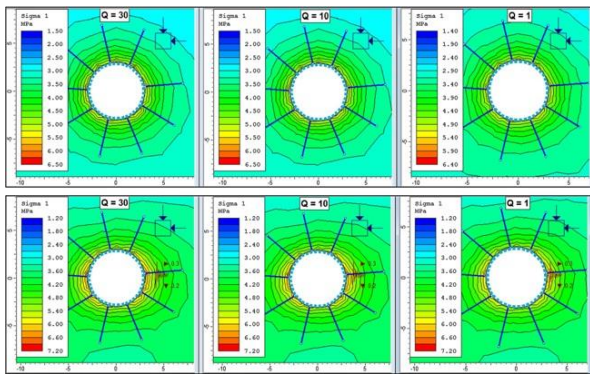


Fig. 3 Contour plot of  $\sigma_1$  around 6-m-diameter tunnel with  $Q = 30, 10$  and  $1$  for static and seismic conditions

### 3.1 Case 1: Continuum rock mass

Numerical modeling was conducted using Phase2 software to analyze various tunnel diameters (6, 12, 18, and 24 m) across different  $Q$  values ( $Q = 1, 10, 30$ ). Figure 4 illustrates the distribution of major principal stress ( $\sigma_1$ ) for a 6-m tunnel excavated in a rock mass with  $Q = 1$ , following the elastic-perfectly plastic model. Under static conditions, the high-stress zone is concentrated around the tunnel invert.

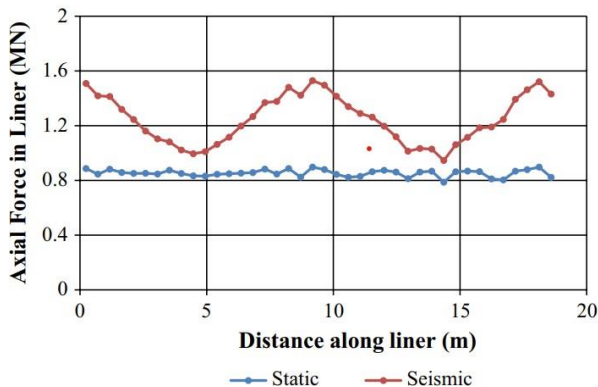


Fig. 4 Axial force on the lining for both static and seismic loading for  $Q = 1$  (6 m dia.)

However, upon the application of seismic loading, characterized by seismic coefficients of  $K_h = 0.3$  and  $K_v = -0.2$ , the area of elevated stress shifts to the tunnel knee, with another high-stress zone developing on the opposite tunnel shoulder, creating two ellipsoidal high-stress regions around the tunnel.

Table 5 presents the percentage increase in support pressure based on tunnel diameter and rock mass quality. The maximum increase in seismic axial force occurs at the tunnel shoulder and knee. Notably, the largest percentage increase in axial force between static and seismic conditions is observed for  $Q = 1$  at a 6 m diameter, while the smallest increase is for  $Q = 10$  at a 12 m diameter.

Table 5 Seismic axial force in tunnel lining for different rock mass qualities

Tunnel dia. (m)	$Q$ value	Maximum axial force in the lining		Percent increase (%)
		Static case (MN)	Seismic case (MN)	
6	1	0.78	0.94	30.5
	10	0.37	0.44	15.9
	30	0.29	0.34	17.2
12	1	0.88	1.03	17.04
	10	0.40	0.46	15
	30	0.31	0.36	16.12

Figure 4 also illustrates the periodic variation of the axial force around the tunnel, revealing similar trends for tunnels with moderate ( $Q = 10$ ) and high-quality rock mass ( $Q = 30$ ). Figure 5 displays the seismic axial force distribution along the liner for different rock classes ( $Q = 1, 10, 30$ ) and tunnel diameters (6 m and 12 m).

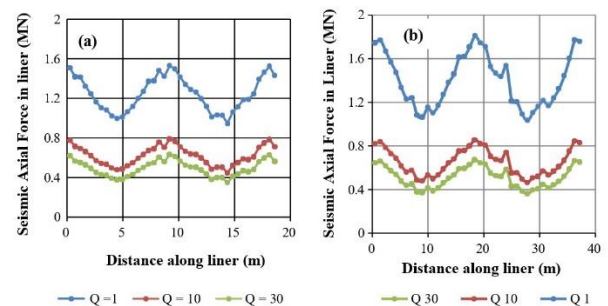


Fig. 5 Axial force on the lining for seismic loading for rock classes  $Q = 1, 10, 30$  for (a) 6-m-diameter and (b) 12-m-diameter tunnel



Overall, seismic loading results in increased axial pressure on the lining, with the magnitude of this increase inversely related to the Q value.

### 3.2 Case 2: Continuum with the interface

In the seismic scenario, the maximum axial force increases compared to the static case for strong rock, regardless of joint orientation. The introduction of a crossing joint in the tunnel is expected to further enhance the maximum axial force when the surrounding rock mass is weakened. Notably, the highest axial force was observed at the knee and shoulder positions rather than at the intersection point between the horizontal joint and the tunnel lining. Vertical joint simulations yielded different locations for the peak axial force, with a similar pattern seen for diagonal joint orientations. Table 6 illustrates the percentage increase in axial force in the lining for various rock diameters with joints.

Table 6 Summary of results for different tunnel orientations

Tunnel dia. (m)	Q value	Maximum axial force in the lining for static case (MN)	Maximum axial force in the lining for seismic case (MN) for various joint types		
			Horizontal joint	Vertical joint	Diagonal joint
6	1	0.88	1.44	1.54	1.53
	10	0.44	0.72	0.78	0.79
	30	0.35	0.58	0.62	0.61
12	1	1.15	1.9	1.8	1.8
	10	0.49	0.84	0.87	0.85
	30	0.37	0.66	0.67	0.66

For the weak rock mass case (Q = 1), the effects of joint weakening do not manifest in the same manner as observed in stronger rock conditions. Figure 6 displays the seismic axial force distribution along the liner for rock classes (Q = 1, 10, and 30) and diameters (6 m and 12 m) across different joint orientations.

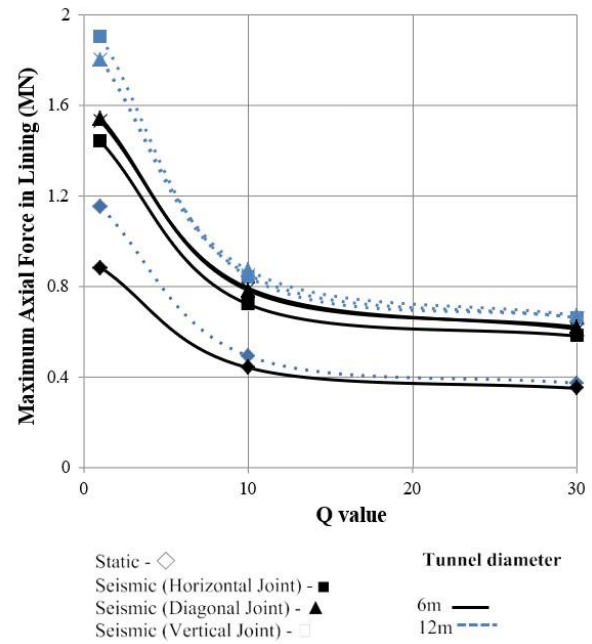


Fig. 6 Axial force in the lining for single-joint simulation at 0°, 45° and 90° for a 6-m-diameter circular tunnel in static load and after superimposing the seismic load combination in weak rock (Q = 1) and strong rock (Q = 30)

### 3.3 Influence of the size of the tunnel

To assess the impact of tunnel size on the force exerted on the lining during an earthquake, various tunnel diameters ranging from 6 to 24 meters were analyzed. The excavation depth was maintained at 100 meters below the surface, with rock mass parameters consistent with those in previous studies.

For poor-quality rocks characterized by a Q value of 1, both the actual axial pressure on the lining and the increase caused by seismic loading was found to decrease as tunnel diameter increased. In contrast, for high-quality rocks represented by a Q value of 30, the variation in axial pressure due to changes in tunnel diameter was relatively minor.

Table 7 displays the percentage increase in support pressure for different tunnel diameters.

Table 7 Summary of the results for different tunnel diameter

Tunnel dia. (m)	Q value	Maximum axial force in lining for static case (MN)	Maximum axial force in lining for seismic case (MN)	% Increase
6	1	0.78	0.94	30.5
	10	0.37	0.44	15.9
	30	0.29	0.34	17.2

12	1	0.88	1.03	17.04
	10	0.40	0.46	15
	30	0.31	0.36	16.12
18	1	0.91	1.08	18.6
	10	0.40	0.48	20
	30	0.31	0.37	19.35
24	1	0.96	1.05	9.3
	10	0.44	0.48	9.09
	30	0.34	0.37	8.10

Meanwhile, Figure 7 illustrates the variation in axial force around the tunnel for rock classes ( $Q = 1, 10,$  and  $30$ ) across diameters of 6 m, 12 m, 18 m, and 24 m under both static and seismic loading conditions.

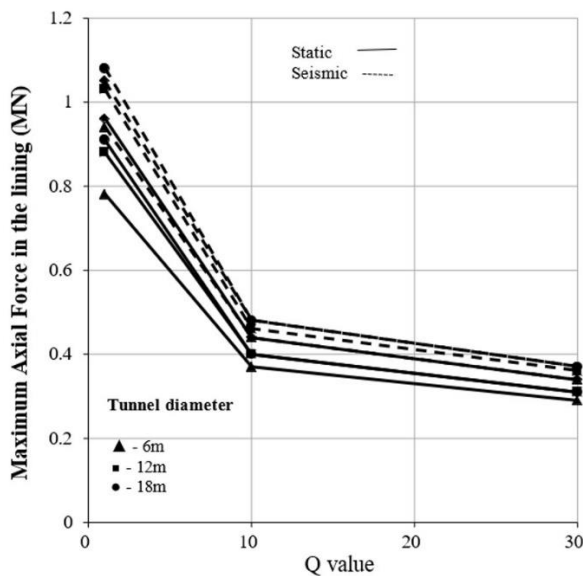


Fig. 7 Variation of the axial force in static and seismic conditions with the rock quality for different tunnel diameter

#### 4 CONCLUSIONS

The expansion of infrastructure in mountainous regions has resulted in a surge in tunnel construction, particularly in seismically active areas, emphasizing the critical need for seismic analysis of tunnels. This study conducted a numerical analysis of circular tunnels in rocks, modeled as both an equivalent continuum and a continuum with interfaces, utilizing Q-based rock mass classifications ranging from 1 to 30. Initially, the research examined the influence of rock mass quality on the forces acting on the tunnel lining under both static and seismic loading conditions. The axial force pattern analysis revealed that under seismic loading, the tunnel exhibits two peaks and two troughs. The findings indicated that for weak rock masses ( $Q = 1$ ), the axial force

difference on the lining between static and dynamic loads ranges from 15% to 20%.

To assess the effects of joint orientation, the study incorporated joints as single interfaces within the model. The Q method suggested that in strong rocks, the deformations occurring along the joints significantly influence jointed rock masses. Conversely, the Q method also indicated that soft rocks can deform independently of their joints, a conclusion supported by the study's results.

Additionally, the study evaluated the impact of tunnel size by increasing the diameter of the circular tunnel from 6 to 20 meters at a depth of 100 meters under seismic loading, with increments of 6 meters. The results revealed that the seismic axial force in the lining increases for poor rock mass ( $Q = 1$ ), while the effect of tunnel diameter on seismic axial force is minimal for strong rock mass.

#### REFERENCES

- Barton, N., Lien, R., Lunde, J., 1974. Engineering classification of rock masses for the design of tunnel support. *Rock Mechanics* 6, 189–236. <https://doi.org/10.1007/BF01239496>
- Forcellini, D., 2019. Numerical simulations of liquefaction on an ordinary building during Italian (20 May 2012) earthquake. *Bull Earthquake Eng* 17, 4797–4823. <https://doi.org/10.1007/s10518-019-00666-5>
- Forcellini, D., 2017. Cost assessment of isolation technique applied to a benchmark bridge with soil structure interaction. *Bull Earthquake Eng* 15, 51–69. <https://doi.org/10.1007/s10518-016-9953-0>
- Hashash, Y.M.A., Hook, J.J., Schmidt, B., I-Chiang Yao, J., 2001. Seismic design and analysis of underground structures. *Tunnelling and Underground Space Technology* 16, 247–293. [https://doi.org/10.1016/S0886-7798\(01\)00051-7](https://doi.org/10.1016/S0886-7798(01)00051-7)
- Hoek, E., Brown, E.T., 1997. Practical estimates of rock mass strength. *International Journal of Rock Mechanics and Mining Sciences* 34, 1165–1186. [https://doi.org/10.1016/S1365-1609\(97\)80069-X](https://doi.org/10.1016/S1365-1609(97)80069-X)
- Jain, A., Rao, K.S., 2022. Empirical correlations for prediction of tunnel deformation in squeezing ground condition. *Tunnelling and Underground Space Technology* 125, 104501. <https://doi.org/10.1016/j.tust.2022.104501>
- Jaramillo, C.A., 2017. Impact of seismic design on tunnels in rock – Case histories. *Underground Space* 2, 106–114. <https://doi.org/10.1016/j.undsp.2017.03.004>
- Li, J., Ma, G., 2010. Analysis of Blast Wave Interaction with a Rock Joint. *Rock Mech Rock Eng* 43, 777–787. <https://doi.org/10.1007/s00603-009-0062-0>
- Pandey, N.K., Satyam, N., Gupta, K., 2024. Landslide-induced debris flows and its investigation using r.avaflo: A case study from Kotrupi, India. *J Earth Syst Sci* 133, 97. <https://doi.org/10.1007/s12040-024-02315-1>
- Pandey, N.K., Venkatesh, K., Pandey, H.K., Srivastava, S., 2023. Numerical Modeling and Analysis of Rock Slope in Markundi Hills, Sonbhadra. *Indian Geotech J* 53, 1103–1113. <https://doi.org/10.1007/s40098-023-00730-7>
- Rawat, V., Satyam, N., 2024a. Effect of fibre-reinforced microbial-induced calcite precipitation on the mechanical properties of coastal soil. *Soil Use and*

- Management 40, e13078.  
<https://doi.org/10.1111/sum.13078>
- Rawat, V., Satyam, N., 2024b. Enhancing the durability of coastal soil treated with fiber-reinforced microbial-induced calcite precipitation (MICP). *Applied Ocean Research* 150, 104106.  
<https://doi.org/10.1016/j.apor.2024.104106>
- Sedarat, H., Kozak, A., Hashash, Y.M.A., Shamsabadi, A., Krimotat, A., 2009. Contact interface in seismic analysis of circular tunnels. *Tunnelling and Underground Space Technology* 24, 482–490.  
<https://doi.org/10.1016/j.tust.2008.11.002>
- Sharma, M., Satyam, N., Reddy, K.R., 2022a. Comparison of improved shear strength of biotreated sand using different ureolytic strains and sterile conditions. *Soil Use and Management* 38, 771–789.  
<https://doi.org/10.1111/sum.12690>
- Sharma, M., Satyam, N., Reddy, K.R., Chrysochoou, M., 2022b. Multiple heavy metal immobilization and strength improvement of contaminated soil using bio-mediated calcite precipitation technique. *Environ Sci Pollut Res* 29, 51827–51846.  
<https://doi.org/10.1007/s11356-022-19551-x>
- Sun, Q.Q., Dias, D., 2019. Assessment of stress relief during excavation on the seismic tunnel response by the pseudo-static method. *Soil Dynamics and Earthquake Engineering* 117, 384–397.  
<https://doi.org/10.1016/j.soildyn.2018.09.019>
- Vardakos, S.S., Gutierrez, M.S., Barton, N.R., 2007. Back-analysis of Shimizu Tunnel No. 3 by distinct element modeling. *Tunnelling and Underground Space Technology* 22, 401–413.  
<https://doi.org/10.1016/j.tust.2006.10.001>





Bronze Sponsor:

# Our credentials continue to change Colombo's skyline.

Over 30 years ago, our firm commitment to professional excellence etched itself on constructions that changed the face of Colombo

Today, that attribute is as consistent as it always was.



# Sanken



Sanken Construction (Pvt)Ltd. 295, Madampitiya Road, Colombo 14.  
Tel: 0112 522 942, E-mail : [sanken@sanken.lk](mailto:sanken@sanken.lk), Web: [www.sankenconstruction.com](http://www.sankenconstruction.com)



**ADVANCEMENTS IN GROUND IMPROVEMENT  
TECHNIQUES FOR SRI LANKAN EXPRESSWAY  
CONSTRUCTION**

**By**

**Dr. Asiri Karunawardena, Director General, National  
Building Research Organisation (NBRO)**



Eng. (Dr.) Asiri Karunawardena is the Director General/ Chief Executive Officer of the National Building Research Organization (NBRO) of Sri Lanka. NBRO is the main focal point for landslide disaster risk reduction in Sri Lanka and it is taking a leading role in promoting resilient and safe infrastructure construction in the country.

Dr. Karunawardena graduated as a Civil Engineer and obtained his master's degree in Geotechnical Engineering from the University of Moratuwa, Sri Lanka. Thereafter, he obtained Doctor of Engineering from Kyoto University, Japan. His major fields of work are related to Landslide risk reduction, Geotechnical Engineering applications, Resilient constructions, etc. He has engaged in many large-scale infrastructure development projects including major highway constructions in Sri Lanka as a Geotechnical Expert. He has authored over 10 peer-reviewed technical papers in the above fields. He is a Chartered Engineer and a member of the International Society of Soil Mechanics and Geotechnical Engineering (ISSMGE).

As the Director General of the institute, he leads a team of multidisciplinary professionals to reduce the losses due to disasters by integrating disaster risk reduction into the planning and development process in the country to achieve the vision of safer built environment and sustainable development gains.







# Advancements in Ground Improvement Techniques for Sri Lankan Expressway Construction

A. Karunawardena

*Director General, National Building Research Organization, Sri Lanka*

**ABSTRACT:** The construction of Expressways in Sri Lanka involved extensive ground improvement work as many parts of the Expressway traverse through flood plains and marshy ground consisting of very soft peat, organic soils, and clays. Depending on the ground conditions, various ground improvement methods including removal and replacement, preloading, preloading with vertical drains, dynamic compaction, vacuum consolidation, gravel compaction piles, and piled embankments were applied to improve the soft soil to build the embankments with heights varying from 2m to 15m. In the construction of the Southern Expressway project, embankments of about 4 km in length were constructed by improving the peaty soil basically by the application of the heavy tamping method. The length of the embankments that were built by improving the peaty soil by vacuum-assisted surcharging is around 2.5 km. The details of the field instrumentation program and field monitoring program to assess the soft ground improvement are presented. The performance of the ground improvement was evaluated in terms of the degree of consolidation, improvement of the physical and engineering properties, increase in pre-consolidation pressure, and gain in shear strength of the peaty soil. The results of the post-construction surface settlement monitoring of the expressway carried out up to date reconfirm that the ground improvement work was very successful, and the expected residual settlements are well below the allowable limit of the contract.

**Keywords:** Peat, Consolidation, Embankment, Settlement, Stability

## 1 INTRODUCTION

The Southern Highway is Sri Lanka's first E-Class highway that links the Sri Lankan capital Colombo with Matara, a major city in the south of the island. The length of 96 km section from Colombo to Galle had been completed and opened to traffic in November 2011. Many parts of the highway traverse through flood plains and marshy ground consisting of very soft peat, organic soils, and clays. Especially, in the major flood plain of Welipenna River, Bentota River, and Gingaga River areas, thick peat and organic clay deposits were found. These problematic soils have low shear strength, high compressibility, and low bearing capacity, and therefore need to be improved to avoid excessive settlement and prevent stability failure during expressway embankment construction. Also, these peaty soils possess high creep settlements and therefore it is necessary to improve the soft ground to control the post-construction settlements (Karunawardena (2007)). Many ground improvement methods have been used on soft soil to improve its bearing capacity and minimize the anticipated settlement in this section of the Southern Expressway Project. Ground improvement methods such as surcharging, surcharging with pre-fabricated vertical drains, rock replacement, heavy tamping, vacuum consolidation, and piled embankment have been used to improve the soft soil

in order to control the post-construction settlements and to ensure the stability of the highway embankment.

This paper presents the ground improvement methods applied in a section of the Southern Expressway between Ch.0+000 km to Ch.66+160 km to improve the peaty soil, with some background information on the design methodology. In the first 34 km of the highway, about 50% of the area is covered by soft ground, and from 34 km to 66 km, the distance covered by the soft ground is around 12 km. In this project, embankments of about 4 km in length were constructed by improving the peaty soil basically by the application of heavy tamping method. The length of the embankments that were built by improving the peaty soil by vacuum-assisted surcharging was around 2.5 km. The problems encountered during ground improvement work and embankment construction and the solutions given for the same are highlighted and discussed. The details of the laboratory and field investigations carried out before and after ground improvement, the field instrumentation program, and the field monitoring program that was carried out during and after the construction of highway embankment to assess the soft ground improvement are presented.

## 2 DETAILS OF THE SUBSOIL PROFILE

Many geotechnical investigations have been carried out since the inception of the project in order to assess the condition of the soft ground. At the preliminary stage, to provide information to bidders and to facilitate initial designs, boreholes were carried out at 500 m intervals. After commencement, boreholes were carried out at about every 50 m interval in order to provide the necessary information for the detailed design.

Site investigation consisted of boreholes with Standard Penetration Test (SPT), hand auguring, Cone Penetration Test with pore pressure measurement (CPTu) as in-situ testing, and a series of laboratory tests such as index property tests, unconsolidated undrained triaxial compression tests, and conventional consolidation tests.

The investigation identified that the soft ground area of the highway mainly consisted of peat, organic clay, alluvial clay, and loose sand deposits. The distribution of soft soil deposits along the highway trace from Kottawa to Kurundugahahetekma is shown in Fig. 1.

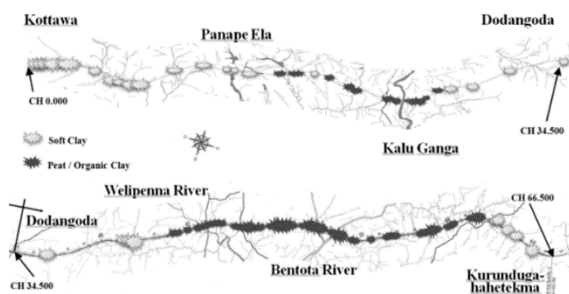


Fig. 1 Distribution of soft ground areas

Silty clay and silty sand were found as topsoil in most of the lowland areas up to a depth of 1.5 m to 3.0 m. This was followed by sand to lateritic soil and the thickness of the layers varied from 1 m to 5 m.

In the flood plains of Panape, Kalu Ganga, Welipenna, and Bentota river areas subsoil consisting of mainly peat, organic clay, very soft inorganic clay, and silt layers was found. The total average thickness of the compressible layer was in the range of 4 m to 11 m. In some areas, loose silty sand layers were present under the above compressible layers. In the valley areas between hillocks, instead of cohesive inorganic clays, very loose to loose silt and sand were found ranging from 0.5 m to 4m thickness. The details of the Geotechnical properties of the subsoil have been given by Karunawardena et al. (2009) and Karunawardena et al. (2011).

## 3 DESIGN OF SOFT GROUND IMPROVEMENT

Soft ground improvement design had to be carried out in order to control the settlements and to ensure the stability of the highway embankment as required in the technical specification. According to the technical specification, the embankment had to be designed and constructed by improving the soft ground in order to control the continued settlement to 15cm at the road center after a period of 3 years following the acceptance of the paving. In addition, the maximum residual differential settlement had to be not more than 0.3% change in grade over longitudinally within three years after construction. In order to achieve the above criteria, most or all of the primary settlements and some of the secondary settlements that would have occurred under the final embankment height alone were forced to take place by improving the soft ground.

The soft ground was improved mainly by using the following methods based on the subsoil conditions. Soft clay of shallow thickness was improved by placing a surcharge load. Shallow peat and organic clay deposits were removed and replaced with rock in order to support the embankments. The subsoil with relatively thick soft clay layers were improved by installing vertical drains and placing a surcharge load. The embankments on the relatively thick peat and organic deposits were constructed by improving the ground with heavy tamping method and the vacuum consolidation method from sections 0.0 km to 34.5 km and from 34.5 km to 66.5 km respectively.

In the rock replacement method, all compressible layers of the subsoil were removed and replaced with rock, completely eliminating the settlements. In the ground improvement method of application of surcharge load with or without vertical drains, future settlement of the highway embankment was controlled as required in the contract by designing an appropriate surcharge load. Most or all of the primary settlement and some of the secondary settlement that would have occurred under the final embankment height alone were forced to take place under the surcharge load. In addition, it was expected that the soil beneath the embankment would become over-consolidated or stiffer due to the surcharging of the ground. The aim of applying the surcharge was to eliminate 100% of primary consolidation settlement and enough secondary settlement such that the residual settlement is within acceptable performance limits. The residual settlement for a given length of time after construction was estimated as the remaining secondary settlement that occurs during the required time after the eliminated equivalent time of secondary compression has elapsed. In the design of

the surcharge, it was expected to have a 1.1 over consolidation ratio (OCR) for inorganic clays and 1.2 to 1.3 OCR for peat and organic clays in order to reduce the secondary settlements during the operation period.

The additional treatments were done after improving the ground in the bridge and underpass approaches in order to smooth the transfer of expected differential settlements between the approach embankment and the bridge deck. After the ground improvement, the approach area within the improved peat layer was replaced with rock within the approach embankment areas in order to eliminate the secondary settlements. The approach embankments on thick peat layers were constructed with special geogrid arrangements in order to have a smooth gradient between the approach embankment and the bridge deck.

#### 4 EMBANKMENT CONSTRUCTION ON PEATY SOIL

Embankments over peaty deposits in the Southern Expressway between Ch. 0.000 km to Ch 34.500 km were constructed by improving the peaty soil using the heavy tamping method whereas the vacuum consolidation technique was applied to improve the peaty soil in the section between Ch.34.500 km to 66.500 km. This Chapter presents the details of the heavy tamping method and the vacuum consolidation techniques applied in the project.

##### 4.1 Heavy Tamping Method

The heavy tamping method resulted in a quick decrease in the void ratio of the peaty soil and instantaneous settlement of ground under impact. Heavy tamping method was designed to enforce the settlements that would be caused by the construction of earth embankments on soft ground by applying impact energy. Different energy levels had to be imparted by considering the anticipated settlement of the compressible layer under the respective designed embankment heights. In the estimation of settlements, all primary consolidation settlements and secondary settlements at the end of 3 years after construction were considered. The estimated settlement of peaty soil layers of different thicknesses under various embankment heights is shown in Fig. 2. In the calculation of settlement, the values of 0.428, 0.0428, 0.05, and 20 kPa were used for the parameters  $c_c/(1+e_0)$ ,  $c_r/(1+e_0)$ ,  $c_\alpha$ , and  $P_c$  respectively where  $c_c$  is the compression index,  $e_0$  is the initial void ratio,  $c_r$  is the recompression index,  $c_\alpha$  is the coefficient of secondary consolidation and  $P_c$  is the pre-consolidation pressure.

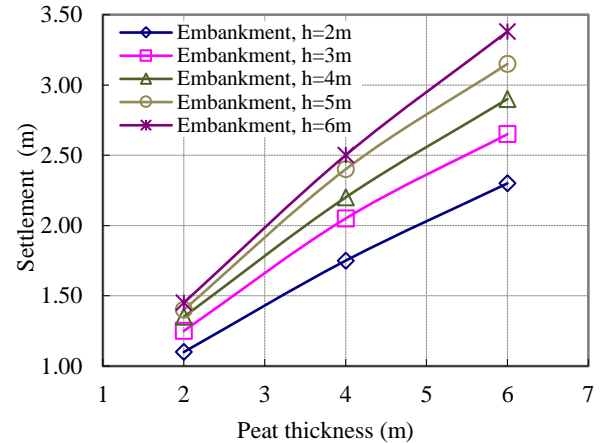


Fig. 2 Predicted settlement in peaty clay due to different embankment heights

The energy level required to enforce the designed settlement was estimated using the graph shown in Fig. 3. First, the soft soil, which was to be consolidated, was overlain by a working platform of lateritic soil to facilitate the movement of machinery. Then, a strong type of fiber drain (band drain) was installed by a machine in the soft subsoil in a square pattern with a spacing of 1 m. The required energy was applied to the soil by dropping a large weight on the ground surface repeatedly in phases on a grid pattern over the entire full base width of the embankment using multiple passes. A high energy level was applied in 5 phases whereas only 4 phases were used to apply a low energy requirement.

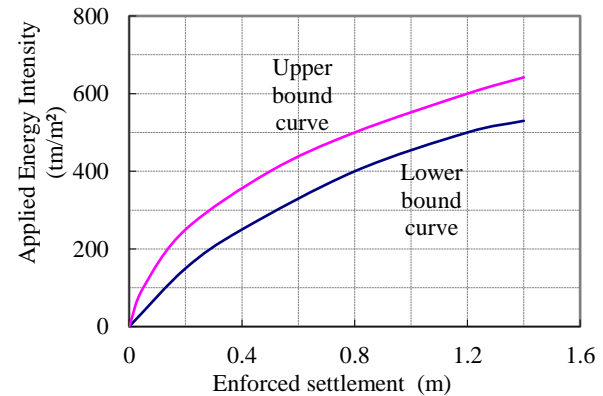


Fig. 3 Relationship between the enforced settlement and applied energy (Karunaratne (2007))

The energy intensity per phase was gradually increased from 15% - 20% of the total energy intensity to 30% - 40% at the last phase prior to the ironing phase. The spacing of the prints of the

pounder dropped on the square grid was estimated as  $2H$  to  $2.5H$ , where  $H$  is the thickness of the compressible layer. As the ground strength improved the spacing was reduced in the subsequent phases. In the ironing phase, a smaller drop height was used at very close spacing to remove surface unevenness and to compact the soil at shallow depths.

During tamping, once the depth of the crater formed by the drop of the pounder exceeded the height of the pounder, the crater was backfilled and leveled with soil. The dimension of the crater was recorded in order to calculate the volume of soil introduced. The above process was continued in all phases of the tamping operation. Using the crater fill volumes, the enforced settlements were calculated and if the enforced settlement was less than the required then another phase of tamping was introduced until the required settlement was achieved.

The weight of the pounder was 15 tons and it was built by stacking and bolting a series of 25 mm thick mild steel plates, 2 m by 2 m in plan area. A 60-ton capacity mobile crane that was equipped with an automatic lifting and release mechanism of the pounder was used in the tamping operation. The height of the drop is governed by the pounder dimension, crane capacity, and boom configuration and hence, was found to be a maximum of 8 m in this operation. The depth of improvement generally depends on the total amount of energy applied to the soil, which is a function of the weight of the tamper and the drop height as shown in the following equation as reported by Lukas (1995).

$$D = n\sqrt{WH}$$

In the above equation,  $D$  is the depth of soft/loose soil to be improved,  $W$  is the weight of the tamper (pounder) in tons,  $H$  is the height of drop in m and  $n$  is a constant ranging from 0.3 to 0.6 and for the peaty soils found in the site it was taken as 0.35. According to the above data, the practically possible improvement depth that could be achieved in the present operation was about 3.5 m to 4 m.

However, according to the investigation, it was observed that the soft compressible layer thickness was higher than above in most of the locations and therefore the underneath deeper soft layers were not improved properly by heavy tamping. These underneath deeper soft layers were improved after the heavy tamping operation by keeping a surcharge load for a sufficient period of time. Fig. 4 illustrates the major steps in the heavy tamping ground improvement adopted in the project.

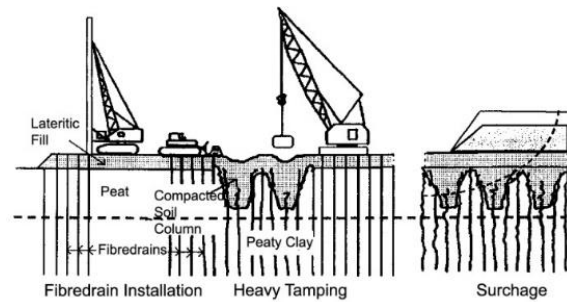


Fig. 4 Major steps in heavy tamping ground improvement.

#### 4.2 Effect of the Fiber Drain Installation for the Tamping Energy

The in situ permeability of peat is relatively higher than that of ordinary clays and therefore it was assumed that quick dissipation of excess pore water pressure would occur within the peat during the tamping operation. However, it was noted that the process of pore water pressure dissipation was rather slow, and therefore no further densification can be achieved by imparting additional energy to the soils. This could have been due to the rapid reduction of permeability of the peaty soil as a result of damage to the structure of the soil, the presence of a substantial amount of clay content, and long drainage paths. Therefore, it was noted that the energy level required to achieve the designed enforced settlement was very high as the excess pore pressure was not allowed to dissipate as expected. Having experienced the above difficulty, it was decided to install special strong type fiber drains in the peaty soil prior to the tamping in order to eliminate the development of high excess pore water pressure during the heavy tamping operation. Fig. 5 shows the applied tamping energy level in order to achieve the designed enforced settlement with and without fiber drain installation in similar ground conditions. As shown in Fig. 5, the energy that was required to achieve the designed enforced settlement in fiber drain installed peaty ground was significantly lower than the energy required without fiber drains. This clearly shows that part of the applied energy was wasted in compressing the 'incompressible' water. Therefore, the provision of a strong band drain such as a fiber drain to withstand heavy tamping impact is useful in reducing the required tamping energy level as described in Karunaratne (2007).



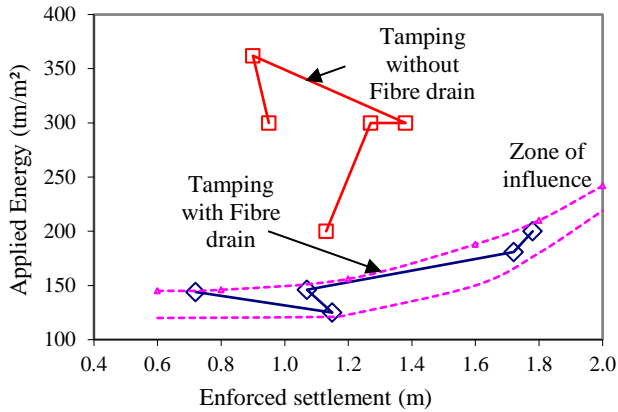


Fig. 5 Comparison of Applied energy vs. Enforced settlement with and without fiber drains

### 4.3 Vacuum Consolidation Method

The vacuum consolidation was carried out using the “Compact Vacuum Consolidation” (CVC) patent by Maruyama Industry, Japan. A brief description of the method adopted at the site is given below and the schematic construction is shown in Fig. 6.

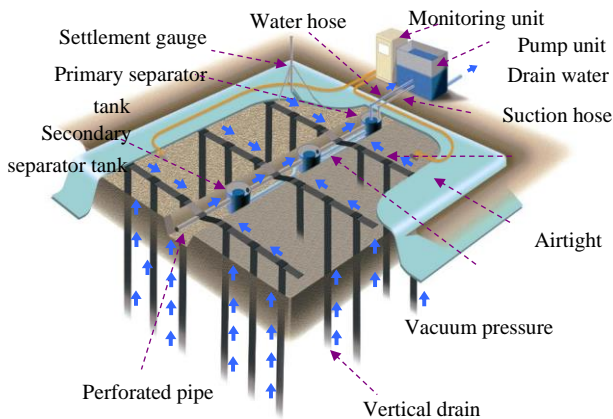


Fig. 6 Schematic construction of compact vacuum Consolidation

In the application of the vacuum consolidation method, about a 1.0 m to 1.5 m thick fill was constructed on the original ground surface to form a working platform for the band drain installation machine. Band drains were installed by a machine up to a designed depth from the original ground surface in a square pattern with a spacing of 1 m. Thereafter, flexible horizontal drains (300 mm wide and 4 mm thick) were laid on top of the fill with a horizontal spacing of 1 m and then connected to the vertical band drains in order to ensure adequate horizontal drainage capacity. Subsequently, the tank system was installed and connected to the designed

pipe systems. Small ditches were excavated perpendicular to the horizontal drains at 20 m intervals and filled with aggregates after placing perforated pipes. Instrumentation such as settlement plates, displacement stakes, electrical piezometers, and differential settlement gauges were also installed at the designed depths. After the installation of vertical drains, horizontal drains, perforated pipes, and separator tanks, the surface of the treatment area was covered by a protection sheet. Thereafter, an air-tight sheet was laid on top and the periphery trench system was constructed to provide air-tightness and the necessary anchorage at the boundary of the treatment area. Vacuum pressure was then applied using a vacuum pumping system patented by Maruyama Industry Co. Ltd, Japan by connecting the suction and water hoses to the vacuum pump. After confirming that there were no leaks through the air-tight sheet, filling was commenced.

It was expected to apply the surcharge by means of a vacuum pressure of 70kPa to compensate for the primary consolidation settlements and to minimize the secondary settlements that can take place in the proposed highway embankment. However, in many areas, the applied vacuum pressure was less than the designed value, and therefore the above-designed surcharge was applied by means of both vacuum pressure and embankment fills. The designed load was kept until the expected settlement was completed.

### 5 FIELD MONITORING PROGRAM

An extensive monitoring program was carried out to understand the field behavior of the foundation soil due to the different ground improvement methods. The improvement of the soft ground was monitored through the measurement of settlement and the excess pore water pressure during the construction period. Settlement plates were installed at the top of the soft layer or on top of the pioneer layer and piezometers were installed at the middle of the soft layer. The settlement stakes were installed near the toe of the embankments to check the stability during the construction. In addition to the above, in the areas improved by vacuum consolidation, a vacuum pressure monitoring unit was used to measure the vacuum pressure at the pump and under the air-tight sheet. Also, a water discharge meter was used to measure the rate and the total discharged water flow due to the vacuum operation. An automatic data acquisition unit was connected with the piezometer, vacuum pressure monitoring unit, and water discharge meter to keep continuous records. The locations of the instrumentation and the field monitoring data for the embankment constructed

using the vacuum consolidation method are shown in Fig. 7 and Fig. 8 respectively.

Installed instruments were monitored at selected time intervals to investigate the performance of the intended ground improvement process and the stability of the embankments. The filling rates and the vacuum pressure were adjusted when the stability of the embankment was seen to be at risk, based on the field monitoring data. During the first two weeks of the vacuum operation, the vertical settlement and lateral movement devices were monitored twice a day and the frequency of monitoring was increased with the progress of the embankment construction work. After the construction of the embankment up to the required level, the monitoring frequency was reduced to once a week. But daily records of the vacuum pressure at the pump and under the sheet as well as piezometer readings were taken from the beginning to the completion date of the treatment.

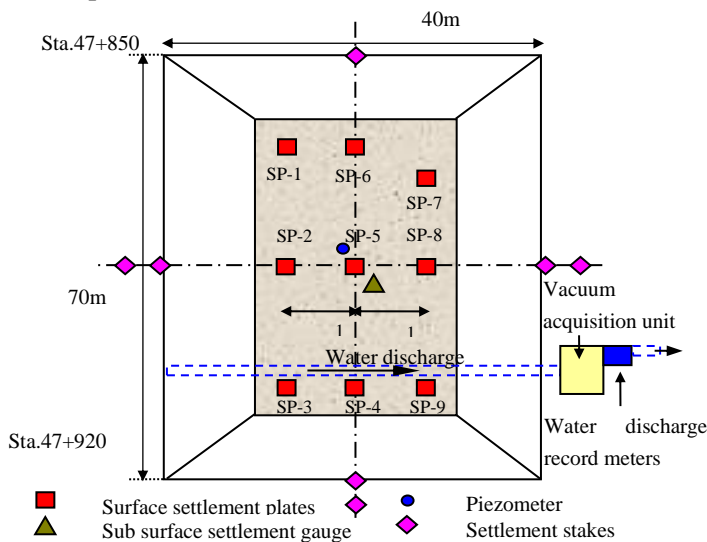


Fig. 7 Plan of the embankment and instrumentation layout

## 6 ASSESSMENT OF THE SOFT GROUND IMPROVEMENT

The performance of the ground improvement was evaluated in terms of the degree of consolidation, improvement of the physical and engineering properties, increase in pre-consolidation pressure, and gain in shear strength of the peaty soil.

### 6.1 Estimation of Degree of Consolidation

The ground improvement achieved was investigated by calculating the degree of consolidation using the observed field settlements before the termination of the vacuum operation and the removal of the surcharge. The degree of consolidation is calculated as the ratio of the current settlement to the expected

ultimate primary settlement. In the present work, ultimate primary settlement and the degree of consolidation were estimated by means of the Asaoka (1978) and hyperbolic (Tan et al. (1991)) methods using the measured field settlement data. The graphical plot of the Asaoka method based on the observed settlement under the center of the embankment (SP 5) at the vacuum consolidated ground improvement section from Ch.47+850 km to Ch. 47+920 km is shown in Fig. 9.

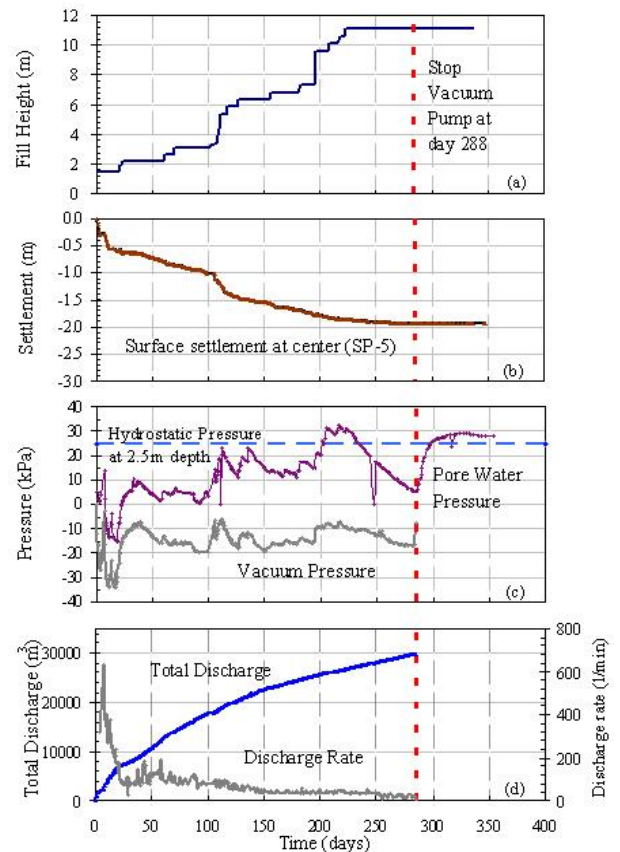


Fig. 8 Field monitoring data

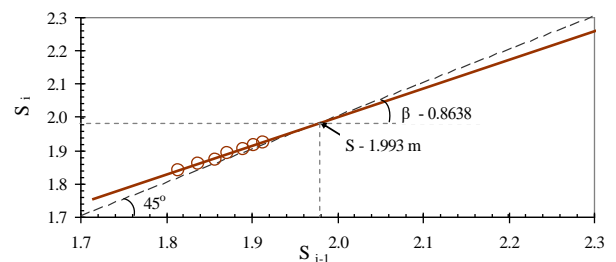


Fig. 9 Graphical plot of Asaoka method

It is seen that at the end of CVC treatment, the achieved degree of consolidation is around 97%. The degree of consolidation was also calculated based on the pore water pressure measurements (PWP), and laboratory consolidation testing of peaty samples after the treatment program. The comparison of the degree of consolidation for each method is shown in Table 1.

Table 1. Estimation of the degree of consolidation

Location	Degree of Consolidation		
	Asaoka Method	Laboratory Data	PWP
Ch. 45+380 – Ch. 45+430	97.83%	83.10% 73.87%	79.46%
Ch. 47+850 – Ch. 47+920	97.10%	100.00% 100.00%	100.00%
Ch. 52+950 – Ch. 53+000	97.57%	80.21% 90.91%	100.00%
Ch. 53+660 – Ch. 53+730	96.65%	96.70% 83.62%	68.71%

If the degree of consolidation from the PWP measurement is assumed to be accurate, the Asaoka Method accurately estimates the degree of consolidation in treatment areas 47 + 850 to 47 + 920 and 52 + 950 to 53 + 00 whereas the Asaoka method over-predicts the degree of consolidation in treatment areas 45 + 380 to 45 + 430 and 53 + 660 to 53 + 730. However, in treatment areas 53 + 660 to 53 + 730 the degree of consolidation from the laboratory test results agrees very well with the same estimated from the Asaoka method. Therefore, based on this investigation it can be concluded that the degree of consolidation estimated from the Asaoka method is reasonably accurate.

In order to assess the secondary settlements, for each monitoring point, the long-term settlement was predicted by extrapolating the secondary settlement rate over a period of 3 years. Predictions were made by preparing a plot of displacement against log (time) for each settlement plate, with the best-fit line through the data extended to define the likely settlement after 3 years. The surcharge was removed only after confirming the residual settlement by considering both the primary and secondary consolidation settlements as described above.

Table 2. Change in peat thickness, water content, and void ratio due to CVC improvement

Location	Peat Layer Thickness (m)		Water Content (%)		Void Ratio		% Change in Thickness of Peat	% Change of Water Content	% Change of Void Ratio
	Initial	Final	Initial	Final	Initial	Final			
Ch.45+380- Ch.45+430	7.70	2.30	378.3	163.6	6.83	3.916	70.13	56.75	42.66
			406.8	137.3	10.11	3.805			
Ch.47+850- Ch.47+920	4.70	2.00	370	141.0	5.54	1.810	57.45	61.89	67.33
			398	168.0	5.58	1.940			
Ch.52+950- Ch.53+000	5.85	2.85	378.3	175.7	4.10	1.900	51.28	53.56	53.66
			471.2	105.8	9.35	2.580			
Ch.53+660- Ch.53+730	5.25	2.76	111.6	86.6	3.06	1.810	47.43	22.40	40.85
			122.9	79.7	2.66	2.000			

### 6.2 Improvement of Physical and Mechanical Properties of Peat

A site investigation was carried out to assess the actual ground improvement in the areas improved by the heavy tamping and vacuum consolidation method just before the removal of the surcharge. The investigation was carried out in the improved as well as the adjacent unimproved area in order to assess the ground improvement. Site investigation comprised of advancing boreholes with Standard Penetration Test (SPT), collection of undisturbed soil samples, performing of Field Vane Shear Test, Cone Penetration Test (CPT), and performing of laboratory tests. The improvement of the physical and mechanical properties of peat due to heavy tamping improvement is described in Karunawardena (2011). The observed subsoil in one of the CVC improved areas deduced from the borehole investigation is shown in Fig. 10. In the same figure recorded SPT values are also plotted along the depth.

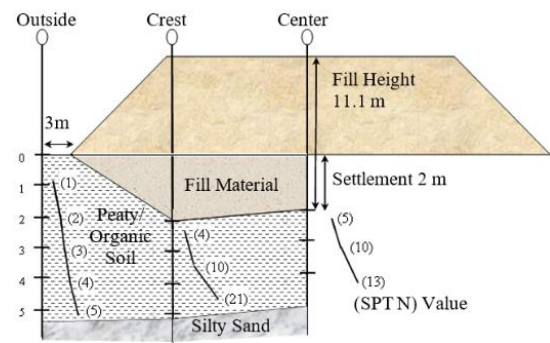


Fig. 10 Subsoil profile of improved and unimproved area

The observed change in the peaty soil layer thickness, the changes in water content, and the void ratio due to CVC ground improvement are given in Table 2. Accordingly, the initial thickness of the peat layer has been reduced by 50%-60% after ground improvement. The above reduction reasonably agreed with the percentage change of water content and void ratio values obtained from peaty soil collected from the improved and unimproved areas. The summary of laboratory test results from the peat samples collected from the improved and unimproved area of Ch.47+850 to Ch.47+920 is given in Table 3. Consolidation tests revealed a significant reduction in the compression index which is proportional to primary consolidation settlement. The compression index of the peat layer has reduced from a range of 2.65 to 2.13, to as low as 0.90 as a result of the ground improvement. The average reduced value is about 1.65.

Table 3. Summary of laboratory test results

Location	Depth (m)	$W_n$ (%)	$e_o$	$c_c$	$c_\alpha$	$C_u$ (kPa)
Improved Area – BH1	3.0	227	4.21	1.80	0.055	85
Improved Area – BH2, 5	3.5	266	4.50	1.95	0.061	120
Unimproved Area – BH3	3.5	141	1.81	0.90	0.037	55
Unimproved Area – BH3	4.5	168	1.94	1.94	0.048	70
Unimproved Area – BH3	2.5	370	5.54	2.13	0.110	22
Unimproved Area – BH3	3.5	398	5.58	2.65	0.120	33

The reduction of secondary compression is very important as the secondary compression phenomenon is dominant in the peaty soil. The results of long-term consolidation tests carried out in the improved and unimproved peaty samples are shown in Table 3. It reveals that the coefficient of secondary consolidation has reduced from a range of 0.10 to 0.13 to a range of 0.03 to 0.06. Subsequently the ratio of  $c_\alpha/c_c$  has decreased from 0.050 to 0.029 due to ground improvement. The estimation carried out based on the above information assures that the residual settlement would be less than 150 mm by the end of 3 years after construction as required in the contract (Karunawardena (2009)).

### 6.3 Increase in Preconsolidation Pressure and Undrained Cohesion

It is expected that the subsoil behave in an over-consolidated state during the service life of the structure after the completion of ground improvement. This can be verified by the pre-

consolidation pressure determined through the 1-D consolidation test. Consolidation tests carried out from section Ch.47+850 to Ch.47+920 indicated that the pre-consolidation pressure of the peaty soil found under the embankment has increased from 28 kPa – 38 kPa range to 160 kPa – 180 kPa range after ground improvement as shown in Fig. 11. The expected load induced on the peaty layer due to the proposed embankment is around 145 kN/m<sup>2</sup>. Therefore, the subsoil will behave under the over-consolidated state with an Over Consolidation Ratio (OCR) of 1.2 to 1.3 during the service life of the highway and hence will only give rise to very small settlements in the future.

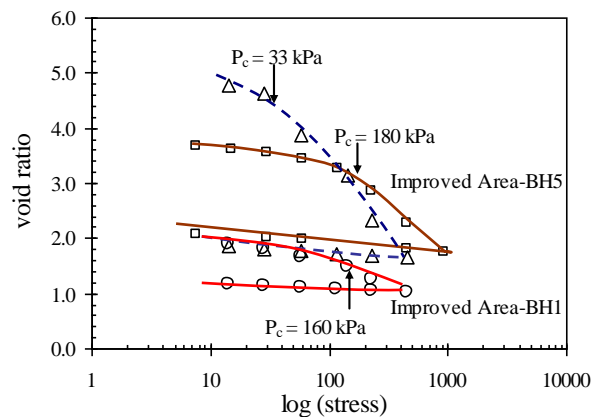


Fig. 11 Consolidation Test Results

Consolidation test results related to some other sections also indicated that the pre-consolidation pressure of the peaty soil found under the embankment has increased as shown in Table 4. Table 4 also shows the expected load induced on the peaty layer due to the proposed embankment and the subsoil over consolidation ratio. According to the data in Table 4, the subsoil will behave under the over-consolidated state with an Over Consolidation Ratio (OCR) of 0.98 to 1.33. It should be noted here that even though the applied vacuum pressure and the fill surcharge load are adequate to yield an OCR value in the range of 1.2 to 1.3, sometimes the calculated OCR is less than the anticipated value. This might be due to the inaccurate  $P_c$  value obtained from the consolidation test as a result of sample disturbance.



Table 4. Increase in pre-consolidation pressure and undrained cohesion

Location	Expected Load (kPa)	P <sub>c</sub> (kPa)	OCR	C <sub>u</sub> (kPa)	( $\Delta c_u / \Delta \sigma'_v$ )
Ch.45+380- Ch.45+430	160.0	180 160	1.13 1.00	79.0 57.0	0.49 0.36
Ch.47+850- Ch.47+920	145.0	200 180	1.37 1.25	55.0 70.0	0.36 0.45
Ch.52+950- Ch.53+000	152.5	150 170	0.98 1.11	41.5 38.2	0.27 0.25
Ch.53+660- Ch.53+730	150.0	170 147	1.13 0.98	54.0 50.5	0.36 0.34

The SPT and Field Vane Shear results indicate that the strength has improved in the compressible layer due to the ground improvement and as a result, the status of the compressible layer has been changed from a very soft to medium stiff state. The strength gained due to ground improvement was investigated by calculating the ratio between the increments of undrained shear strength of peaty soil and the effective stress ( $\Delta c_u / \Delta \sigma'_v$ ). The undrained cohesion of the peaty soil was determined from unconsolidated un-drained triaxial tests and the preconsolidation pressure was obtained from oedometer tests on undisturbed soil samples. The ratio between the increment of undrained shear strength of peaty soil and the effective stress after the treatment program was obtained to be 0.25 to 0.49.

## 7 OBSERVED SETTLEMENT AFTER PAVEMENT CONSTRUCTION

The surface settlement of the highway embankment constructed over the improved soft ground was monitored by installing the settlement markers at 50 m intervals after the construction of the road pavement. Initially, for about a 6 month period, before the road was opened to traffic, surface settlement was monitored at both the center and the edge of the embankment. The observed settlements were in the range of 0 mm to 5 mm in most of the ground-improved sections except at very few locations where high embankments were constructed over thick peat deposits by improving the vacuum consolidation method. The observed surface settlement in those areas was around 10 mm to 20 mm at the end of six months after the construction of the pavement. After the highway was opened to traffic in November 2011, settlement monitoring was carried out only along the edge of the highway embankment considering safety

reasons. The observed total surface settlement up to September 2012, ten months after opening to traffic, is shown in Fig. 12. The observed settlement was less than 5 mm in most of the sections, and in only two locations the settlement exceeded 20 mm. The maximum observed settlement was 35 mm and the settlement prediction using the monitoring data indicates that the estimated residual settlement is less than 15 mm at the end of 3 years after the handing over of the project.

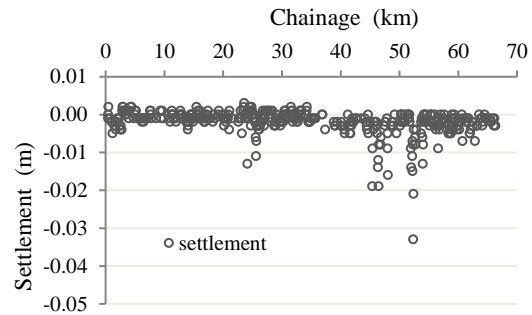


Fig. 12 Results of the surface settlement monitoring

## 8 CONCLUSION

This paper presents the successful application of ground improvement work carried out in the construction of the Southern Highway project in Sri Lanka. Ground improvement methods such as heavy tamping method and vacuum consolidation techniques were applied to construct the high embankments over thick peaty deposits. In both methods, a surcharge load had been applied to over-consolidate the peaty soil. Field monitoring data obtained during the construction period indicates that the primary consolidation settlement due to the final load of the highway embankment has already been completed and the secondary settlement had been reduced to control the residual settlement within acceptable performance limits. Investigations carried out at the site show that both physical and mechanical properties of the peat have improved significantly and the peaty soil will behave in an over-consolidated state with a ratio of 1.2 to 1.3 during the service life of the highway. The results of the post-construction surface settlement monitoring of the expressway carried out up to date reconfirm that the ground improvement work was successful and the expected residual settlements are well below the allowable limit in the contract.

## ACKNOWLEDGMENT

The author is grateful to the Road Development Authority of Sri Lanka, Oriental Consultants Co., Ltd., Japan, and the National Building Research

Organization Sri Lanka for the necessary approval and support extended towards writing this paper.

## REFERENCES

- Asoka, A. (1978). Observational Procedure of Settlement Prediction, *Soil and Foundation*, 18(4):87-101.
- Karunawardena, A. (2007). Consolidation Analysis of Sri Lankan Peaty Clay using Elasto-viscoplastic Theory.” Doctoral Thesis, Kyoto University, Japan.
- Karunawardena, A. and Nithiwana, W., (2009), Construction of a trial embankment on peaty ground using vacuum consolidation method for a highway construction project in Sri Lanka, *Soil Mechanics and Geotechnical Engineering*, Alexandria 2009, 17th International Conference, Vol. 3, pp. 2200-2203
- Karunawardena, A. and Toki, M. (2011). Application of the Heavy Tamping Method on Sri Lankan Peaty Clay for the Construction of a Highway Embankment, *Soil Mechanics and Geotechnical Engineering*, Hong Kong, China 2011, 14th Asian Regional Conference
- Lukas, R. G. (1995). Geotechnical Engineering Circular No. 1, Dynamic Compaction, Federal Highway Report. FHWA-SA-95-037, U.S.A.
- Tan, T.S., Inoue, T. and Lee, S.L., ( 1991). Hyperbolic method for consolidation analysis, *Journal of Geotechnical Engineering*, 117(11): 1723–1737
- Technical report on Heavy Tamping Trial, (2007). Oriental Consultants Co., Ltd., Japan, Southern Transport Development Project, JABIC founded Section, Sri Lanka

Bronze Sponsor:



**sierra**

**SETTING STANDARDS LOCALLY TO MEET INTERNATIONAL QUALITY**



ROAD CONSTRUCTION



POWER



TELECOMMUNICATION



WATER SUPPLY &  
SEWERAGE



PILLING



BUILDING

[www.sierra.lk](http://www.sierra.lk)





**POST-CONSTRUCTION SETTLEMENTS OF  
EXPRESSWAYS**

**By**

**Prof. Saman Thilakasiri, Senior Professor, Sri Lanka Institute  
of Information Technology (SLIIT)**



Prof. Saman Thilakasiri is a Senior Professor at the Faculty of Engineering, Sri Lanka Institute of Information Technology (SLIIT). He holds a First-Class Honors Engineering Degree from the University of Moratuwa, Sri Lanka, a Master's Degree with Distinction from Imperial College, London, UK, and a PhD from the University of South Florida, USA. With a robust academic career spanning over three decades since 1990, Prof. Thilakasiri has served in various academic capacities.

In addition to his academic pursuits, he has extensive experience as a senior engineer on numerous national-level projects. He obtained chartered status from the Institution of Engineers Sri Lanka (IESL) in 2003 and became a Fellow of the same institution in 2007. Prof. Thilakasiri has also gained valuable experience from prestigious educational institutions in the USA, UK, and Australia, serving as a research student, adjunct faculty, and research fellow.

Before joining SLIIT in 2014, he held significant administrative roles at the University of Moratuwa, including Director of Undergraduate Studies and Postgraduate Research Coordinator for the Faculty of Engineering. His diverse expertise in engineering and education continues to make a substantial impact on the field in Sri Lanka and beyond.





# Measurements and Prediction of the Post-Construction Settlements of Highways

H. S. Thilakasiri

*Sri Lanka Institute of Information Technology (SLIIT), Sri Lanka*

**ABSTRACT:** Organic soil deposits, formed from decomposed plant and animal residues, pose significant challenges for construction due to their low shear strength and high compressibility. The majority of these deposits are found in temperate regions, with only 8-11% located in tropical areas, such as Sri Lanka. Sri Lankan organic soil deposits, concentrated in the western and southern coastal regions, particularly in areas like Muthurajawela and Kotte (Lappalainen, 1996), exhibit unique geotechnical challenges. These deposits, formed under tropical conditions, are primarily amorphous with high degrees of decomposition and variable organic content. Due to the increasing use of treated soft grounds for highway construction, it is crucial to critically understand the properties and engineering behavior of these soil deposits. The study involved extracting undisturbed soil samples from 13 locations along the Colombo-Katunayake Expressway and Outer Circular Highway. After the construction of the Colombo Katunayake Expressway, some points along the highway were earmarked to measure the post-construction settlements. These measured settlements were compared with the various post-surcharge secondary consolidation prediction methods, such as those proposed by Ladd (1971) and Mesri et al. (1997), the Hyperbolic method against actual field settlement data. The comparison is shown. Then,  $C^{\alpha}/C_{\alpha}$  method put forward by Mesri et al. (1997) was modified according to the Sri Lankan conditions, and a good match between settlement prediction was shown.

## 1 INTRODUCTION AND RESULTS

After the construction of the Colombo Katunayaka Expressway (CKE), some points were installed with settlement measuring nails and those points were measured for settlement from time to time. Those measured settlements were compared

with the prediction methods given by Ladd (Ladd, 1971), Mesri (Mesri et al., 1997), and Hyperbolic (Tan et al., 1991) methods. The loading of the highway is shown in Figure 1.

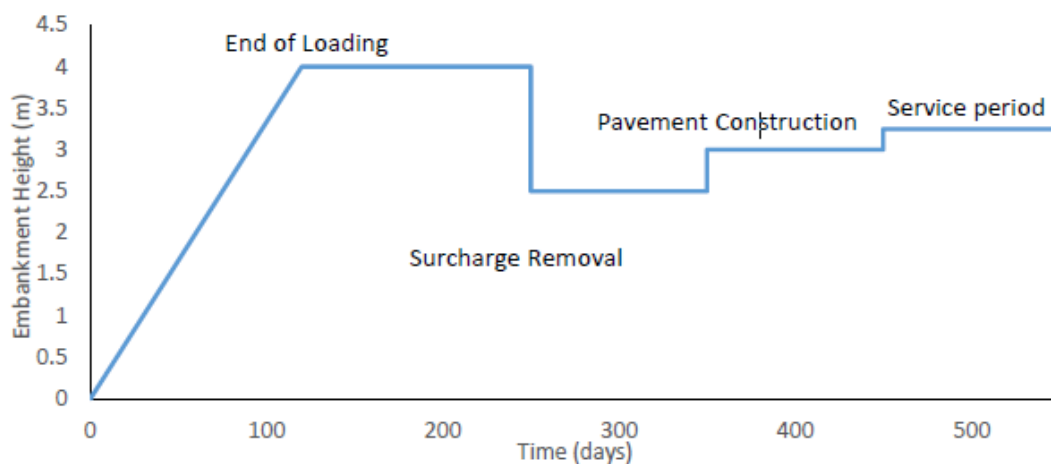


Fig. 1 – Loading of the sections considered.

According to the first two methods mentioned above, the effective overburden pressures in each loading phase were calculated, and the over-consolidation ratio (OCR) was determined. In the

Ladd method, the Amount of Surcharge (AOS) was then calculated, which is equivalent to  $OCR - 1$ . The Ladd method introduces an adjustment for AOS, commonly referred to as Adjusted Amount of Surcharge (AAOS) when the primary consolidation

underneath the embankment has not been completed. After that, the post-surcharge secondary consolidation settlement can be conveniently predicted by  $C\alpha$  determined, referring to the applicable relationship.

On the other hand, in the Mesri method, once the OCRs are calculated, the relevant  $t/t_l$  ratio should be calculated where  $t$  is the time in which the post-surcharge secondary consolidation should be determined and  $t_l$  is the time of the end of primary consolidation. Then, with the  $R = OCR - 1$  and time ratios, the relevant  $C\alpha$  can be determined using the graphical relationships provided in Mesri method.

The third method, (the hyperbolic method) does not involve any such calculations. The settlement

monitoring data during the construction period was used to determine the hyperbolic parameters relevant to the Sri Lankan low organic content clayey soils beneath the embankments. Afterward, the post-surcharge secondary consolidation settlement of the embankment sections was calculated using the hyperbolic parameters for the construction period. As the hyperbolic method doesn't discuss the post-surcharge secondary consolidation settlement, it was assumed that the post-surcharge secondary consolidation would behave similarly to that of normally consolidated soil. The comparison is shown in Figure 2.

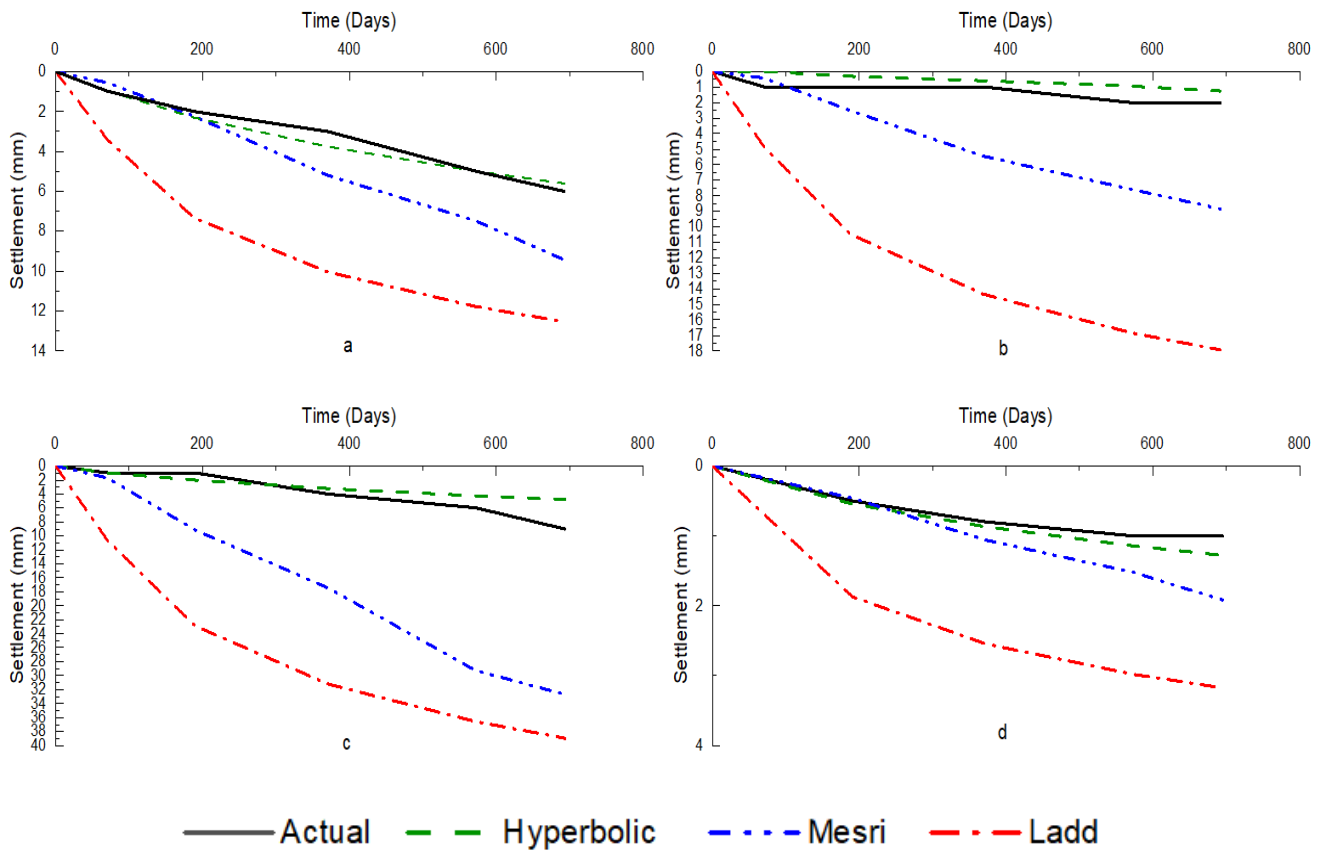


Fig. 2 – Comparison of the actual measured settlements with the prediction methods.

For the prediction method of Mesri, Figure (3a) was used to determine the predicted post-construction settlements. Figures (3a) to (3c) show that the shape of the curve depends on the location

of the peat deposit. The low organic soils found in Sri Lanka may be different. Therefore  $C''\alpha/C\alpha$  was developed for Sri Lankan peaty soils, as shown in Figure 4.



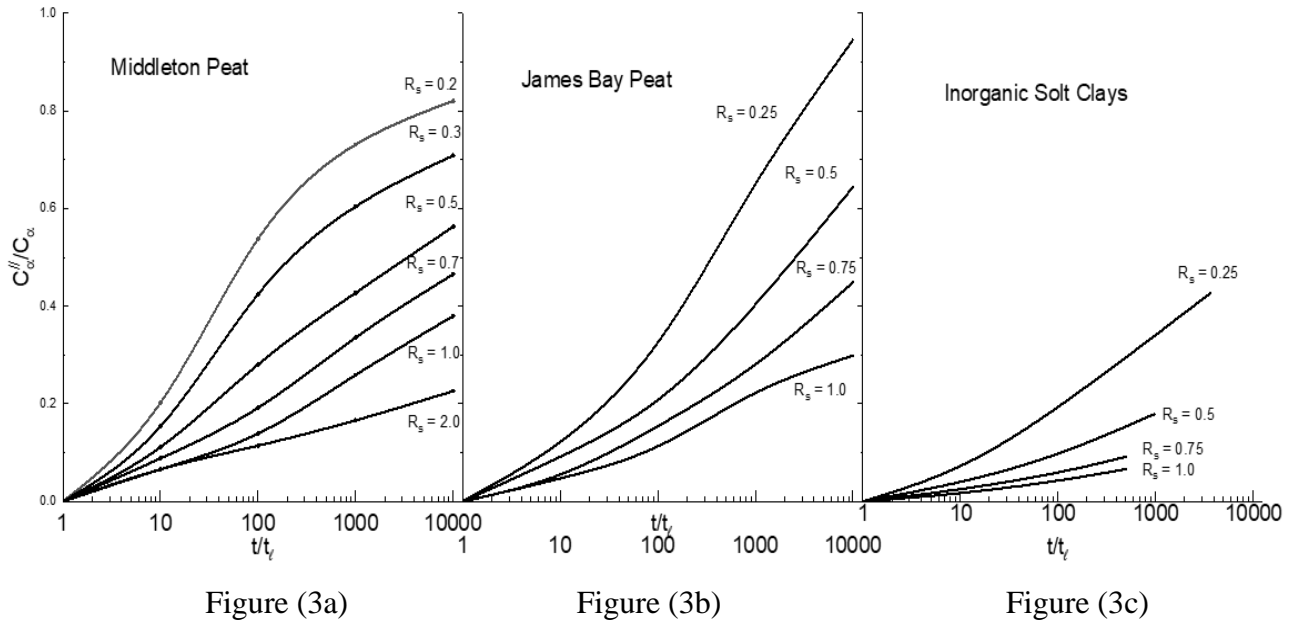


Fig. 3 – Variation of Secondary consolidation coefficient.

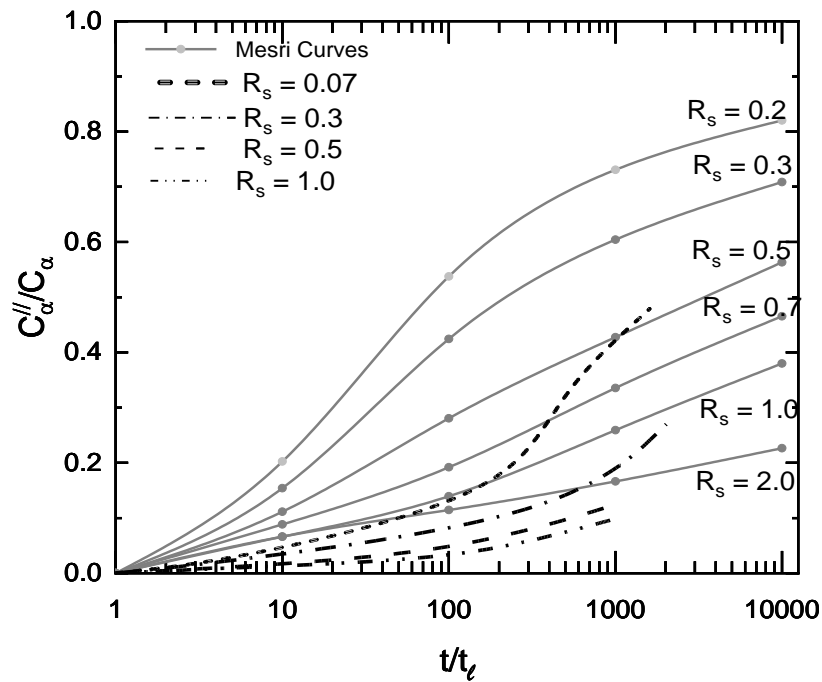


Fig 4. -  $C''/C_\alpha$  variation for Sri Lankan Peaty soil.

Using the above-developed curves, the comparison study was done. The results are shown in Figure 5.

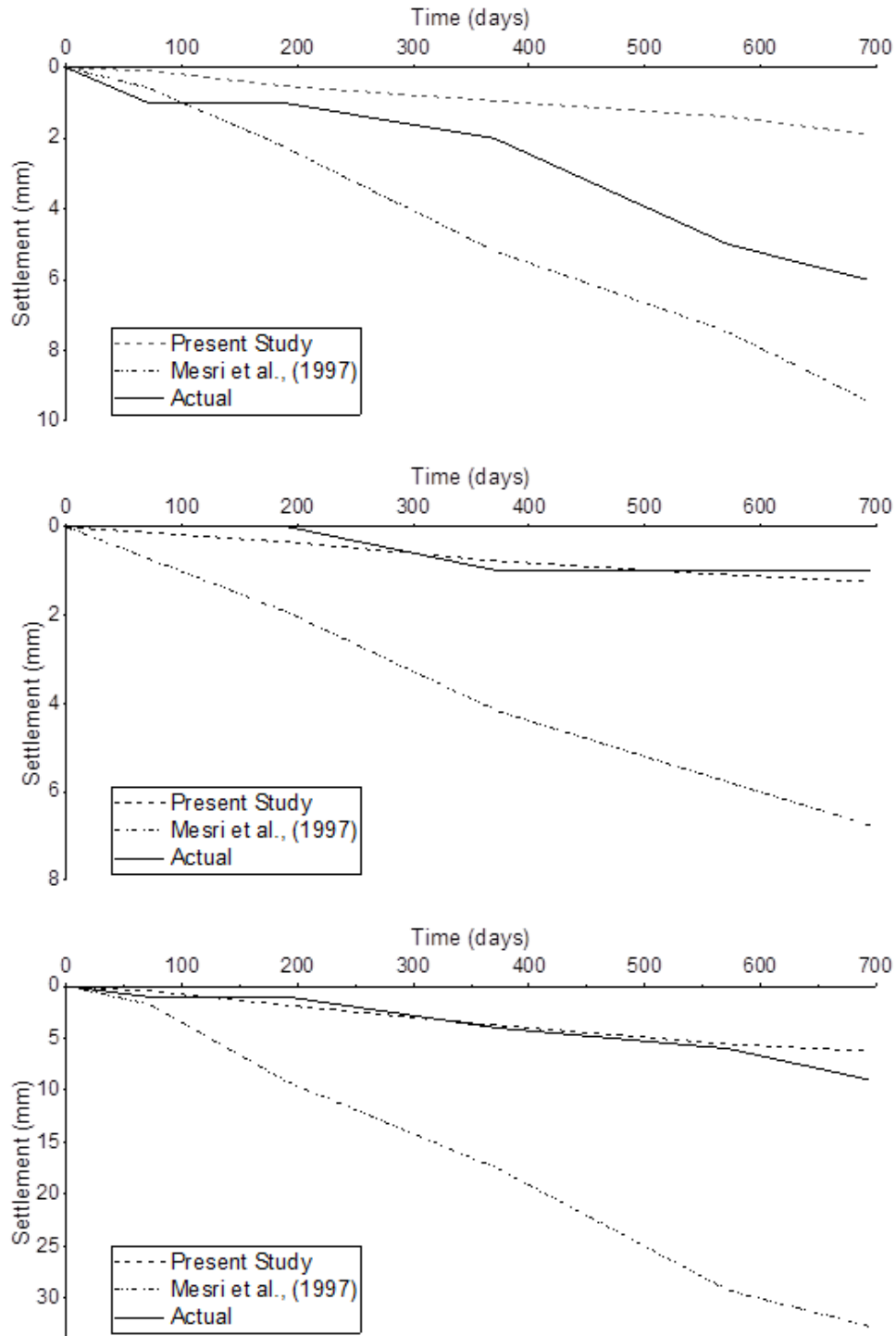


Fig. 5 – Comparisons of the actual measured settlements with the Predicted settlements.

## 2 CONCLUSIONS

The hyperbolic method, though not usually used for post-surge secondary settlement prediction, can be used for short-term predictions.

Mesri method if modified to suit specific geological conditions, can be accurately used in settlement prediction.

The  $c'_\alpha/c_\alpha$  vs Time Ratio curves for low organic clayey soils can be used to accurately predict post-surge secondary consolidation.

Laboratory testing should be carried out to further improve the proposed  $c_{\alpha}''/c_{\alpha}$  vs Time Ratio curves

- Include more surcharge efforts ( $R = OCR - 1$ )
- Longer time periods
- Different curves for a wider range of organic content

## REFERENCES

- Ladd, C. C. (1971). Secondary compression of clays. *Journal of the Soil Mechanics and Foundations Division, American Society of Civil Engineers (ASCE)*, 97(7), 1613–1641.
- “Lappalainen Espoo (Finland)],” E. [ed. ; G. S. of F. (1996). *Global peat resources. Finland.* <https://doi.org/https://doi.org/>
- Mesri, G., Stark, T., Ajlouni, M., & Chen, C. (1997). Secondary Compression of Peat with or without Surcharging. *Journal of Geotechnical and Geo - environmental Engineering*, 123, 411–421. [https://doi.org/10.1061/\(ASCE\)1090-0241\(1997\)123:5\(411\)](https://doi.org/10.1061/(ASCE)1090-0241(1997)123:5(411))
- Tan, T., Inoue, T., & Lee, S. (1991). Hyperbolic Method for Consolidation Analysis. *Journal of Geotechnical Engineering*, 117(11), 1723–1737. [https://doi.org/10.1061/\(ASCE\)0733-9410\(1991\)117:11\(1723\)](https://doi.org/10.1061/(ASCE)0733-9410(1991)117:11(1723))

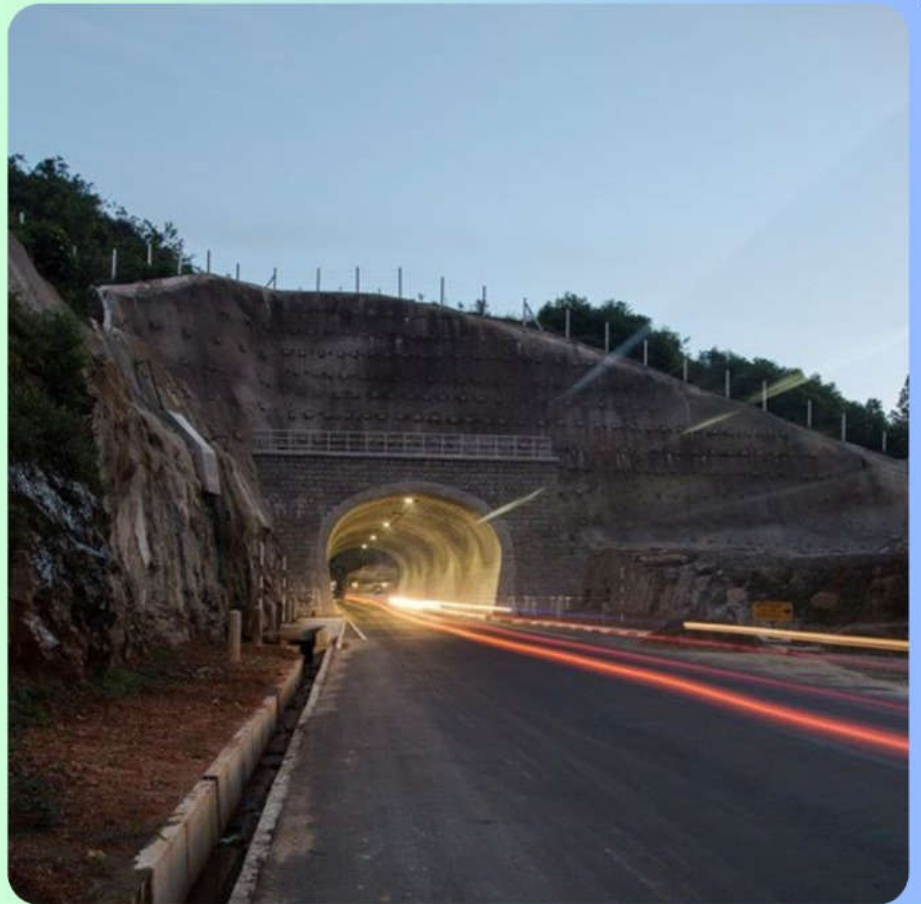






Bronze Sponsor:

**ELS CONSTRUCTION (PVT)LTD**  
**ENGINEERING & LABORATORY**  
**SERVICES (PVT)LTD**



**QUALITY IS**  
**OUR**  
**TRADEMARK**

- ✓ BRIDGE CONSTRUCTION
- ✓ PRE-CAST
- ✓ PILING
- ✓ GEOTECHNICAL INVESTIGATION
- ✓ LABORATORY TESTING
- ✓ SOIL NAILING & SLOPE STABILIZATION
- ✓ MARINE CONSTRUCTION

📍 NO 62/3, NEELAMAHARA  
ROAD, KATUWAWALA, BORALESGAMUWA, SRI LANKA

☎ (94) 11 4309494, (94) 11 2519727

✉ ELS@ELSLANKA.COM

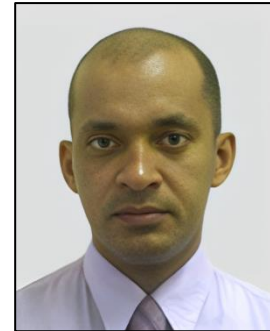
🌐 WWW.ELSLANKA.COM



**FAILURE OF GRAVEL COMPACTION PILE (GCP)  
IMPROVED EMBANKMENT – A CASE STUDY**

**By**

**Prof. Nadeej Priyankara, Professor, Department of Civil and  
Environmental Engineering, University of Ruhuna**



Prof. N. H. Priyankara is a prominent figure in Geotechnical Engineering, currently serving as a Professor in the Department of Civil and Environmental Engineering at the University of Ruhuna. With a Ph.D. in Geotechnical Engineering from Tohoku University, Japan, an M.Eng. from the Asian Institute of Technology (AIT), Thailand, and a B.Sc. (Hons.) from the University of Moratuwa, he possesses extensive expertise in his field. Prof. Priyankara is a Chartered Engineer and a Corporate Member of the Institute of Engineers Sri Lanka (IESL), actively contributing to professional organizations such as the Sri Lankan Geotechnical Society (SLGS) and the International Society of Soil Mechanics and Geotechnical Engineering (ISSMGE).

His accolades include the 10<sup>th</sup> Vice-Chancellor's Award in 2013 for the highest research grants and winning the Project Day Competition organized by SLGS in 2000. His research interests span soft ground improvements, slope stability, foundation design, landfill clay liner development, and sustainable construction using waste materials. Dedicated to advancing geotechnical engineering, Prof. Priyankara's research emphasizes practical applications in infrastructure, soil stabilization, and pavement construction. He continues to inspire the next generation of engineers through his teaching and contributions to Sri Lanka's engineering community.







# Failure of Gravel Compaction Pile (GCP) Improved Embankment – A case study

N. H. Priyankara

*Department of Civil and Environmental Engineering, University of Ruhuna, Sri Lanka*

**ABSTRACT:** Due to the scarcity of good lands, it becomes necessary to utilize marshy lands consist of soft soil for infrastructure development. Soft soil has a problematic nature due to its high moisture content, high compressibility, high void ratio and very low shear strength. Hence, it is a responsibility of the geotechnical engineers to overcome these issues by adopting suitable ground improvement techniques. Gravel Compaction Pile (GCP) is one of the most popular soft ground improvement techniques used in the field. This technique has been successfully applied during the construction of Colombo-Katunayaka expressway project and Outer Circular highway project. However, GCP technique has been failed in the Southern Expressway Extension Project from Matara to Beliatta section. Therefore, in this research study, the causes of the failure of the GCP improved embankment section were studied based on the field records. The subsurface soil profile was critically analysed using borehole logs as well as GCP installation records. The slope stability of the embankment during construction was analysed using Matsuo and Kawamura's method based on the field monitoring data. Further, the shear strength parameters of the GCP improved composite ground at different stages of construction were back calculated using GEOSLOPE SLOPE/W software. Finally, based on the analysis, possible reasons for the GCP improved embankment failure were presented.

**Keywords:** Gravel Compaction Pile (GCP), Matsuo and Kawamura's method, Slope stability analysis, very soft peaty clay

## 1 INTRODUCTION

The rapid development and population growth of a country would make land very scarce by raising the demand for a substantial number of infrastructures. The scarcity of suitable lands for construction encourages the widespread use of areas underlined by weak soil deposits that are considered either marginal or inappropriate. Due to the scarcity of suitable lands, a considerable percentage of the number of infrastructure development projects in Sri Lanka such as the Colombo – Katunayake expressway, Southern expressway, Outer Circular highway and Central expressway were constructed on flood plains and marshy terrain made up of extremely soft peat, organic soils, and clay [1][2][3][4][5][6].

The road embankment construction over peat deposits is quite challenging, because of the poor peaty soil properties such as high moisture content, high compressibility, high void ratio and very low shear strength [2][3][4][6][7]. The primary consolidation of the peat is very high with significant secondary compression [1][2][3]. Madhusanka and Kulathilaka, 2015 [4] reported that Sri Lankan peaty soil has a high moisture content of about 300 %, low shear strength of about 0.99 kN/m<sup>2</sup>, and a compression index ( $C_c$ ) of 1.51. Further, Karunawardena et al., 2017 [1] stated that

peaty clay found from Outer circular highway has compression index of 1.95 and undrained shear strength of 7.2–19.0 kPa. As such, peaty soil does not provide favourable conditions for construction on them. Therefore, geotechnical engineers face many challenges because the peaty soil cannot support high loading, and construction can result in excessive settlement. In order to overcome these challenges, there are two ways, namely transfer the structural load to underlying hard stratum through piles or improve the engineering properties of soft soil. However, the transferring of load through piles to the hard stratum is not an economical solution for roads occupying a large plan area and moderately loaded buildings. Improving engineering properties of soft soil is the most economical option and it is a responsibility of the geotechnical engineers to find appropriate ground improvement technique/s based on the subsurface soil conditions.

Gravel Compaction Pile (GCP) is one of the most popular soft ground improvement techniques, that aim to increase load-bearing capacity and reduce settlement by densification of subsoil [1][7]. The installation of GCP consists of sequence of routine work as shown in Figure 1. In this method, 40 cm diameter casing is forced into the ground up to the required depth under vibration with a frequency of 10 Hz [8]. Then, casing is retracted

stepwise while supplying granular material into the casing and compact the granular material by casing tip under vertical vibration. As this process is repeated, a well compacted 70 cm diameter Gravel Compaction Pile (GCP) is created.

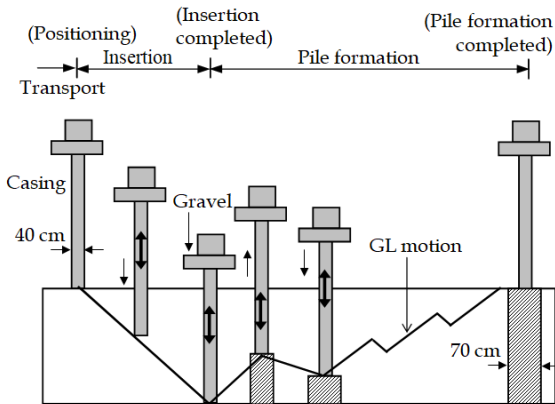


Fig 1 GCP construction procedure

Even though GCP technique has been successfully utilized in the Colombo–Katunayake expressway project and Outer Circular highway project [1][2] to improve soft soil in Sri Lanka, this technique was failed when it was applied for the soft soil improvement in Southern Expressway Extension Project from Matara to Beliatta (Section – 1), causing huge financial loss to the contractor. As such, this paper presents the detail analysis of cause of GCP improved embankment failure and lessons that can be learnt from the incident.

## 2 DETAILS OF GCP TRIAL EMBANKMENT

To expand the expressway network in Sri Lanka, Government of Sri Lanka had decided to extend the existing Southern expressway from Matara to Mattala (Figure 2), which was implemented under four phases namely Matara to Beliatta (Section-1), Beliatta to Wetiya (Section-2), Wetiya to Andarawewa (Section-3) and Hambantota to Mattala via Andarawewa (Section-4) [9].

Section 1 of the Southern Expressway Extension Project from Matara to Beliatta, is mainly going through the Nilwala flood plain which consists of 10.1 km viaducts, 0.6 km bridges/underpass/drainage box culverts, 15.3 km non-treatment area and 4.0 km soft ground treatment area. By considering the sub surface soil profile, initially Gravel Compaction Pile (GCP) technique had been proposed to use as the soft ground treatment method. In order to show the performance of the GCP improved ground, a trial embankment section was done at the chainage (Ch.) 7+405 to 7+475. The typical cross section of the GCP improved embankment is shown in Figure 3.

It can be noted that Existing Ground Level (EGL) is about 0.250 m MSL whereas design Road

Finished Level (RFL) is about 9.760 m MSL. The side slope of the embankment was planned to maintain as 1:1.5 (1 vertical to 1.5 horizontal) above the berm section and 1:1.8 in below the berm. Width of the carriageway is 24.40 m.

### 2.1 Subsurface soil profile

The subsurface soil profile in the trial area was investigated by advancing five numbers of boreholes as illustrated in Figure 4. Two boreholes namely BH-21 and BH-22 were done in the initial stage of the project at the centre line at the Ch. 7+405 and 7+500, respectively and three boreholes namely BH-04, BH-05 and BH-06 were done in the detail design stage at Ch. 7+452 covering the entire cross section.

According to the borehole logs at Ch. 7+405 (BH-21) and Ch. 7+500 (BH-22), soft soil thickness was identified as 17.0 m and 13.0 m, respectively. The subsurface soil profile across the Ch. 7+452 can be idealized as shown in Figure 5. It can be seen that soft soil thickness significantly varied from left to right, where soft soil thickness on Left Hand Side (LHS) is about 4.0 m whereas that on Right Hand Side (RHS) is about 16.0 m.

### 2.2 Geotechnical parameters of subsurface soil

The physical and engineering properties of the subsurface soil based on field and lab test data are summarized in Table 1.

Based on the data presented in the Table 1, it can be noted that subsurface mainly consists of very soft peaty clay followed by completely weathered rock layer. The peaty clay consists of very high moisture content with very high void ratio. Both laboratory triaxial tests and in-situ vane shear test results illustrated that peaty clay has very low shear strength. Furthermore, laboratory oedometer test results indicated that peaty clay has high compression index with very high modified compression index of about 0.3. The average coefficient of consolidation in vertical direction ( $C_v$ ) and modified secondary compression index were found as 0.8 m<sup>2</sup>/year and 0.1, respectively. For a conservative design, coefficient of consolidation in horizontal direction ( $C_h$ ) was assumed as 0.8 m<sup>2</sup>/year.

### 2.3 Gravel Compaction Pile (GCP) installation

Before installation of GCP, 1.5 m high soil fill had been placed on the existing ground as the working platform for the movement of GCP installation machine. Based on the geotechnical parameters presented in the Table 1, GCP were installed at 1.3 m spacing in the Right-Hand Side (RHS) and at 1.6 m spacing in the Left-Hand Side (LHS) in square pattern as there is a considerable variation

of the soft soil thickness from LHS to RHS as shown in Figure 5. The spacing of the GCP was taken as 1.6 m when the soft soil thickness is less than 10 m and vice versa. With the help of vertical vibrating excitation of the vibro-hammer, casing was penetrated through the soft soil to the hard stratum. When the applied current (about 35 A) of the GCP

machine to penetrate the casing was significantly increased (up to about 80A), driving of the casing was terminated as depicted in Figure 6. When the required current to penetrate the casing is significantly increased, that implies casing has been reached to the hard stratum.

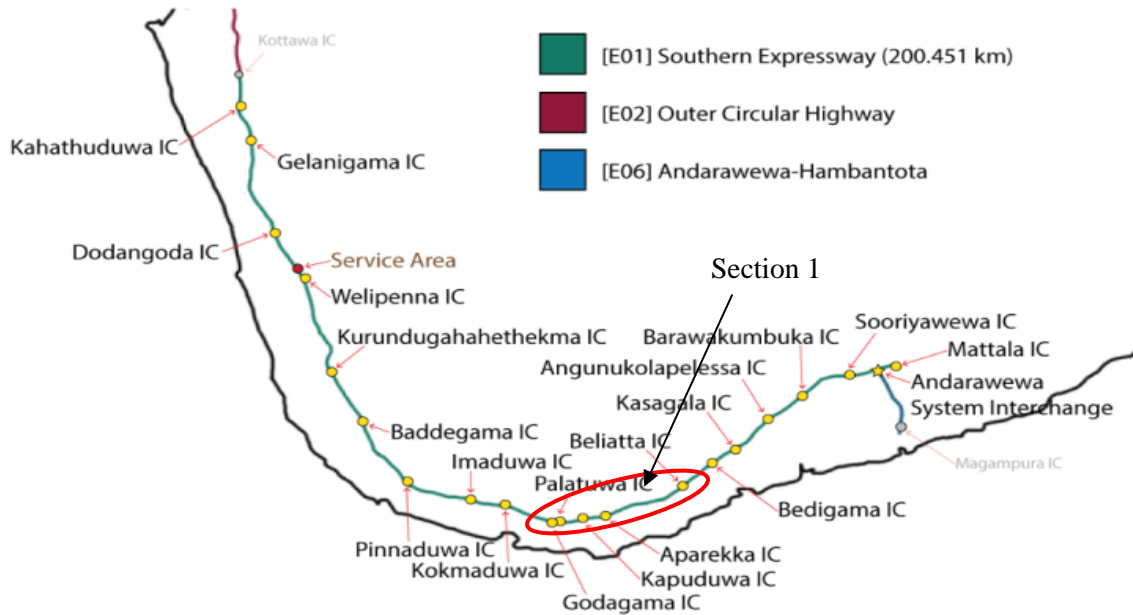


Fig 2 Project location – Southern Expressway Extension Project (Section 1)

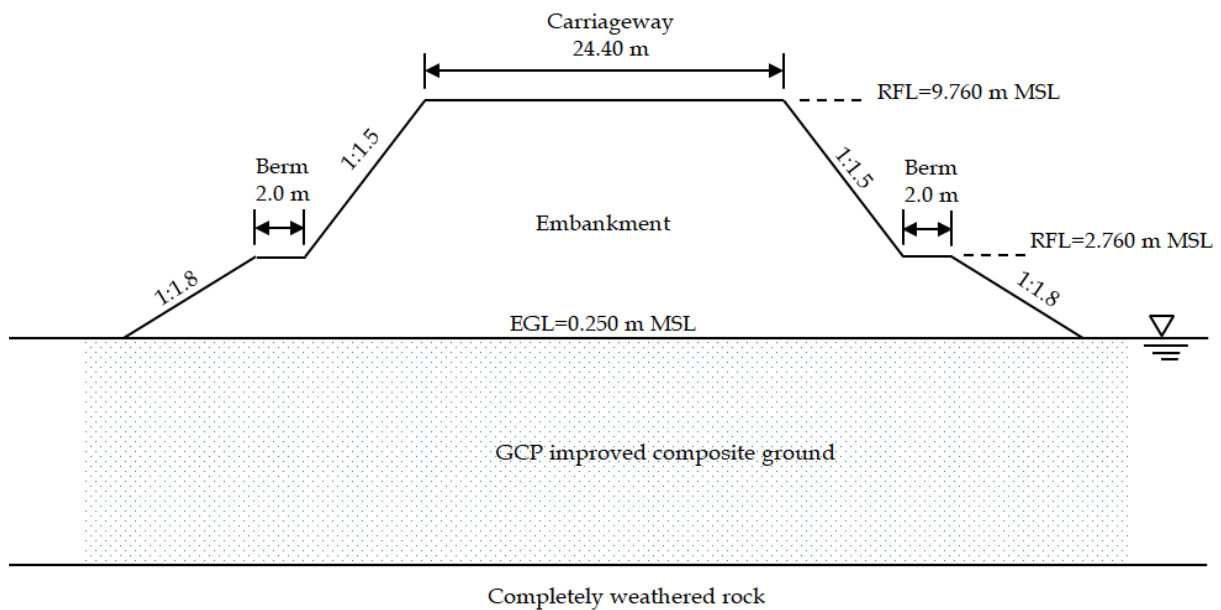


Fig 3 Typical embankment at Ch. 7+405 – 7+475

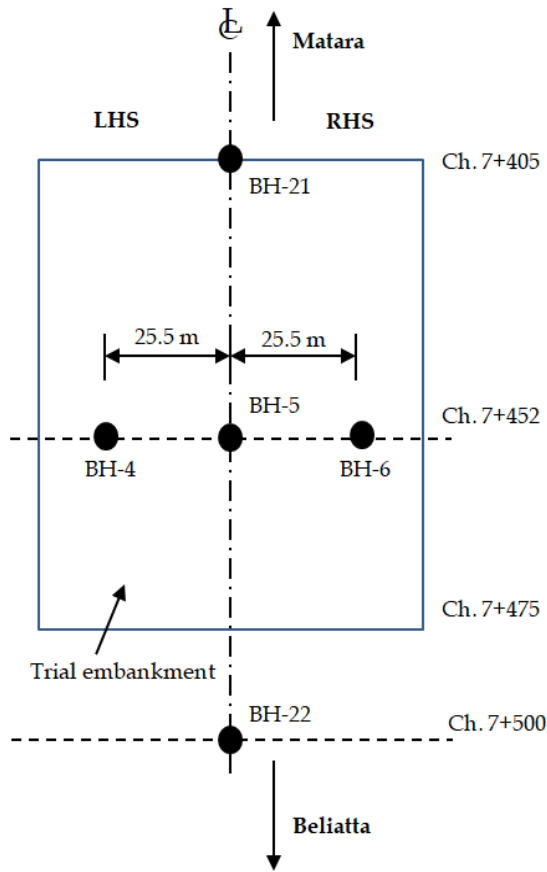


Fig 4 Borehole locations within the GCP trial embankment section

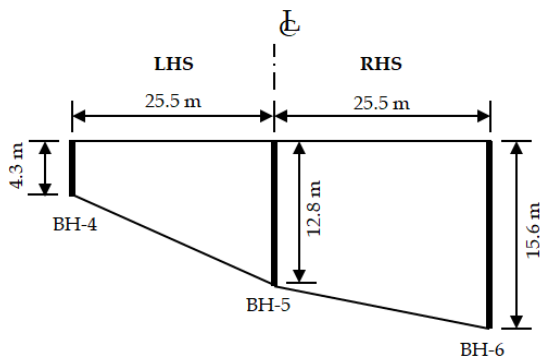


Fig 5 Variation of soft soil thickness across Ch. 7+452

Table 1 – Properties of subsurface soil

Property	Value
Soil type	Blackish grey very soft peaty clay
Natural moisture content (%)	107 – 150
Unit weight (kN/m <sup>3</sup> )	11.38 – 12.85
Coefficient of consolidation ( $C_v$ ) (m <sup>2</sup> /year)	0.8 – 1.5
Compression Index ( $C_c$ )	0.997 – 1.140
Initial void ratio ( $e_0$ )	2.40 – 2.62

Modified Compression Index	
$C_c' = \frac{C_c}{1 + e_0}$	0.28 – 0.33
Modified Secondary Compression Index ( $C_{\alpha}'$ )	0.08 – 0.1
Undrained shear strength ( $C_u$ ) (kPa)	5.75
Undrained friction angle ( $\phi_u$ )	0
Liquid Limit (%)	109 - 159
Plastic Limit (%)	51 - 72

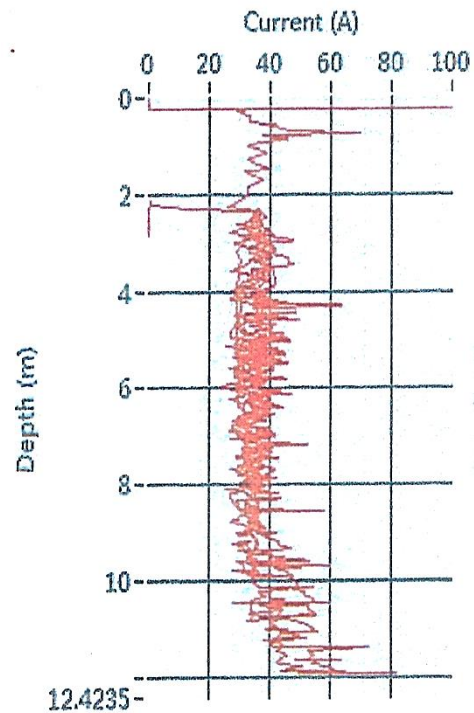


Fig 6 GCP termination criteria based on the current at Ch. 7+470

Further, based on the GCP installation records, variation of soft soil thickness along a particular cross section can be identified as shown in Figure 7. By combining borehole logs and GCP installation records, variation of soft soil thickness within the trial embankment section can be idealized as shown in Figure 8.

Based on this idealization, it can be seen that soft soil thickness in RHS is varied from 12-18 m whereas in the LHS, it is about 4-10 m. Especially, in Ch. 7+405 to 7+420, even in LHS soft soil thickness is varied from 16-18 m. This clearly illustrates the heterogeneous nature of the subsurface soil profile.



2.4 Quality Assurance of GCP

The quality of the GCP was investigated at thirteen (13) GCP locations by conducting Dynamic Cone Penetration Test (DCPT) at the center of the GCP [10][11][12]. Then, the measured DCPT-M values were converted into SPT-N values using the correlation as shown in Equation 1.

$$SPT - N = \frac{DCPT - M}{1.5} \quad (1)$$

The variation of SPT-N values over depth at different GCP locations are presented in Figure 9.

It can be clearly seen that the SPT-N values are gradually increased with the depth due to overburden pressure. Even though SPT-N values are increased with depth, when the overburden correction was applied to estimate the SPT-N value, the corrected SPT-N values are around 40–50 irrespective of the depth. This implies GCP was properly compacted.

Then friction angle of the compacted GCP materials ( $\phi_s$ ) was estimated using Equation 2 [13], where  $\phi_s$  is the friction angle of GCP and N is the field measured SPT-N value.

$$\phi_s = 0.3N + 27 \quad (2)$$

By taking the average SPT-N value of 16 as indicated in Figure 9, it can be calculated that the friction angle of the GCP material  $\phi_s$  is about  $32^\circ$ .

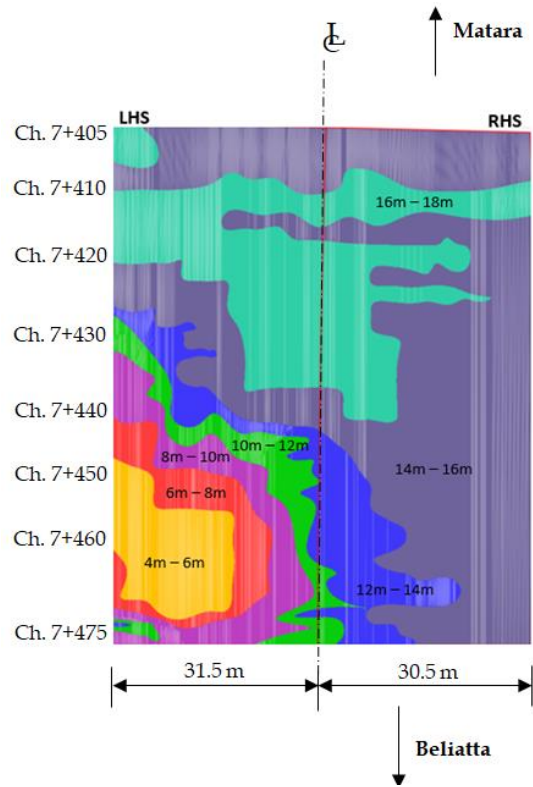


Fig 8 Soft soil thickness contour map within the trial embankment section

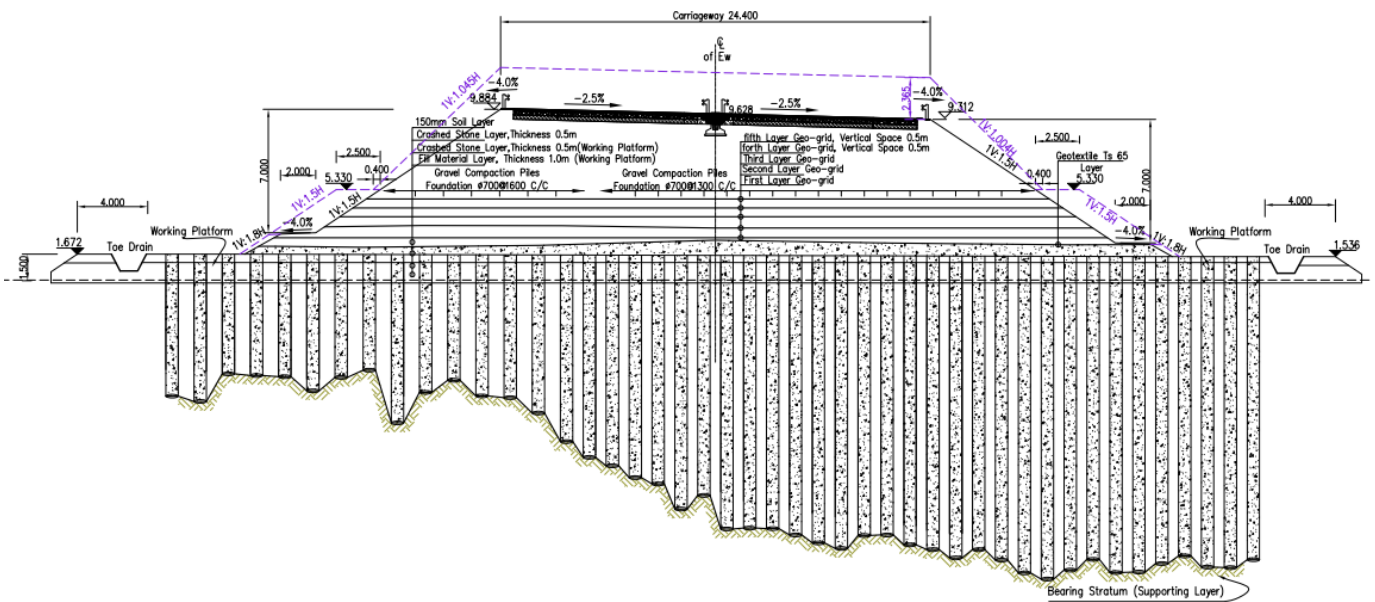


Fig 7 Typical GCP installation records at Ch. 7+460

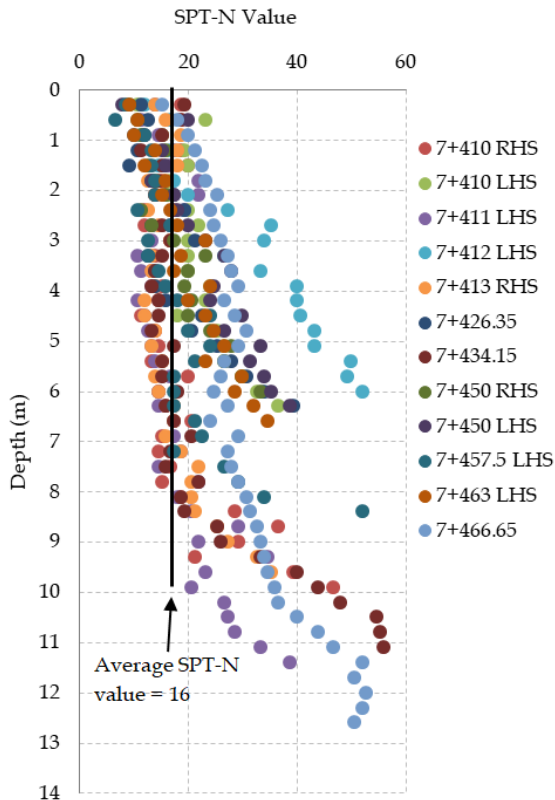


Fig 9 SPT N value over depth at GCP locations

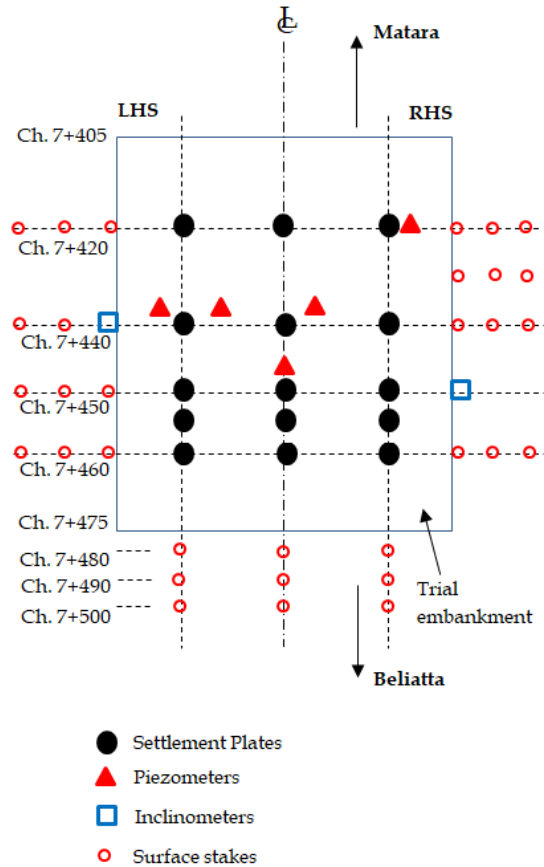


Fig 10 Instrumentations in the GCP trial section

### 2.5 Embankment construction and field instrumentation

Soon after the GCP installation, 0.5 m thick gravel mat was placed as a drainage layer. After that a geotextile was laid as a separator and embankment filling was started. The performance of embankment during construction was evaluated based on the field instrumentation and monitoring data. During the construction of the embankment, the field behaviour was monitored using the 16 settlement plates, 5 vibrating wire piezometers, 2 inclinometers, and 38 surface stakes. The field instrumentation arrangement is shown in Figure 10. Settlement plates were used to measure the settlement of the soft soil underneath the embankment, while piezometers and inclinometers were used to measure the variation of the pore water pressure and lateral displacement of the ground respectively.

Lateral displacement measurements obtained from inclinometers indicated the continuous horizontal movement of the subsoils over the depth under the embankment, while surface stakes are installed near the toe of the embankment were used to measure the lateral movement of the subsoil, close to the ground surface (not vary with depth). Further, surface stakes were installed near the toe of the embankment to check the stability during the construction.

### 3 FIELD OBSERVATIONS

The embankment was constructed in four phases; such as Embankment construction - Stage 1, Waiting period, Berm construction and Embankment construction – Stage 2. The summary of the trial embankment construction is illustrated in Table 2. The graphical presentation of the four phases of the embankment construction is shown in Figure 11.

It can be noted that due to up heaving of the ground during GCP installation, working platform elevation before starting the embankment filling was about 2.0 m MSL. The settlement of the subsurface soft ground due to embankment construction is presented in Figure 12. It can be seen that settlement in the RHS is much higher than that of LHS, where settlement after 277 days at RHS and LHS were about 1.35 m and 0.3 m, respectively. The variation of lateral displacement in RHS of the embankment over depth at different time intervals is illustrated in Figure 13. The variation of rate of lateral displacement over time at RHS of the embankment at the critical depths is shown in Figure 14.

In order to verify the slope stability of the embankment, excess pore water pressure dissipation is one of the key parameters to be

considered. Dissipation of excess pore water pressure during the embankment construction is very important for the consolidation of the subsurface soil to become stiffer and gain strength.

To monitor the excess pore water pressure dissipation, it is necessary to install the piezometer before starting the embankment construction. According to the information provided, 3 piezometers were installed soon after the GCP installation. However, none of the piezometer was under working condition during the embankment construction - stage 1. As such, 2 more piezometers were installed about 60 days after the embankment construction was began, which means after construct the embankment up to 4.0 m MSL elevation.

According to the data obtained, the variation of pore water pressure over time was drawn for Ch. 7+450 and Ch. 7+435 at depths of 3.75 m and 8.45 m, respectively as shown in Figure 15. It can be clearly seen that pore water pressure is gradually increasing with time during all the phases. Even during the waiting period, without filling the embankment, there is no any dissipation of excess pore water pressure.

Table 2 Summary of trial embankment construction

Phase	Details	Duration (Days)
0	Platform construction and GCP installation	-
1	Embankment construction – Stage 1	100
2	Waiting period	89
3	Berm construction	40
4	Embankment construction – Stage 2	48

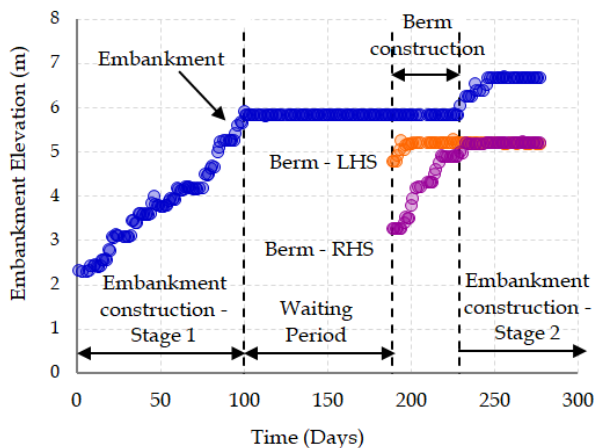


Fig 11 Variation of embankment elevation over time at Ch. 7+455

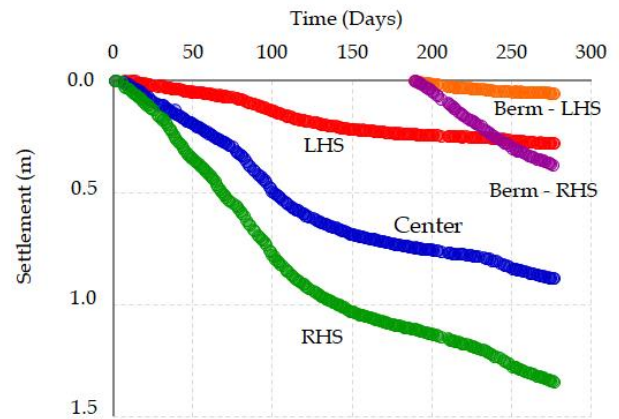


Fig 12 Settlement over time at Ch. 7+455

#### 4 ANALYSIS

##### 4.1 Slope stability based on Matsuo and Kawamura method

It has been widely recognized that the failure of a soft ground is closely related to the magnitude and history of the deformation which taken place before final failure. This makes the use of information which is practically possible measurements in the field to control the construction of the embankment to be safe and efficient. When the soft ground is under loading, in addition to the consolidation, there is a possibility for horizontal flow (shear deformation). This fact makes it difficult to theoretically distinguish the displacement and the failure of soft ground. It is obvious that failure occurs when the progress of shear deformation is faster than the consolidation settlement. Therefore, the graphical method proposed by Matsuo and Kawamura, 1977 [14] is commonly used to estimate the stability of the embankments constructed on the soft ground based on the field monitoring data as shown in Figure 16.

The Figure 16 indicates a relationship between settlement and ratio of lateral displacement to settlement, and each curve is corresponding to a different Factor of Safety (FOS) values vary from 1.0 to 1.67. Then, based on the obtained field monitoring data, embankment settlement versus ratio of lateral displacement to settlement was plotted in Matsuo and Kawamura’s diagram as shown in Figure 17. This clearly indicates the variation of Factor of Safety (FOS) at different depths of the soft soil against slope failure of embankment at different phases of construction.

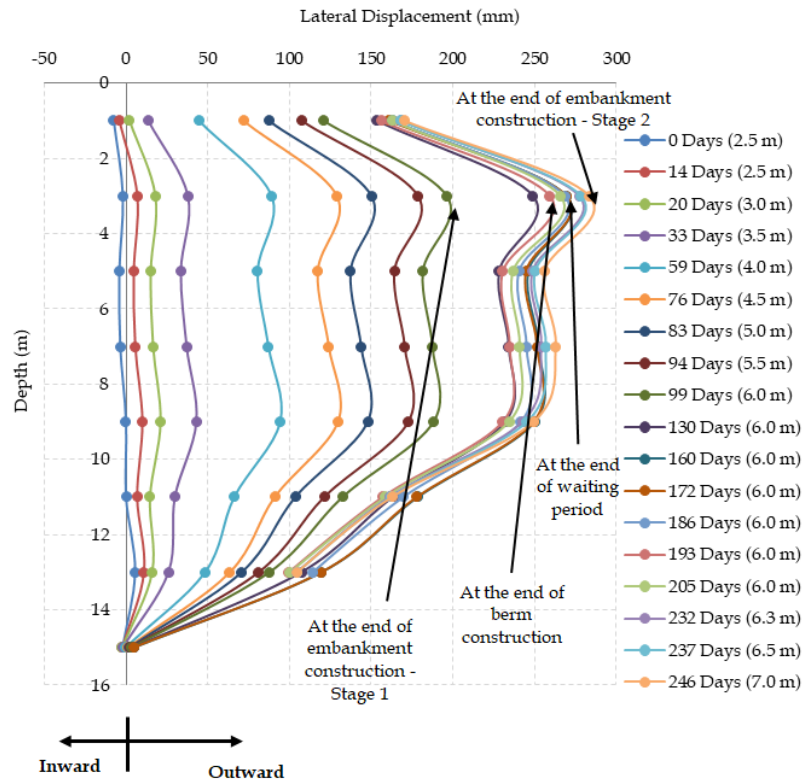


Fig 13 Variation of lateral displacement over depth at RHS of the trial embankment

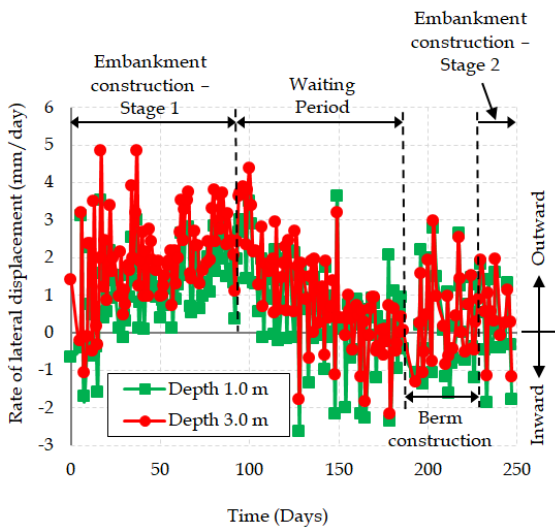
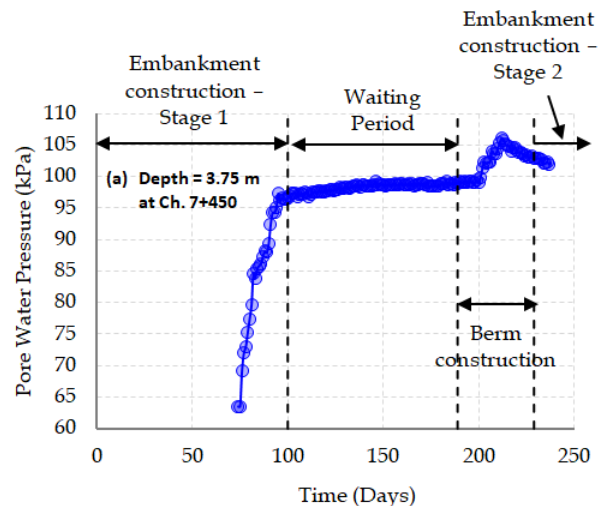


Fig 14 Variation of rate of lateral displacement over time for RHS of embankment at Ch. 7+455

It can be noticed that FOS gradually decreases with the increase of embankment construction – Stage 1 due to huge lateral displacement of about 200 mm in right side of the embankment as depicted in Figure 17 and Figure 13. The significant outward lateral movement can be observed up to a depth of 12.0 m at the end of Stage 1 of embankment construction. The rate of lateral displacement per day has been increased up to 4-5 mm/day as indicated in Figure 14. According to the field practices, if the rate of lateral displacement is in

between 4 to 5 mm/day, frequent monitoring is required. Further, FOS at the end of Stage 1 of embankment construction can be estimated as 1.24. Therefore, the embankment filling was stopped as indicated in Figure 11 (waiting period) expecting an improvement in FOS.

The continuous increase of pore water pressure (Figure 15) during embankment construction – Stage 1 clearly indicated the unsafe nature of the embankment at that phase. As such, embankment construction was stopped for a period of 89 days (waiting period) expecting the dissipation of excess pore water pressure to improve the stability.





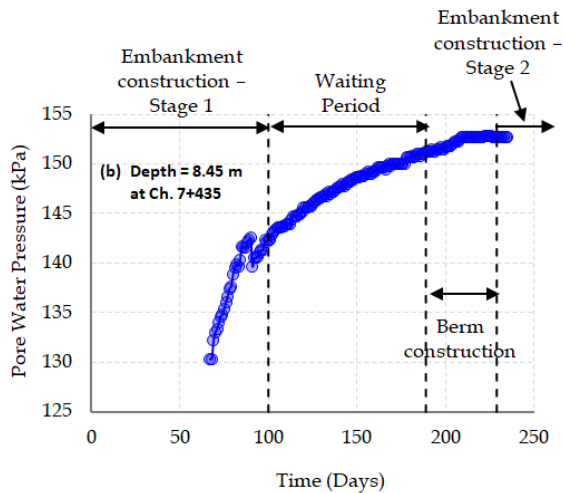


Fig 15 Variation of pore water pressure with time

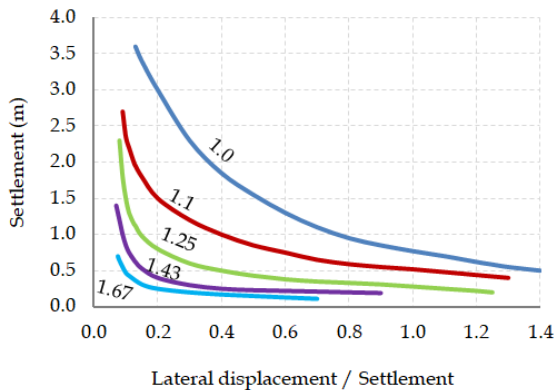


Fig 16 Matsuo and Kawamura's diagram [14]

Even though, there is no any dissipation of excess pore water pressure during the waiting period, the rate of increment of pore water pressure has been significantly decreased at shallow depth as illustrated in Figure 15 (a). However, at greater depth [Figure 15 (b)], pore water pressure has been increased even during the waiting period. This behaviour clearly indicated that existing Gravel Compaction Piles were not effectively help to transfer the pore water at greater depth to the ground surface during the Stage 1 of the embankment construction. However, during the design stage, generally, it is assumed that pore water in the soft ground flow towards the GCP due to higher horizontal permeability of the soft soil and collected pore water transfer to the ground surface through the GCP. Based on field monitoring data, it seems that vertical drainage path (GCP) has been significantly reduced due to smear effect and/ or higher horizontal permeability of soft soil has been diminished due to disturbance during GCP installation. As a result, excess pore water pressure has not been dissipated during the embankment

construction – Stage 1 and even during the waiting period. Moreover, it can be noted that if length of the GCP is more, the vertical drainage through the GCP due to capillary action may not be effective. Even though, rate of lateral displacement has been significantly reduced during the waiting period, additional 70 mm outward lateral movement can be observed during the waiting period. As such, this behaviour further reduces the FOS against embankment slope failure up to 1.20 even during the waiting period.

Then, a berm has been introduced up to the elevation of 5.33 m MSL in both RHS and LHS of the embankment to reduce the lateral displacement. The newly introduced berm and revised design cross section is indicated in the dotted line in the Figure 7. It is well known that berm provides an additional lateral support against outward movement of the embankment. Berm construction and settlement due to berm construction are depicted in Figure 11 and Figure 12, respectively.

It can be noted that settlement due to berm construction in RHS is about 0.4 m where as in LHS is about 0.05 m. This clearly indicates the variation of soft soil thickness across the trial embankment area. By providing the berm, embankment was moved about 10 mm into the inward direction as illustrated in Figure 13. Further, rate of lateral displacement has been changed to 1-2 mm/day in inward direction as depicted in Figure 14. However, there is no any reduction in pore water pressure due to berm construction. It can be clearly seen that settlement versus lateral displacement to settlement ratio graphs in the Matsuo and Kawamura's [14] plot have been moved to left indicating a slight improvement in the stability. This behaviour is clearly illustrated in the enlarge view of the variation of FOS at the depth of 3.0 m at different phases of embankment construction in the same figure.

Once the FOS has increased and indicated a slight improvement in stability, embankment construction – Stage 2 has been started as shown in Figure 11. When the embankment elevation increased up to 7.0 m MSL, embankment was again started to move in the outward direction as presented in Figure 13. Even though, rate of lateral displacement is about 2.0 mm/day, the FOS curves in the Matsuo and Kawamura's [14] plot moved in the vertical direction indicating further reduction in FOS. The FOS values of depths 3 m to 7 m are about 1.13 – 1.17 which is less than the required minimum FOS of 1.20 for short term stability [15]. Therefore, it is clearly indicated that the embankment is unstable at this stage.

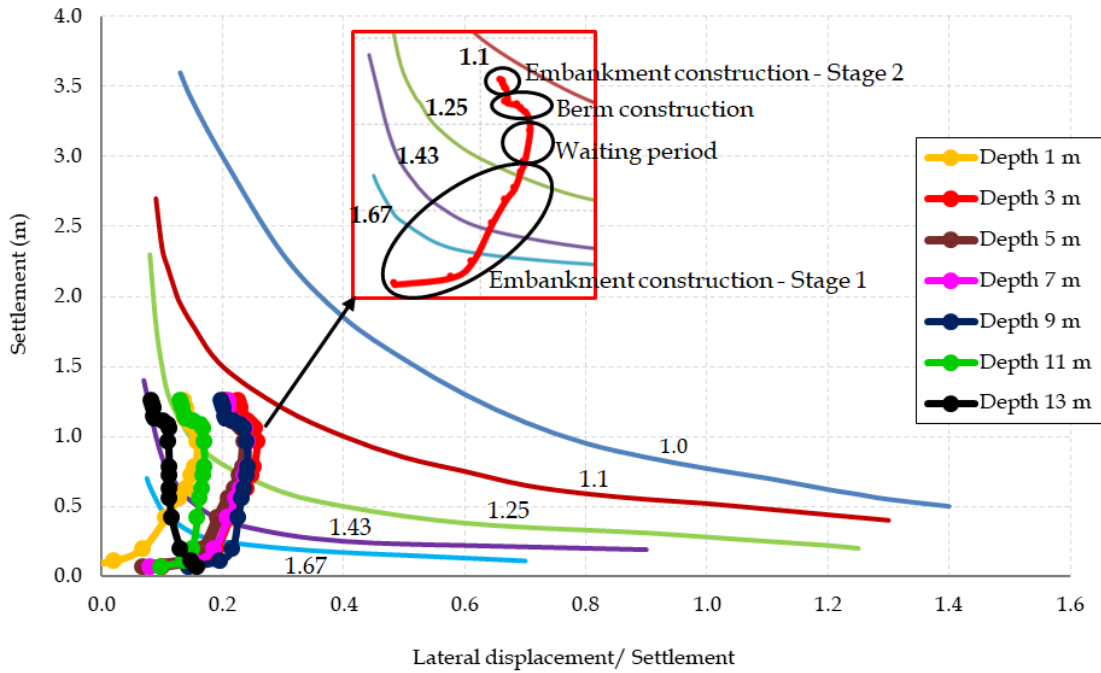


Fig 17 Variation of FOS in RHS of the embankment using Matsuo and Kawamura Method [14] at Ch. 7+455

#### 4.2 Determination of shear strength parameters based on Back Analysis

The above embankment conditions were numerically modelled using GEOSLOPE SLOPE/W software as shown in Figure 18. Using the back analysis technique, shear strength parameters of GCP improved composite ground at different phases of the embankment construction were estimated. Spencer’s method was used as the constitutive model while “Entry and Exit” method was used to generate the slip surfaces. Since soft soil is critical in RHS of the embankment, only RHS of the trial embankment section was considered for the slope stability analysis. In the model, it was assumed that only the soft soil portion below the embankment was improved with GCP and the water table was maintained at the existing ground surface. According to the field observations, only 3 numbers of GCPs were installed beyond the toe of the embankment. In addition, 200/200 geogrids (tension in both transverse and longitudinal direction is 200 kN/m<sup>2</sup>) were placed in the embankment to enhance the slope stability.

The geotechnical parameters of other materials (except GCP improved composite ground) used for the analysis is shown in Table 3. Effective shear strength parameters ( $c'$  and  $\phi'$ ) were used for embankment fill material and completely weathered rock while undrained shear strength parameters ( $c_u$  and  $\phi_u$ ) were used for unimproved ground for the analysis. Based on the GCP spacing and diameter, area replacement ratio ( $a_s$ ) was estimated as 0.228.

Further, it was assumed that unit weight of the GCP improved composite ground ( $\gamma_{avg}$ ) does not vary with the embankment fill height, and average shear strength method was used to compute the unit weight of GCP improved composite ground [7] as presented in Equation 3. By taking unit weight of GCP material as 22 kN/m<sup>3</sup>, the average unit weight of GCP improved composite ground can be estimated as 14.28 kN/m<sup>3</sup>.

$$\gamma_{avg} = \gamma_{GCP} a_s + \gamma_{clay} (1 - a_s) \quad (3)$$

In this analysis, assuming that FOS obtained through Matsuo and Kawamura method [14] is correct, shear strength parameters of the GCP improved composite ground were estimated from trial-and-error method. Since friction angle of the GCP improved composite ground is governed mainly by the GCP material, it was assumed that friction angle of GCP improved composite ground is not varying with the embankment height. As such, the average friction angle ( $\phi_{avg}$ ) of GCP improved composite ground is estimated using the Equation 4 [7], where  $\mu_s$  is the stress ratio in GCP. By taking stress concentration ratio ( $n$ ) as 3,  $\mu_s$  was estimated as 2.06.

$$\tan \phi_{avg} = \mu_s a_s \tan \phi_s \quad (4)$$

The shear strength parameters obtained through back analysis are shown in Table 4 and critical failure surfaces at different stages of embankment construction are illustrated in Figure 19. Based on above explanation, the friction angle of the GCP

improved composite ground can be computed as 16.4<sup>0</sup>.

Table 3 Material parameters used for SLOPE/W analysis

Material	$\gamma$ (kN/m <sup>3</sup> )	$C$ (kPa)	$\phi$ (°)
Embankment Fill	20	5	32
Completely Weathered Rock	21	10	38
Unimproved ground	12	5.75	0
GCP improved ground	14.28	-	-

Based on the results presented in Table 4, it can be noted that undrained cohesion ( $c_u$ ) gradually decreases with the increment of embankment height. According to Skempton and Bjerrum, 1957 [17], undrained shear strength gain depends on the applied external load and degree of consolidation of the soft soil. The phase 1 to phase 3 of the embankment construction is under the same applied external vertical load (embankment height = 6.0 m). Even though, 229 days has been spent for the construction from beginning to phase 3, there is no any improvement in shear strength gain during this period due to less dissipation of excess pore water pressure. Poor dissipation of excess pore water pressure may result in the very slow primary consolidation. Further, introduction of berm was not made any influence on the shear strength gain even though it reduces the outward movement of the embankment.

As such it is very clear that there is no any shear strength gain of soft soil due to GCP installation and stage construction of the embankment. The continuous reduction of FOS and outward lateral movement of embankment led to abandon the GCP ground improvement technique in the project and huge financial loss has been occurred to the contractor.

Table 4 Back analysis results

Construction phase	FOS		Shear strength parameters	
	Matsuo and Kawamura	SLOPE/W	Cohesion $c_u$ (kPa)	Friction angle $\phi_u$ (°)
Stage 1	1.240	1.240	17.3	16.4
Waiting period	1.200	1.203	15.7	16.4
After berm construction	1.205	1.209	12.0	16.4
Stage 2	1.130	1.131	12.0	16.4

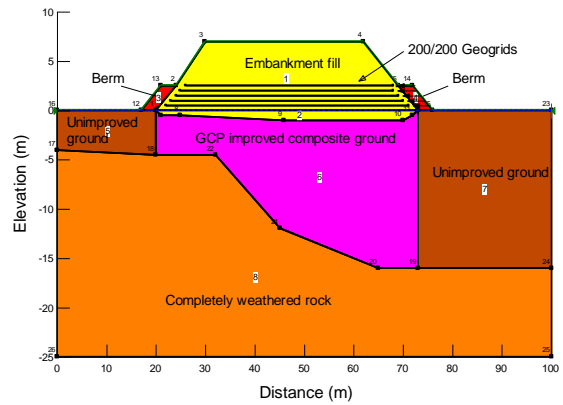
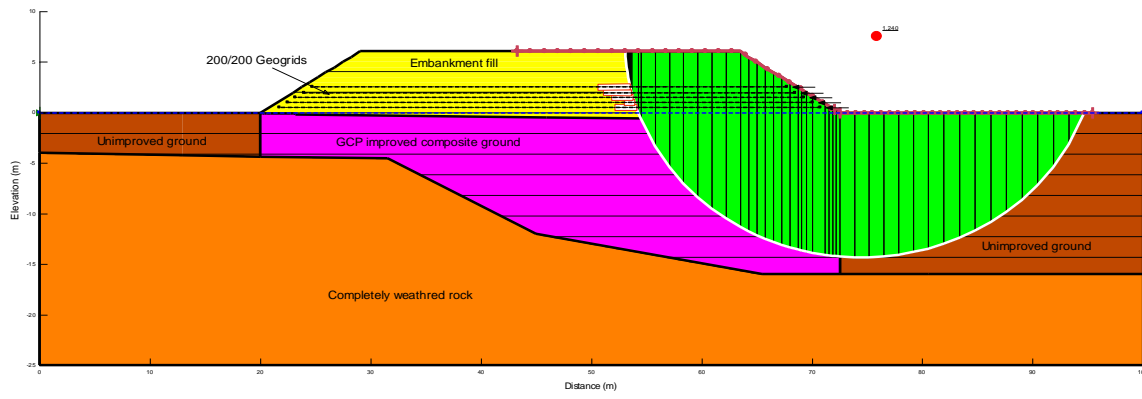


Fig 18 Numerical Model used for the back analysis

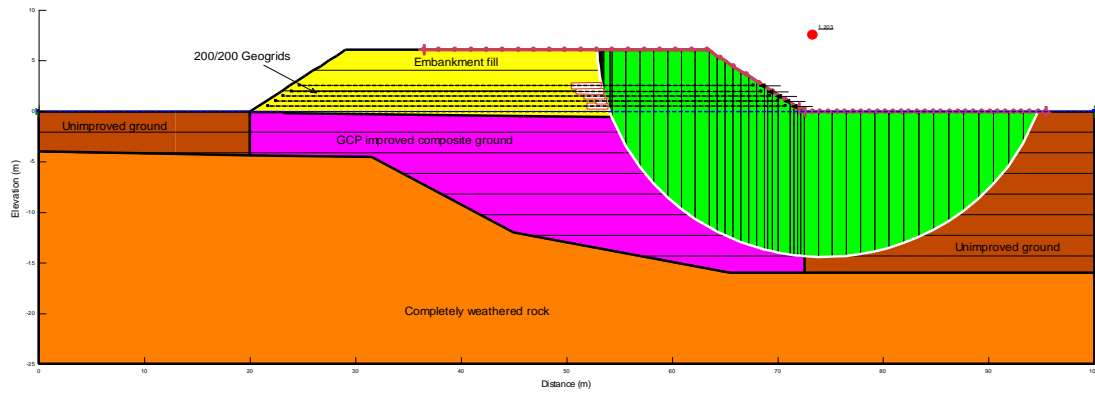
## 5 CONCLUSIONS

Based on this research study, the following conclusions can be drawn;

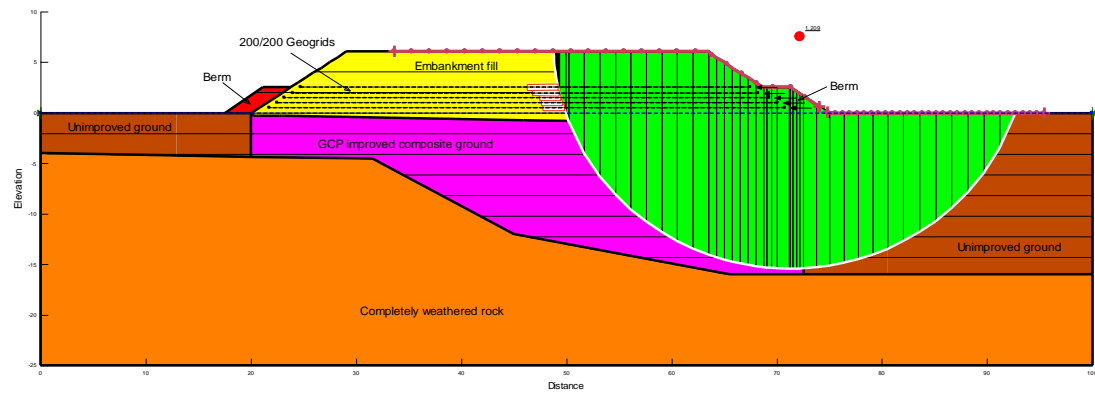
- According to limited borehole investigations, soft soil thickness in the RHS was identified as 15.6 m and GCP spacing was decided by taking average soft soil thickness as 13.7 m. However, during GCP installation, it was realized that average soft soil in the RHS is about 16 m and some locations it may around 18 m. As such it can be concluded that GCP spacing was decided by wrong interpretation of the soft soil thickness. This clearly indicates the importance of proper site investigation prior to start the GCP installation.
- As per depth measurements carried out during the GCP installation, soft soil thickness was higher than the value considered for the GCP design. However, no precautions have been taken to revise the original design or no countermeasures have been implemented before start the embankment filling. Hence it is a good practice to revise the original design if the field records indicate somewhat different soil profile than the soil profile used for the original design. By reducing the GCP spacing than the original design by installing additional GCP in between already installed GCPs, shortcomings in the original design can be eliminated.
- It was noticed that only 3 numbers of GCPs were installed beyond the toe of the embankment. However, it was realized that only 3 numbers of GCPs are not sufficient to provide toe support to the embankment due to high thickness of the soft soil. If the soft soil thickness is more, by installing precast concrete piles as toe support, adequate stability can be achieved against slope failure.



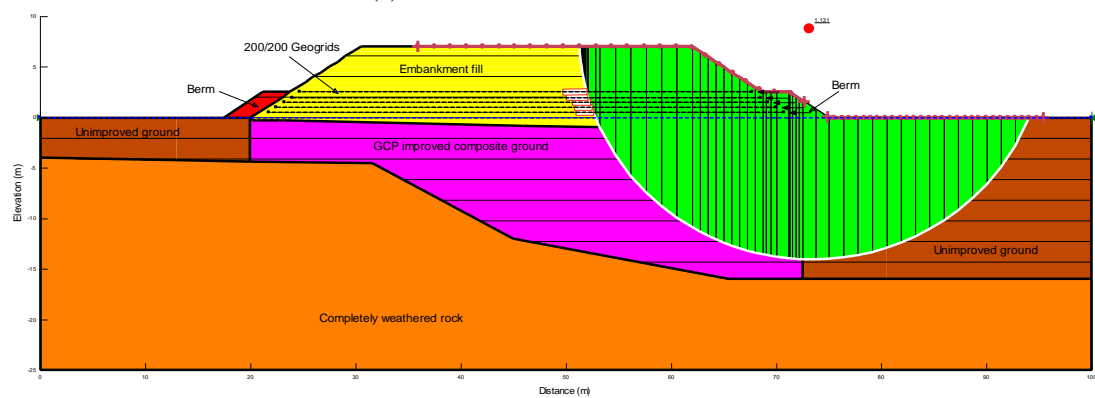
(a) At the end of embankment construction – Stage 1



(b) At the end of waiting period



(c) At the end of berm construction



(d) At the end of embankment construction – Stage 2

Fig19 Critical failure surfaces at different stages of embankment construction



- Trial embankment construction was started immediately after the GCP installation. However, it is a well known factor that due to disturbance during GCP installation, the strength and stiffness of surrounding soft soil is reduced. Hence, it is necessary to keep adequate time to stabilize the surrounding soft ground to recover its strength. The waiting period can be decided based on the pore pressure measurements using piezometers.
  - It can be noted that in the trial embankment section, piezometers were installed after start the embankment construction. This clearly indicates that embankment filling was started without proper monitoring of pore water pressure. Hence, it is recommended to establish proper field monitoring system, prior to start the embankment construction.
  - Based on the field observations and data analysis, it can be concluded that when the soft soil thickness is more than 10 – 12 m, it is really difficult to improve the soft ground without any reinforcement. Hence it is strongly recommended to select the most suitable ground improvement technique by accurately interpreting the soft soil thickness.
  - The slow rate of dissipation of excess pore water pressure after embankment loading is due to the shear failure of the soft soil. Due to disturbance of the soft soil during GCP installation and other field activities, higher horizontal permeability of soft soil diminishes and increases the smear zone surrounding GCP. As a result, the vertical drainage path within the GCP reduces causing reduction in dissipation of pore water pressure. This behaviour clearly indicates the importance of proper maintenance of field activities without disturbing the subsurface during GCP ground improvement.
  - Once the shear failure has occurred, the strength of the soft soil reduces to its residual value and it takes longer time to regain its original strength [16]. After the shear failure, even providing lateral supports by constructing berm will not be successful.
3. Kulathilaka, S.A.S. & Fernando, M. (2015) “Effect of preload on secondary consolidation of peaty clay,” International Conference on Geotechnical Engineering (ICGE – 2015), pp. 371-374
  4. Madhusanka, K.A.C. & Kulathilaka, S.A.S. (2015). “Possible use of Paddy Husk Ash in Improvement of Engineering Characteristics of Peaty Clay,” International Conference on Geotechnical Engineering (ICGE – 2015), pp. 407-410
  5. Saputhanthri, D.R. & Kulathilaka, S.A.S. (2011) “Enhancement of engineering characteristics of peaty clay due to mixing with cement,” Annual Transactions of the Institute of Engineers Sri Lanka, pp. 118-126
  6. Priyankara, N.H., Wijesooriya, R.M.S.D., Wickramasinghe, W.R.M.B.E. & Yapa, S.T.A. (2009) “Suitability of Quarry dust in geotechnical applications to improve engineering properties,” Engineer -Journal of this Institution of Engineers Sri Lanka, Vol. 42, No. 3, pp. 7-13
  7. Bergoda, D.T., Anderson, L.R., Miura, N. & Balasubramaniam, A.S. (1996) “Soft ground improvement: in low land and other environments”, American Society of Civil Engineers, New York, pp. 427.
  8. Nozu, M. & Ohbayashi, J. (1998) “Application of the static sand compaction pile method to loose sandy soil”, Proceeding of International Symposium on Problematic soils, IS – TOHOKU, Vol. 2, pp. 751-755
  9. <http://rda.gov.lk/supported/project-progress-pmu/esepe/esepe.html>, visited, 13/07/2023
  10. Spagnoli, G. (2007) “An empirical correlation between different Dynamic Penetrometers” , Electronic Journal of Geotechnical Engineering (EJGE), Vol. 13, pp. 1-11
  11. Marawan, M.S. & Ahmed, F. (2013) “Estimation of deformation modulus of gravelly soils using dynamic cone penetration tests, “ Ain Shams Engineering Journal, Vol. 4, pp. 633-640
  12. Salagoda, R. & Yoon, S. (2003) “Dynamic Cone Penetration Test (DCPT) for Subgrade Assessment Final report,” FHWA/IN/JTRP-2002/30
  13. Shioi, Y. & Fukui, J. (1982) “Application of N-value to Design of foundation in Japan,” 2nd ESOPT, Vol. 1, pp. 40-93
  14. Matsuo, M. and Kawamura, K. (1977) “Diagram for construction control of embankment on soft ground”, pp 37-52.
  15. ICTAD Publication No. – SCA/5, (2009) “Standard specifications for construction and maintenance of roads and bridges”.
  16. Priyamali, M.W.S. & Priyankara, N.H. (2023) “The influence of Preconsolidation pressure on undrained shear strength characteristics of peaty clay in Sri Lanka”, Engineer - Journal of this Institution of Engineers Sri Lanka, (Accepted).
  17. Skempton, A.W. & Bjerrum, L. (1957) “A contribution to the settlement analysis of Foundations on Clay”, Geotechnique, Vol. 7, pp. 168-178.

## REFERENCES

1. Karunawardena, A., Ooka, A. & Nithiwana, W. (2017) “Improvement of Sri Lankan Peaty Clay using the Gravel Compaction Pile Method for the Construction of a Highway Embankment.,” Proceedings of the 19th International Conference on Soil Mechanics and Geotechnical Engineering, Seoul 2017, pp. 3003-3006
2. Karunawardena, A. & Toki, M. (2013) “Design and Performance of Highway Embankments Constructed over Sri Lankan Peaty Soils,” Proceedings of the 18th International Conference on Soil Mechanics and Geotechnical Engineering, Paris 2013, pp. 2949-2952

**Associate Partner:**



**Gold Sponsor:**



**Silver Sponsors:**



**Bronze Sponsors:**



**SRI LANKAN GEOTECHNICAL SOCIETY**

A member Society of the International Society for Soil Mechanics and Geotechnical Engineering (ISSMGE)